UNIVERSITY OF CALIFORNIA
RIVERSIDE

Influences on T Cell Migration Behavior in the Inflamed Brain

A Dissertation submitted in partial satisfaction
of the requirements for the degree of

Doctor of Philosophy

in

Biochemistry and Molecular Biology

by

Kathryn Elizabeth McGovern

June 2016

Dissertation Committee:

Dr. Emma H. Wilson, Chair
Dr. Kathryn A. DeFea
Dr. Monica J. Carson

The Dissertation of Kathryn Elizabeth McGovern is approved:

Committee Chairperson

University of California, Riverside

ACKNOWLEDGEMENTS

There are so many people to thank for making my time here at UC Riverside the best it could possibly be. First, my deepest respect and highest esteem go to my advisor, Dr. Emma Wilson. Her direction, creativity, enthusiasm and shining example constantly inspired me and always drove me to be a better scholar. She has been patient, critical, encouraging, and supportive. She made me the scientist (and public speaker!) that I am now and her gift for forging collaborations gave my career the best start possible. There is no better mentor in the world for me.

I am thankful to my dissertation committee, Dr. Monica Carson and Dr. Kathryn DeFea. Both have been accessible, supportive, and extremely generous with their time. I can't imagine a better team to both challenge and train me. Apart from my committee, I am also grateful to the PIs and labs that make up UCR's Host-Pathogen Group. Drs. Nair, Lo, and Messaoudi have influenced me greatly with their advice, honesty, vast knowledge, and humor. My labmates Phil Nance, Shahani Noor, Clement David, Danielle Worth, and Tyler Landrith made every day of work in the lab fun. It makes me so happy to be able to call you all colleagues and friends.

My family- my parents and grandmother- made me the person that I am through their love and support. My in-laws kept both my husband and myself fed on a nearly weekly basis and gave us a place we could completely relax. Finally, my loving husband comforted me when I needed it but most importantly, he kept

me laughing and kept me going. I don't think I will ever find the right words to express how much my family's love has meant to me over the years.

Every person mentioned above was there for me during both my tears and triumphs. This dissertation would have never coalesced without them.

Chapters 1 and 4 of this dissertation, in part, are reprints of material published in the following articles and are used here with the permission of the publishers.

Kathryn E. McGovern and Emma H. Wilson. Dark side illuminated: imaging of *Toxoplasma gondii* through the decades. *Parasites & Vectors.* 6(1): 334. doi: 10.1186/1756-3305-6-334. 22 November 2013. (Review.)
PMID: 24267350

Kathryn E. McGovern and Kathryn A. DeFea. Molecular mechanisms underlying β-arrestin-dependent chemotaxis and actin-cytoskeletal reorganization. *Handbook of Experimental Pharmachology*. 219:341-59. doi: 10.1007/978-3-642-41199-1_17. 5 November 2013. (Invited Book Chapter.)
PMID: 24292838

Kathryn E. McGovern and Emma H. Wilson. Role of Chemokines and Trafficking of Immune Cells in Parasitic Infection. *Current Immunology Reviews*. 9(3) 157-168. doi: 10.2174/1573395509666131217000000. February 2014. (Invited Review.)
PMID: 25383073

ABSTRACT OF THE DISSERTATION

Influences on T Cell Migration Behavior in the Inflamed Brain

by

Kathryn E. McGovern

Doctor of Philosophy, Graduate Program in Biochemistry and Molecular Biology
University of California, Riverside, June 2016
Dr. Emma H. Wilson, Chairperson

Cell migration is an integral function of immunity. Control of cellular infiltration and behavior are critical to prevent inflammation-induced pathology while still combating infection. Nowhere in the body is this balance more important than the CNS. As an immune privileged site, the brain needs a potent response that is compatible with the surrounding sensitive tissue. Chronic infection with the parasite *Toxoplasma gondii* provides a model of balance. T cells must migrate efficiently within the brain to find sites of infection and keep parasites from replicating. Many factors can influence cell behavior once leukocytes enter the brain. This dissertation examines the role two molecules play in T cell migration during chronic *Toxoplasma* infection.

First, the role of the intracellular adaptor protein β-arrestin 2 (β-arr2) is examined in T cell migration in response to the chemokine CCL21. β-arr2 is required for migration of naïve cells and those isolated from the brain. Chemotaxis studies demonstrate this requirement is a result of mediating migratory speed. Next, β-arr2's role in cell trafficking to infected tissue is tested

in vivo. Finally, using two-photon microscopy β-arr2 is shown to mediate migratory speed of infiltrating T cells in the brain. Together these data define the specific role for β-arr2 in regulating T cell velocity in the CNS.

Next, the effect of the matricellular glycoprotein SPARC is discussed. Infected astrocytes are the source of SPARC in the infected brain, the same source as CCL21. Novel binding partners for SPARC- CCL21 and CCL19- are reported, expanding the potential roles of SPARC to include the maintenance of chemokine signals in the brain. SPARC's presence enhances T cell migration in response to CCL21. Finally, two-photon imaging reveals SPARC enhances T cell access to the brain and slightly enhances T cell migration behavior within the brain. These data demonstrate how SPARC cooperates with other proteins in the brain matrix to contribute to T cell behavior.

Lastly, additional levels of regulation for chemokine dependent cell migration are considered and potential areas of further investigation are proposed. This dissertation provides new insight into T cell migration during a protective immune response in the brain.

TABLE OF CONTENTS

LIST OF FIGURES

CHAPTER ONE

Introduction

1.1 The Biology of *Toxoplasma gondii*

1.1.1 Discovery and Prevalence

When Charles Nicolle, Louis Manceaux and Alfonso Splendore first described *Toxoplasma gondii* in 1908, their depiction of the parasite was similar and very detailed (1,2). Both papers, presented days apart, describe *T. gondii* as a parasite found both inside and outside of nucleated cells, never in red blood cells, having a rounded or piriform shape, and with a length of 5-8 mm. Splendore describes the wasting exhibited by all the rabbits he was studying before they succumbed to infection. He goes on to describe the hypertrophied and discolored spleen, the enlarged liver and lymph nodes and the ulcerated small intestine. He even describes, in addition to the parasite's commonly observed "kidney-shaped form", the presence of cysts, 8-40 mm in diameter. Nicolle and Manceaux focus their efforts on describing *T. gondii's* morphology and systematically recounting in which types of tissues the parasite is found in the gundis they were studying. Both papers underscore *T. gondii's* similarity to *Leishmania*, so much so that Nicolle and Manceaux proposed to call their new parasite, *Leishmania gondii* (1,2).

It is now known that *Toxoplasma* is an obligate intracellular parasite that can invade any nucleated cell in any warm-blooded animal. The prevalence rate of this parasite is very high, with recent estimates between 15-30% in the US and

UK and up to 80% in parts of Europe and South America. Infection stimulates a proinflammatory immune response with systemic parasitemia contained within one to two weeks. The host remains infected for life and a continuous T cell response is required to prevent reactivation of *Toxoplasma* cysts, primarily located in the brain. Severe pathology therefore manifests in the immune compromised, most commonly observed as Toxoplasmic encephalitis.

1.1.2 Life Cycle

Though a wide variety of animals can serve as a secondary host, this apicomplexan parasite's definitive host is the cat and *T. gondii* can only sexually reproduce in the digestive system of the cat (Figure 1). Highly resilient *T. gondii* oocysts are shed with the cat's feces and contaminate the soil and water (3). Secondary hosts become infected by ingesting contaminated food or water. Once eaten, oocysts convert to tachyzoites and disseminate throughout the body, invading and quickly replicating within any nucleated cell. Pressure from the immune system, namely the production of IFNγ by Th1 cells controls parasite replication. In response, tachyzoites convert to slowly replicating bradyzoites and encyst. Tissue cysts can be found in any tissue, but they are predominately found in the brain for the remainder of the host's lifetime.

1.2 Chemokines and Cell Migration During *Toxoplasma* Infection

As with all infections, parasites induce inflammation - that is the mobilization, proliferation and recruitment of leukocytes to the site of infection. This immune cell trafficking and the effector functions of these cells can control the pathogen or exacerbate pathology. In comparison to viral or bacterial invasion, parasites are complex eukaryotic pathogens often with multiple lifecycle stages within the mammalian host. Their characteristic ability to manipulate the host immune response and tendency to cause chronic infections adds further complexity to the recruitment and maintenance of cellular immune responses within infected tissues.

Chemokines are essential regulators of cell trafficking. They are a large family of small cytokines named for their ability to induce chemotaxis in cells expressing the appropriate receptors and categorized into four subfamilies (C, CC, CXC, CX_3C) depending on the sequence position of conserved cysteine residues. Chemokines play multiple roles in physiology including during development for directed cell guidance and hematopoiesis in addition to mediating inflammatory responses (4-9). However, perhaps because of the inherent requirement for continuous migration of cells, the influence chemokines exert on the immune system has been extensively studied. This includes the role they play in lymphocyte homeostasis, which requires several chemokines, primarily CCL19 (ELC, EBV-induced chemokine, MIP-3b) and CCL21 (SLC, exodus 2), the

ligands for CCR7. CCL21 is required for T cell circulation within and between primary and secondary lymphoid organs (10-13) as well as the homeostatic expansion of naïve CD4+ T cells (10). Moreover, CCR7 signaling cooperates with CXCR5 signaling on B cells to orchestrate B cell migration within the lymph nodes and B cell access to T cell help. This is in addition to the expression of CXCL13 within the B cell follicle that controls B cell retention and organization in this area of the lymph node (14-16). However, ultimately our immune system has evolved for efficient and optimal defense against invading pathogens. This dissertation will focus on the role chemokines, specifically CCL21, and subsequent cell trafficking in the rapid, coordinated and long-term immune defense against parasitic infection.

1.2.1 Chronic Infection

In the case of *T. gondii*, parasites persist in the brain after trafficking to the CNS as free parasites (17,18) or inside infected cells (19,20). Parasites can appear in the brain as early as 10 days after initial exposure (21) and remain there for the lifetime of the host (22). Control of parasite replication and maintenance within cysts depends on IFNγ production by infiltrating T cells (23-26). Two major chemokine ligand/receptor systems are important for T cell recruitment and behavior within the chronically infected brain: CCL21/CCR7 and CXCL10/CXCR3. Both CCL21 and CCL19 are upregulated in the brain during infection and linear strands of CCL21 can be observed within the brain parenchyma associated with

migrating CD8+ T cells (27,28). In addition, CCL21 is required for efficient CD4+ T cell migration from extraparenchymal sites into the brain parenchyma (29) (Figure 3C). This was demonstrated in *plt/plt* mice (deficient in CCL19 and CCL21-ser) and transgenic GFAP-CCL21 mice (where CCL21 is constitutively over-expressed under the astrocyte specific promoter, GFAP). In wild type mice chronically infected with *T. gondii*, immune infiltrates can be observed in the perivascular spaces and meninges, in addition to the tissue parenchyma (29). In mice lacking CCL19/CCL21, significantly higher numbers of CD4+ T cells are recruited to the brain. However, these cells accumulate in the extraparenchymal spaces. In contrast, mice overexpressing CCL21 displayed little accumulation of CD4+ T cells in extraparenchymal spaces and instead cells were found dispersed throughout the brain instead of focused in the frontal cortex where *T. gondii* primarily resides (29).

Ligands for CXCR3, CXCL9 and CXCL10, are significantly upregulated in the brain upon infection (30). CXCL10 is required for a protective antigen specific CD8+ T cell population within the CNS. Whether this is through recruitment or retention of these cells is not known, however in the absence of CXCL10 there is a 60% reduction in the T cell population at this site (30). CXCL9 and CXCL10 are found at perivascular areas in the brain suggesting a role in recruitment across the blood brain barrier (31). However, the role of CXCR3/CXCL10 signaling in the *Toxoplasma* infected brain seems more fundamental than trafficking across

this barrier. Recent mathematical modeling of CD8+ T cell behavior demonstrates that these cells undergo a Lévy random walk, characterized by sudden long ‘flights’. This is an optimal search strategy conserved throughout the animal kingdom and at the cellular level (30) and suggests that these cells are not undergoing gradient-guided migration. However CXCR3 signaling is required for CD8+ T cell migratory speed (30) as blockade of CXCL10 signaling leads to a significant reduction in cell velocity without changes in the search strategy of the cell. Ultimately more work is needed to determine if or when guided migration within infected tissue occurs, how local gradients act, and the effect differential downstream signaling of competing chemokines may have on cell behavior and optimal parasite control.

1.3 β-arrestins in Immune Responses and Cell Migration

1.3.1 CCR7 Biology

Cell migration is a critical aspect of the immune response. There is a continuous redistribution of cells from the primary and secondary lymphoid organs to infection sites, which must be tightly controlled to provide efficient protection from invading pathogens while minimizing immune related pathology. Chemokines and their receptors are major regulators of the cell trafficking required to mediate an immune response. For example, CCR7 is a well-known homing receptor, expressed on mature dendritic cells (DCs) naïve and memory T cells, and naïve B cells. DCs continuously scavenge for antigen in peripheral tissues and upregulate CCR7 to migrate to the secondary lymphoid tissues and present antigen (32,33). Naïve T cells present in the lymph node express high levels of CCR7. Once they are presented with their cognate antigen by DCs, they downregulate CCR7 to migrate out of the lymph node and into the periphery. When these now antigen experienced T cells reach inflamed tissue, CCR7 is again acquired to facilitate lymphocyte migration into the tissue from the blood (34-37). Central memory T cells reside in lymphoid tissue and express high levels of CCR7, but down regulate the receptor as they proliferate after a subsequent antigen stimulation to mobilize to inflamed tissue (38). On the other hand, $CCR7^{low}$ effector memory T cells reside in the tissues and upregulate CCR7, induced by restimulation with antigen. Further, CCR7 expression on B

cells will prompt them to migrate toward the lymph node's T cell zone to receive CD4 T cell help, critical for promoting effective B cell responses (39,40).

CCR7 has two ligands, CCL19 and CCL21, which bind to their receptor with equal affinity (41). They only share 32% sequence homology and the main structural difference between them is CCL21's C-terminal glycosaminoglycan binding domain, allowing CCL21 to remain immobilized while CCL19 is soluble (42-46). Both ligands are constitutively expressed on the high endothelial venules of the lymph node to facilitate lymphocyte entry (40,47). Within the lymph node, CCL21 and CCL19 are expressed by fibroblastic reticular cells and follicular dendritic cells to form the conduits that enable T cell and DC migration and facilitate antigen presentation (48,49). Both ligands are also inducible upon infection to facilitate T cell entry into inflamed tissue (12,28). Thus, interactions between CCR7 and its ligands play a vital role in orchestrating leukocyte trafficking between the periphery and lymphoid tissues.

1.3.2 β-arrestins Downstream of CCR7

As a chemokine receptor, like most other 7 transmembrane domain receptors, CCR7 has two signaling axes. The best known and best conserved axis is the activation of G protein signaling (50). Agonist binding to CCR7 causes a conformational change leading to the exchange of GDP for GTP in the $G\alpha_i$ subunit of the heterotrimeric G protein complex that is coupled to the receptor.

This exchange leads to the dissociation of $G\alpha_i$ from the heterotrimeric complex, which goes on to inhibit adenylyl cyclase activity. Agonist bound receptors like CCR7 are then targeted by G-protein coupled receptor kinases (GRKs) and phosphorylated at the C-terminal tail. Phosphorylated receptors recruit β-arrestins, the molecules responsible for the second signaling axis. β-arrestins are a family of four intracellular proteins, two of which, β-arrestin 1 and 2 (β-arr2) are ubiquitously expressed in mammalian cells (51,52). The most well known actions of β-arrestins include G protein uncoupling, receptor internalization and recycling, but β-arrestins can also scaffold actin remodeling proteins at the leading edge of a migrating cell, promoting gradient sensing and chemotaxis even without the actions of G proteins (53-56). These actions may vary depending on cell type, or may be temporally and spacially regulated within the same cell (57,58).

Despite equal affinity for CCR7, equal activation of G proteins, and equal calcium mobilization, subtle differences elicited by CCL19 and CCL21 have been reported (43,59-61). Bard et al. first reported that CCL19, but not CCL21 leads to receptor endocytosis (62) in human lymphocytes isolated from the blood, but the mechanism through which endocytosis occurs was not investigated. Later, CCL19 mediated β-arr2 binding to CCR7 was detected in stably transfected HEK cells, presumably initiated by phosphorylation of CCR7 at the carboxyterminal serine/threonine cluster (63). A report by Byers et al. revealed CCL21 can also

lead to CCR7 endocytosis, but to a lesser degree than CCL19, such that most of the receptor remains on the cell surface. However, by knocking down β-arr2 in a lymphoma cell line and rescuing β-arr2 expression in arrestin deficient MEK cells, β-arr2 mediated CCR7 internalization was detected only after stimulation with CCL19 (64). CCL21 mediated β-arr recruitment to CCR7 was finally detected in HEK cells using FRET assays by the Lefkowitz group (41). Further, it was determined that phosphorylation of CCR7 by GRK6 occurs after stimulation by either ligand, but phosphorylation by GRK3 only occurs after stimulation with CCL19 (41), pointing to a mechanism for the observed ligand bias and differential chemotaxis.

Chapter 2 of this dissertation focuses on the role of β-arr2 in the migration of primary T cells in response to CCL21 and indeed within the complex environment of the inflamed brain. Data suggest that β-arr2 promotes CCL21 driven chemotaxis of naïve T cells isolated from the lymph nodes and activated T cell isolated from the brain. It is not required for T cells to enter the brain to combat infection, but does mediate efficient migratory speed. This suggests β-arr2's role is not simply pro- or anti-inflammatory in the context of infection, but rather it has a nuanced part to play by bolstering the speed at which T cells must migrate to keep parasite replication under control.

1.4 Extracellular Matrix Remodeling and its Contribution to Cell Migration

The proliferation of intravital microscopy in studies of immune responses is continually showing how the extracellular matrix has an important role not only in supporting, but also influencing cell behavior. It is a dynamic scaffold, continuously remodeled during development but also during injury and inflammation (65). The secreted proteins that make up the ECM are frequently decorated with sulphated glycosaminoglycans (66,67), allowing for interactions with other secreted molecules like chemokines, and influencing the arrangement, concentration, and availability of these factors to infiltrating immune cells (67). Further, the proteins that make up the ECM are targets of enzymatic cleavage during immune cell infiltration and the remaining fragments can also elicit chemotaxis (68-71). Thus the ECM delivers a multitude of signals to modulate immune functions such as activation, polarization, and migration within tissue.

Integral for the ECM's ability to continuously renew, matricellular proteins are another family of secreted proteins. While structurally they are unrelated to each other (72), matricellular proteins function similarly in that they regulate matrix turnover. They are highly expressed during tissue remodeling events like growth and development and following injury or infection. Their expression is tightly controlled to help strike a balance between orchestrated and disordered cell movement. Regulating these events is not a trivial matter. Abnormal growth leads to developmental disorders while aberrant leukocyte infiltration leads to

immune-mediated pathology (73). There are many members of the matricellular protein family (74), but the focus here is on SPARC (secreted protein acidic and rich in cysteine).

1.4.1 SPARC and the Extracellular Matrix

SPARC (also referred to as osteonectin or BM-40) is capable of binding to a variety of different ECM components including but not limited to fibronectin, vitronectin, thrombospondins and at least four different isoforms of collagen (75). Thus, SPARC has the ability to regulate the barrier functions of the ECM, such as regulating immune cell infiltration through basement membranes, in addition to regulating the matrix structure in tissue parenchyma.

SPARC's interaction with collagen is probably best characterized. Early studies observed the co-expression of collagens and SPARC during development and wound healing (76,77) suggesting that SPARC is a chaperone for the initial assembly and distribution of collagen in the matrix. This is supported by the lesser amount of collagen deposited in the skin of SPARC deficient mice (78,79). However, the identification of SPARC's only known receptor, Stabilin-1, on alternatively activated macrophages (80) provides a competing hypothesis. SPARC binds to ECM components in a Ca^{2+} dependent manner. Outside the cell, calcium is abundant and SPARC's affinity for matrix proteins is high. When alternatively activated macrophages are recruited to areas where SPARC

expression is occurring, they target SPARC via Stablin-1 (80). Then the entire SPARC complex is endocytosed. Inside the cell, low calcium concentrations mediate the release and subsequent degradation of matrix and SPARC is exported from the cell. Thus, scavenging SPARC in this way leads to the degradation or clean-up of matrix components.

1.4.2 SPARC and Cell Migration

SPARC's contribution to cell migration is varied. For example, SPARC is often described as a counter-adhesive molecule. Addition of recombinant SPARC to cells in vitro does not lead to complete separation from the culture dish, but does lead to separation from other cells and rounding (81). This is thought to be caused by SPARC's direct interaction with integrins on the cell surface (82) though in vivo may also be due to SPARC binding to ECM fibers to block integrin binding (83).

Matrix turnover is an essential part of injury repair. Therefore we would expect the presence of SPARC to be essential for wound healing and the mediate inflammation. However, the opposite appears to be true. Skin excisions in SPARC null mice close faster than in WT mice (78). This may be due to a variety of factors. Expression of cytokines and other small factors like leptins are increased in SPARC deficient mice and may act in a compensatory manner to help heal the injury (78,84). Further, collagen present in skin is less dense in the

absence of SPARC and therefore could more easily accommodate infiltrating immune cells. Indeed, in a mouse model of peritonitis, SPARC -/- mice exhibit increased neutrophil and leukocyte infiltration (85). Further, dendritic cell migration to the draining lymph node and T cell priming is increased in a mouse model of contact hypersensitivity (79). The same phenotype is observed in a mouse model of salmonella infection due to the inability of SPARC deficient mice to form granulomas. However, in this model, despite enhanced immune cell activation, SPARC null mice die anyway because without granulomas the infection cannot be contained (86). Therefore SPARC's multifaceted roles can lead to unexpected phenotypes in vivo.

The work in chapter three of this dissertation investigates the role SPARC plays in mediating efficient chemokine T cell migration during chronic *Toxoplasma gondii* infection in the brain. Infected astrocytes are a source of both SPARC and CCL21. In vitro, SPARC can bind to CCL21 directly, and when added to chemotaxis assays, SPARC enhances the T cell response to CCL21. In the brain, the absence of SPARC leads to the accumulation of T cells in densely populated clusters, suggesting access to the parenchyma is impaired in SPARC null mice. The velocity, displacement, and meandering index of T cells migrating in SPARC-/- mice are all significantly reduced compared to those migrating in WT mice. All together, these data demonstrate how SPARC promotes CCL21 mediated cell migration and provides optimal access to the infected brain.

1.5 Materials and Methods

Mice

CBA/CaJ, Swiss Webster, C57BL/6, congenic CD45.1 (C57BL/6 background) OTI, dsRed (C57BL/6 background), and GFP (C57BL/6 background) mice were purchased from Jackson ImmunoResearch (West Grove, PA). SPARC null mice on a mixed background were also purchased from Jackson ImmunoResearch and backcrossed onto a C57BL/6 background for at least 9 generations. β-arrestin 2-/- (C57BL/6 background) mice were provided by Robert Lefkowitz (Duke University Medical Center). All mice were bred and maintained in a pathogen free environment and all animal procedures were in accordance with the guidelines on the use and care of laboratory animals set by the national institutes of health and approved by the Institutional Animal Care and Use Committee at the University of California, Riverside.

Parasites

T. gondii Prugniaud and RH strain tachyzoites were maintained *in vitro* in Human Foreskin Fibroblasts (HFF) grown in complete DMEM (90% DMEM, 10% fetal bovine serum (FBS), 1% Penicillin/Streptomycin). After infecting HFFs, parasites were grown in D10 media (70% DMEM, 20% M199, 10% fetal bovine serum, 5% penicillin/ streptomycin, 5% gentamycin). Parasite strains engineered to express ovalbumin grown under selection in the presence of chloramphenicol. Parasites

were purified from culture by passing through a 23-gauge needle followed by passage through a 5μm filter. Parasite suspension was centrifuged at 3000rpm for 10 minutes, resuspended in 1 mL PBS, and counted. Parasites were diluted to 50,000 parasites per mL and 10,000 parasites were injected interperitoneally into each mouse. Me49 and Me49-RFP strains were maintained in infected Swiss Webster and CBA/CaJ mice. To isolate cysts for infection, brains from infected mice were placed in 3mL sterile 1xPBS and passed 5 times through an 18.5-gauge, 20.5-gauge, then a 22.5-gauge needle. The number of cysts in a 30mL aliquot was counted microscopically then brain suspensions were adjusted to 100 cysts/mL and each mouse was infected with 15-20 cysts interperitoneally. All reagents and experiments involving *T. gondii* were conducted under Biosafety Level 2 (BSL2) conditions in compliance with approved Biological Use Authorized protocols.

Systemic Cytokine Measurement

Blood was collected from the tail vein or by cardiac puncture at the time of sacrifice from naïve animals or at 7 days post infection with *T. gondii* and centrifuged at 14,000rpm for 10 minutes at 4^{o}C. Serum was collected and stored at -80^{o}C until IFNγ, IL-12, IL-10, IL-6, TNFα, and CCL2 levels could be measured using the Cytometric Bead Array (BD) according to the manufacturer's instructions.

Cytospins

Peritoneal exudate cells (PECs) were harvested by injecting 3mL of sterile 1xPBS into the peritoneal cavity, agitating the abdomen gently, and withdrawing the PBS with the syringe. 100mL of the cell suspension was spun onto a glass microscope slide with a cytocentrifuge.

Adoptive Transfer

Naïve T cells were purified from the lymph nodes and spleens of WT and β-arrestin 2-/- using T cell enrichment columns (R&D Systems). The enriched suspension was determined to be approximately 90% T cells as assessed by flow cytometry. T cells were resuspended in sterile 1xPBS and 2-5x10^6 cells in 200mL were injected intravenously into each mouse. OVA specific T cells were expanded in culture as previously described (87), resuspended in sterile 1xPBS and 5x10^6 cells in 200mL were injected intravenously into each mouse.

Preparation of Single Cell Suspensions

Mice were sacrificed via asphyxiation with CO2 and perfused with ice cold, sterile 1xPBS. Suspensions of splenocytes and lymphocytes were prepared by passing tissue through a 40mm cell strainer and washing with complete RPMI. Suspensions were centrifuged for 10 minutes at 1200rpm at 4^{o}C. Red blood cells were lysed in 0.86% ammonium chloride solution and washed away with complete RPMI. Brain mononuclear cells (BMNCs) were prepared by mincing

brain tissue with a razor blade and passed 3-5 times through and 18-gauge needle. The suspension was incubated with collagenase/dispase (10mL at 10mg/mL, Roche) for 45 minutes at 37^{o}C and then with DNAse (300mL at 10mg/mL, Sigma) for a further 45 minutes at 37^{o}C. The cell suspension was then passed through a 70mm strainer, washed with complete RPMI and centrifuged at 1200rpm for 10 min at 4^{o}C. The pellet was then resuspended in 60% percoll (GE Healthcare) in complete RPMI and overlaid with 30% percoll in 1xPBS. The percoll gradient was centrifuged at 200rpm for 25 minutes at room temperature. After centrifugation, BMNCs were recovered from the percoll interface and washed with complete RPMI prior to counting, staining and further analysis.

Restimulation Assay

Single cell suspensions of splenocytes and/or BMNCs were diluted to 1-4 x 10^{6} cells/mL. Cells from biological replicates were added in triplicate to a round bottom 96-well plate in 100mL of complete RPMI. Cultures were then treated with media alone, stimulated with PMA (50ng/mL) and Ionomycin (1mg/mL), or stimulated with soluble Toxoplasma antigen (sTAg) for 6 hours at 37^{o}C and 5% CO_2. Brefeldin A (10mg/mL) was added 2 hours prior to harvest to block secretion of cytokines. STAg was prepared from RH tachyzoites as previously described (88).

Transwell Assay

BMNCs and splenocyte suspensions were prepared, diluted to $5x10^6$ cells per mL of assay medium (RPMI with 0.5% bovine serum albumin and 25mM HEPES) and 100mL of each suspension was applied to the transwell insert (5.0mm pore size, Costar). Differing concentrations (50-2000ng/mL) of chemokines (CCL21 or CXCL10, R&D Systems) were prepared in assay medium and 600mL of each concentration was applied to the lower chamber. For the input count, 500mL of assay medium was incubated in an empty well with 100mL of each cell suspension. After a 90 minute incubation, cells were collected from the lower chamber for counting and phenotyping by flow cytometry. Cell numbers were quantified using 5000 count beads per sample (20mm Fluoresbrite (FITC) microspheres, Polysciences).

Flow Cytometry

After counting, $1x10^6$ cells from each sample was transferred to a FACS tube (BD Falcon) and centrifuged at 1200rpm for 5 minutes at 4^oC. Cells were washed in FACS buffer (1xPBS with 1%BSA and 0.01% EDTA) then incubated with a saturating solution of Fc block (eBioscience) for 10 minutes on ice. Samples stained with MHC class I dextramer (Immudex) or class II tetramer (NIH tetramer core facility) were incubated at room temperature for 30 minutes followed by surface staining with a mixture of conjugated antibodies for 30 minutes on ice. Cells were washed and resuspended in 300uL FACS buffer and

analyzed using the BD FACSCanto™ II flow cytometer and Flowjo 8.0. For intracellular staining, cells were first stained surface markers and fixed with 4% paraformaldehyde overnight. Cells were permeabilized with 0.3% saponin (in FACS buffer) and stained with conjugated antibodies raised against intracellular targets for 30 minutes on ice. Cells were then washed in permeabilization buffer and resuspended in FACS buffer.

Real Time PCR

Parasite burden in mice was measured by amplifying the *T. gondii* specific genes B1, SAG1, SAG4 or MAG1. CCL19, CCL21, CXCL10, GAPDH and HPRT transcript was amplified from RNA isolated from cultured astrocytes or whole organs with TRIzol reagent (Invitrogen) according to the manufacturer's instructions. Quantified results represent the fold induction of the target gene at different days post infection or stimulus compared to naïve samples. Primer sequences and protocols have been previously described (27,89).

Immunohistochemistry

Following excision, tissues were flash frozen in isopentane then put into standard sized cryomolds and embedded in Optimal Cutting Temperature (OCT) solution (Tissue-Tek, Torrance, CA) on dry ice and stored at -80^{o}C. Serial sections, 10-25mm thick, were prepared on a standard cryostat (Leica CM1850, Simi Valley, CA) then fixed with 75% acetone/25% ethanol and blocked with 2-5% donkey

serum prior to incubation with purified primary antibodies. Antibodies for SPARC (R&D Systems), CCL21 (Peptrotech), Lamanin (Cedar Lane) and CD4 or CD8 (Ebioscience), or GFAP (Life Technologies, Grand Island, NY) were incubated with blocked tissue samples for 3 hours at room temperature and/or overnight at 4^{o}C followed by appropriate secondary antibodies conjugated to Alexa 488, 568, or 647 at a 1:500 dilution (Life Technologies, Grand Island, NY). Samples were mounted with Prolong Gold with DAPI for nuclear staining. Samples were imaged on a Leica SP5 confocal microscope or a Leica epifluorescent microscope (Leica Optics, Germany). Images were analyzed using Volocity 6.1 (Perkin Elmer, Waltham, MA).

Multiphoton Microscopy

Live tissue was excised from euthanized mice, placed in a 35mm glass bottom dish in cRPMI (RPMI plus 10% fetal-calf serum, 1% pen/strep, 1% glutamine, 1% HEPES, 1% nonessential amino acids, and 0.1% β-mercaptoethanol) and maintained at 37^{o}C with 20% O_2 and 5% CO_2. Imaging was performed on a Zeiss LSM 710 NLO or a Nikon FN1. Samples were excited at 920nm with a Ti:Sapphire laser (Coherent Chameleon) and emitted light was detected with non-descanned detectors. Volocity software was used to measure SHG volume and to quantify cell movement.

Gel Filtration

Recombinant proteins (SPARC, CCL21, CCL19, CXCL10, R&D Systems) were resuspended in PBS according to the manufacturer's instructions. 4mg of each protein combination was mixed in a 1:1 ratio and incubated at 4^{o}C for two hours. The mixture was then loaded onto a column of Sephadex G-50 (Sigma) and eluted in 2mL fractions. Fractions that contained protein were pooled and concentrated with Amicon filters (Millipore, Billerica, MA). Concentrated eluate was mixed with Laemmli buffer and subjected to SDS-PAGE on 10% Tris-HCL gels (Biorad, Hercules, CA) followed by western blot onto nitrocellulose membranes on a semi-dry blotter (Biorad, Hercules, CA). Membranes were blocked with 5% nonfat dry milk then probed with anti-SPARC (R&D Systems), anti-CCL21 (Peprotech), anti-CCL19 (R&D Systems) or anti-CXCL10 (R&D Systems) antibodies. Blots were imaged using an Odessey Infrared Imaging system (Li-COR Biosciences).

Thermophoresis

Microscale thermophoresis analyses were carried out with a Monolith NT.115 instrument (NanoTemper, Munich, Germany). Recombinant murine SPARC was covalently linked to the fluorescent label, NT-495, by NHS coupling according to NanoTemper's instructions. Increasing concentrations of unlabeled CCL21, CCL19, and CXCL10 in Ca^{+2}-MST buffer (50mM Tris, pH7.4, 150mM NaCl, 2mM $CaCl_2$, 0.05% Tween 20) were titrated against 4.5nM of Labeled SPARC. Standard treated capillaries (K002 Monolith NT.115) were loaded with the

samples, and all measurements were performed three times at room temperature. Data evaluation was performed with the Monolith software (NanoTemper, Munich, Germany) and Prism 6 (GraphPad, La Jolla, CA).

T cell Depletion

Mice were infected with the Pru strain of *T. gondii*. On day 28 post infection, the mice were given three intravenous injections every five days of 500mg of anti-CD4 (clone GK1.5, Bio X cell, West Lebanon, NH), anti-CD8 (clone 2.43, Bio X cell, West Lebanon, NH), or IgG control antibodies (Bio X cell, West Lebanon, NH). On the fifth day after the last injection, the mice were sacrificed and their brains, spleens, and lymph nodes were excised to confirm T cell depletion by flow cytometry and to measure parasite burden and transcripts of SPARC, CCL21, CCL19, and CXCL10.

Chemotaxis Assays

Collagen IV coated m-Slide Chemotaxis slides (ibidi, Madison, WI) are were seeded with WT-dsRed CD8+ T cells (500,000 cells/mL) suspended in 2.4 mg/mL Matrigel Matrix (Corning, Tewksbury, MA) according to the manufacturer's instructions. Then, slide reservoirs were filled with assay media on either side, CCL21 on either side, or with media on one side and CCL21 on the other to establish a gradient. Movies were filmed for 20 min at 37^{o}C, 5% CO_2

and 20% O_2. Cell behavior was analyzed with Volocity 5.0 or 6.1 (Perkin-Elmer, Waltham, MA).

Statistics

Survival data was analyzed using the log-rank test. All other data was analyzed with an unpaired, two-tailed student's t test (for Gaussian populations), a Mann-Whitney test (for non-Gaussian populations), or an ANOVA test with a 95% confidence interval (Prism, GraphPad Inc., La Jolla, CA). All data are displayed as means ± SEM.

1.6 FIGURES AND LEGENDS

Figure 1.1. Life Cycle of *Toxoplasma gondii.* An infected cat sheds oocysts in its feces, contaminating the environment (1). Secondary hosts such as birds, mice (2), or livestock (3) become infected by drinking contaminated water or grazing on contaminated land. Once consumed, oocysts convert to tachyzoites and disseminate throughout the host's body. In response, a pronounced Th1 immune response is ellicited that clears the parasite from most tissues. To protect themselves, tachyzoites convert to bradyzoites that form tissue cysts, which can be found in muscle but are predominantly found in the brain (4). Cats then become infected by eating prey that harbor tissue cysts (5). Like other warm blooded animals, humans may become infected by consuming food or water contaminated with cat feces (6) or eating undercooked meat from infected animals (7). Humans may also become infected through organ transplantation or blood transfusion and from mother to fetus (8).

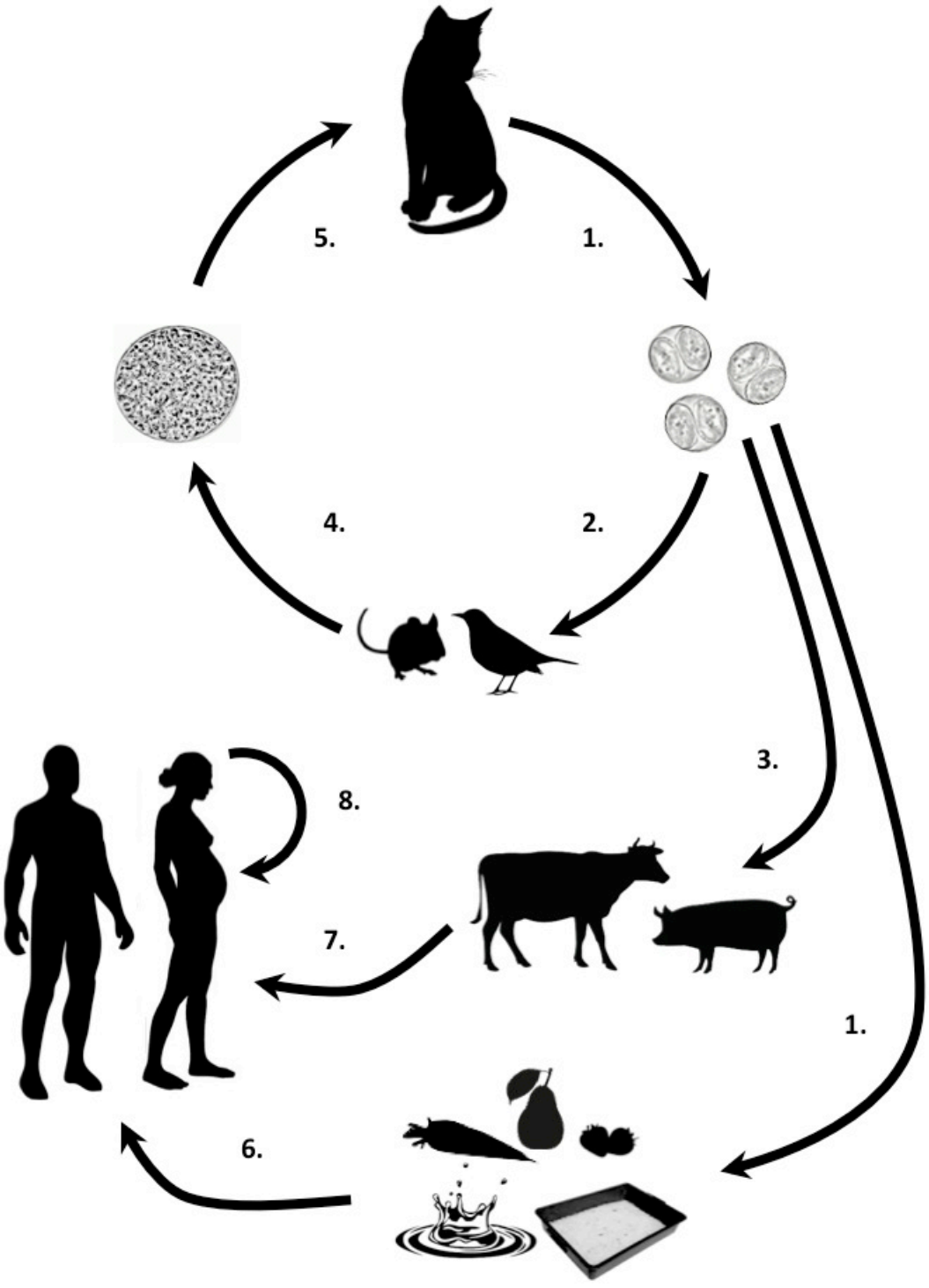
1.
2.
3.
4.
5.
6.
7.
8.
1.

Figure 1.2. Role of CCL21 in response to parasitic infection. (A) Skin resident Langerhans cells (LCs, white) and dermal dendritic cells (DCs, teal) scavenge antigen at the exposure site. LCs are slow to move in the epidermis, but extend their dendrites to scavange antigen (black) from their environment. In contrast, dermal DCs constantly patrol their environment and upon antigen uptake, they upregulate CCR7 and migrate to the lymphatic vessels (LV) following gradients of CCL21 (red) produced by the lymphatic endothelium (green). (B) Once DCs reach the lymph node, they transverse the walls of the high endothelial vessels (HEVs) and enter the parenchyma of the lymph node (1). There, they migrate randomly along a network of fibroblastic reticular cells (light green) coated with CCL21. The migration elicited by CCL21 enables DCs to encounter and present antigen to naïve, CCR7+ T cells and initiate an adaptive response (2). (C) Both neurons (light blue) and astrocytes (green) produce CCL21 in response to injury or insult. CCL21 is necessary to recruit CD4+ T cells into the brain from the perivascular spaces to keep parasite replication under control. CCL21 co-localizes with astrocytic and neuronal markers, appearing as long strands to which migrating T cells associate.

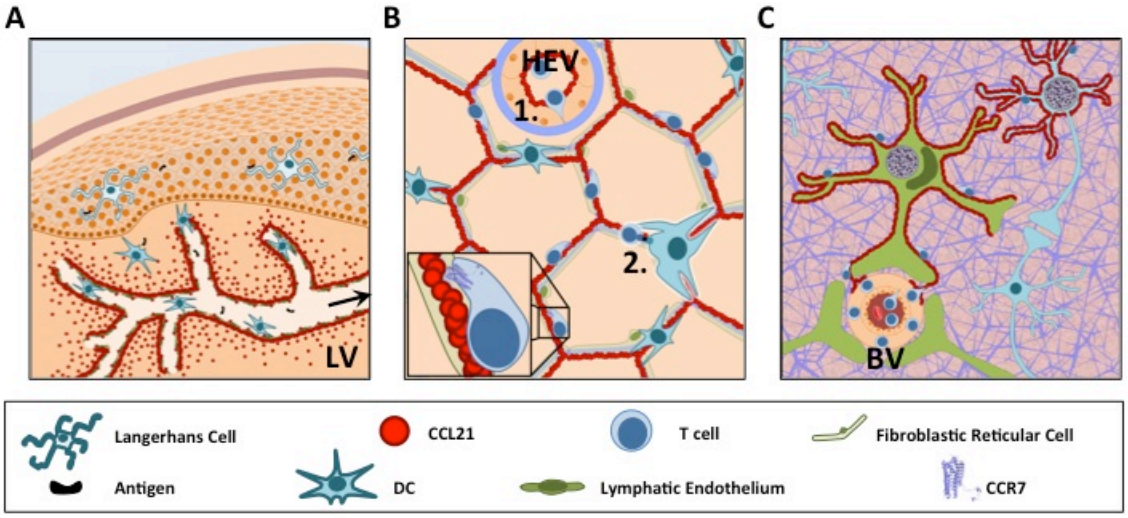
A
B
C
HEV
1.
2.
LV
BV
Langerhans Cell
Antigen
CCL21
DC
T cell
Lymphatic Endothelium
Fibroblastic Reticular Cell
CCR7

Figure 1.3. β-arrestin mediated chemokine receptor endocytosis. According to the model describing receptor turnover, β-arrestins bind to phosphorylated receptors occupied by chemokine. This promotes the clathrin-dependent internalization of the receptor. Once internalized, the occupied receptor can be targeted for lysozomal degredation, or the ligand can be degraded and the receptor can traffic back to the cell surface.

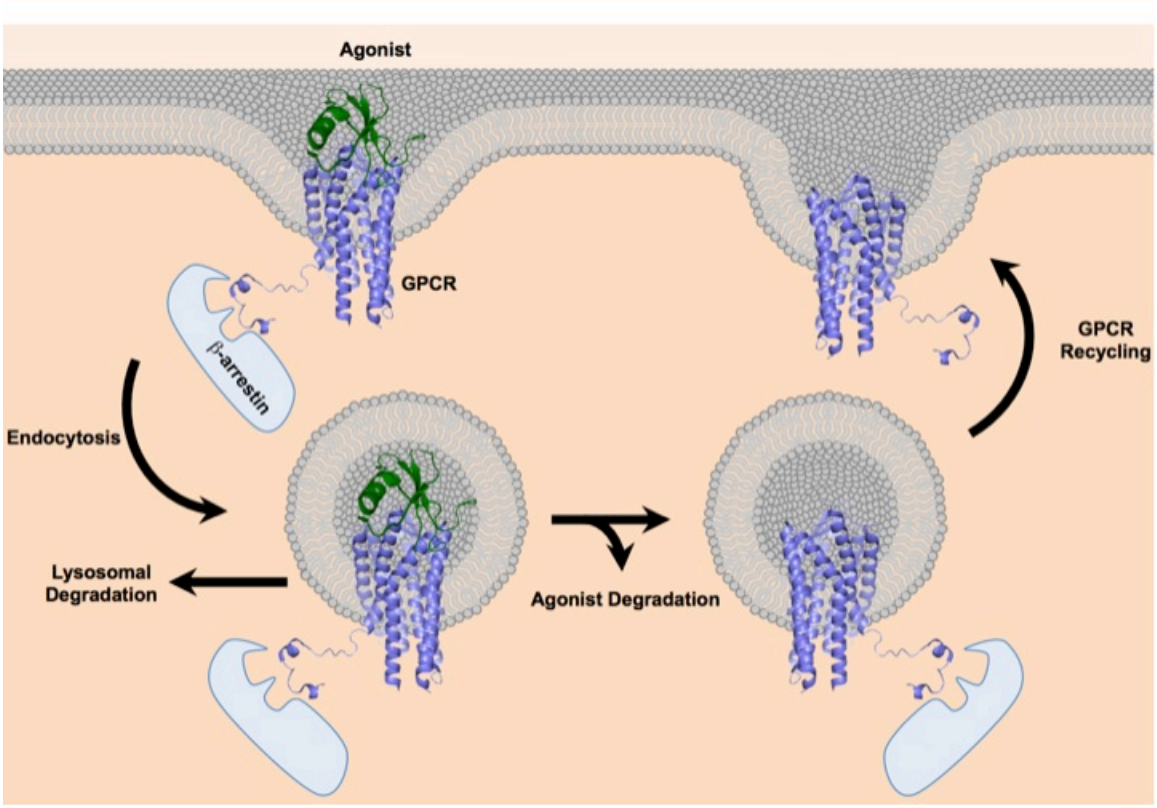
Agonist
GPCR
β-arrestin
Endocytosis
Lysosomal Degradation
Agonist Degradation
GPCR Recycling

Figure 1.4. β-arrestin and actin remodeling. β-arrestins are responsible for keeping a variety of signaling molecules at the leading edge of a migrating cell. To facilitate actin remodeling, β-arrestins bind and inactivate LIM kinase (LIMK) and scaffold cofilin with its activating phosphatase. They can also regulate the activity of Ral, which is important for membrane protrusion. It is thought that β-arrestins act to provide spactiotemporal control of these molecules at the leading edge to promote precise formation of lamellipodia toward a chemokine gradient.

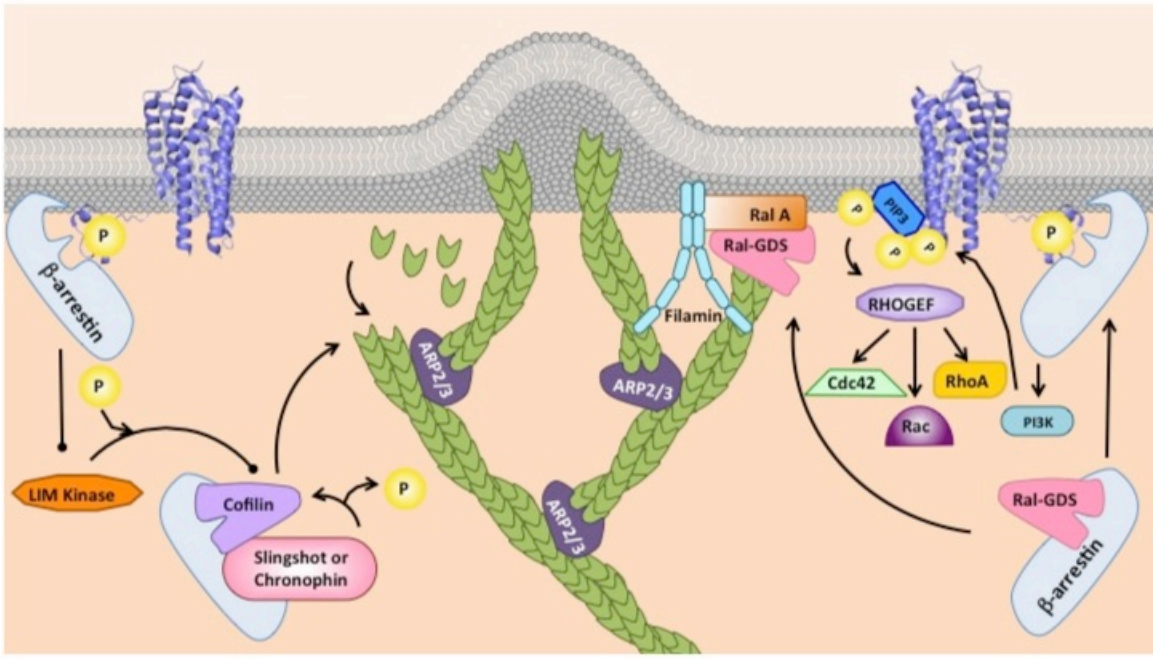
β-arrestin
P
P
LIM Kinase
Cofilin
P
Slingshot or
Chronophin
ARP2/3
ARP2/3
ARP2/3
Ral A
Ral-GDS
Filamin
PIP3
RHOGEF
Cdc42
RhoA
Rac
PI3K
P
Ral-GDS
β-arrestin

Figure 1.5. The many functions of SPARC. (A) Integrins can aggregate on the surface of the cell and bind to matrix molecules like fibronectin to facilitate focal adhesion. (B) SPARC can block focal adhesion by binding to fibronectin and preventing integrins from binding to the matrix. (C) As a regulator matrix assembly, SPARC signaling can directly impact cell migration, proliferation, and survival. (D) SPARC chaperones collagen remodeling by binding to collagen in the matrix. Then stablin-1, the only known receptor for SPARC, takes up both SPARC and the collagen fragment to which it is bound. In this manner, collagen is degraded and stablin-1 is recycles to the cell surface.

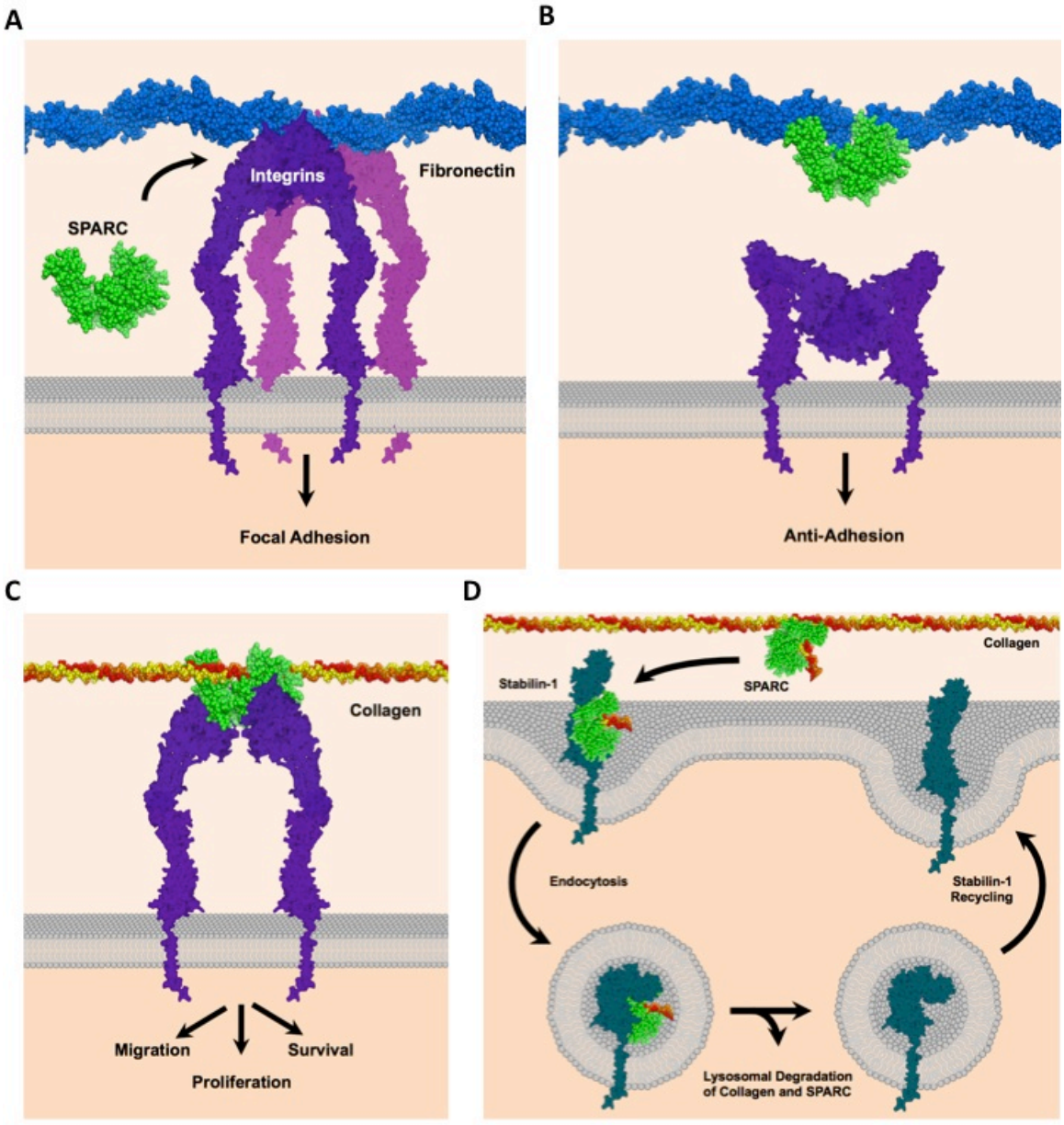
A
Integrins
Fibronectin
SPARC
Focal Adhesion
B
Anti-Adhesion
C
Collagen
Migration
Survival
Proliferation
D
Collagen
Stabilin-1
SPARC
Endocytosis
Stabilin-1
Recycling
Lysosomal Degradation
of Collagen and SPARC

1.7 References

1. Nicolle, C. a. M., L (1908) Sur une infection a corps de Leishman (ou organismes voisons) du gondi. *C R Acad Sci* **147**, 736

2. Splendore, A. (1908) Un nuovo protozoa parassita deconigli incontrato nelle lesioni anatomiche d'une malattia che ricorda in molti punti il Kala-azar dell'uoma. *Rev Soc Sci Sao Paulo* **3**, 109-112

3. Dabritz, H. A., Miller, M. A., Atwill, E. R., Gardner, I. A., Leutenegger, C. M., Melli, A. C., and Conrad, P. A. (2007) Detection of Toxoplasma gondii-like oocysts in cat feces and estimates of the environmental oocyst burden. *J Am Vet Med Assoc* **231**, 1676-1684

4. Nagasawa, T., Hirota, S., Tachibana, K., Takakura, N., Nishikawa, S., Kitamura, Y., Yoshida, N., Kikutani, H., and Kishimoto, T. (1996) Defects of B-cell lymphopoiesis and bone-marrow myelopoiesis in mice lacking the CXC chemokine PBSF/SDF-1. *Nature* **382**, 635-638

5. Tachibana, K., Hirota, S., Iizasa, H., Yoshida, H., Kawabata, K., Kataoka, Y., Kitamura, Y., Matsushima, K., Yoshida, N., Nishikawa, S., Kishimoto, T., and Nagasawa, T. (1998) The chemokine receptor CXCR4 is essential for vascularization of the gastrointestinal tract. *Nature* **393**, 591-594

6. Zou, Y. R., Kottmann, A. H., Kuroda, M., Taniuchi, I., and Littman, D. R. (1998) Function of the chemokine receptor CXCR4 in haematopoiesis and in cerebellar development. *Nature* **393**, 595-599

7. Chong, S. W., Nguyet, L. M., Jiang, Y. J., and Korzh, V. (2007) The chemokine Sdf-1 and its receptor Cxcr4 are required for formation of muscle in zebrafish. *BMC Dev Biol* **7**, 54

8. Vasyutina, E., Stebler, J., Brand-Saberi, B., Schulz, S., Raz, E., and Birchmeier, C. (2005) CXCR4 and Gab1 cooperate to control the development of migrating muscle progenitor cells. *Genes Dev* **19**, 2187-2198

9. Knaut, H., Blader, P., Strahle, U., and Schier, A. F. (2005) Assembly of trigeminal sensory ganglia by chemokine signaling. *Neuron* **47**, 653-666

10. Liu, C., Ueno, T., Kuse, S., Saito, F., Nitta, T., Piali, L., Nakano, H., Kakiuchi, T., Lipp, M., Hollander, G. A., and Takahama, Y. (2005) The role of CCL21 in recruitment of T-precursor cells to fetal thymi. *Blood* **105**, 31-39

11. Misslitz, A., Pabst, O., Hintzen, G., Ohl, L., Kremmer, E., Petrie, H. T., and Forster, R. (2004) Thymic T cell development and progenitor localization depend on CCR7. *J Exp Med* **200**, 481-491

12. Bromley, S. K., Thomas, S. Y., and Luster, A. D. (2005) Chemokine receptor CCR7 guides T cell exit from peripheral tissues and entry into afferent lymphatics. *Nat Immunol* **6**, 895-901

13. Ploix, C., Lo, D., and Carson, M. J. (2001) A ligand for the chemokine receptor CCR7 can influence the homeostatic proliferation of CD4 T cells and progression of autoimmunity. *J Immunol* **167**, 6724-6730

14. Okada, T., Miller, M. J., Parker, I., Krummel, M. F., Neighbors, M., Hartley, S. B., O'Garra, A., Cahalan, M. D., and Cyster, J. G. (2005) Antigen-engaged B cells undergo chemotaxis toward the T zone and form motile conjugates with helper T cells. *PLoS Biol* **3**, e150

15. Luther, S. A., Tang, H. L., Hyman, P. L., Farr, A. G., and Cyster, J. G. (2000) Coexpression of the chemokines ELC and SLC by T zone stromal cells and deletion of the ELC gene in the plt/plt mouse. *Proc Natl Acad Sci U S A* **97**, 12694-12699

16. Reif, K., Ekland, E. H., Ohl, L., Nakano, H., Lipp, M., Forster, R., and Cyster, J. G. (2002) Balanced responsiveness to chemoattractants from adjacent zones determines B-cell position. *Nature* **416**, 94-99

17. Barragan, A., and Sibley, L. D. (2003) Migration of Toxoplasma gondii across biological barriers. *Trends Microbiol* **11**, 426-430

18. Konradt C, U. N., Christian DA, Delong J, Harms-Pritchard G, Herz J, Bzik DJ,Koshy AA, McGavern DB, Lodoen MB, Hunter CA. (2015) Endothelial cells as a replicative niche for pathway entry to the CNS. *In press, Nature Microbiology*

19. Courret, N., Darche, S., Sonigo, P., Milon, G., Buzoni-Gatel, D., and Tardieux, I. (2006) CD11c- and CD11b-expressing mouse leukocytes transport single Toxoplasma gondii tachyzoites to the brain. *Blood* **107**, 309-316

20. Harker, K. S., Ueno, N., Wang, T., Bonhomme, C., Liu, W., and Lodoen, M. B. (2013) Toxoplasma gondii modulates the dynamics of human monocyte adhesion to vascular endothelium under fluidic shear stress. *J Leukoc Biol* **93**, 789-800

21. Sumyuen, M. H., Garin, Y. J., and Derouin, F. (1995) Early kinetics of Toxoplasma gondii infection in mice infected orally with cysts of an avirulent strain. *J Parasitol* **81**, 327-329

22. Wilson, E. H., and Hunter, C. A. (2004) The role of astrocytes in the immunopathogenesis of toxoplasmic encephalitis. *Int J Parasitol* **34**, 543-548

23. Suzuki, Y., and Remington, J. S. (1988) Dual regulation of resistance against Toxoplasma gondii infection by Lyt-2+ and Lyt-1+, L3T4+ T cells in mice. *J Immunol* **140**, 3943-3946

24. Gazzinelli, R., Xu, Y., Hieny, S., Cheever, A., and Sher, A. (1992) Simultaneous depletion of CD4+ and CD8+ T lymphocytes is required to reactivate chronic infection with Toxoplasma gondii. *J Immunol* **149**, 175-180

25. Casciotti, L., Ely, K. H., Williams, M. E., and Khan, I. A. (2002) CD8(+)-T-cell immunity against Toxoplasma gondii can be induced but not maintained in mice lacking conventional CD4(+) T cells. *Infect Immun* **70**, 434-443

26. Suzuki, Y., Orellana, M. A., Schreiber, R. D., and Remington, J. S. (1988) Interferon-gamma: the major mediator of resistance against Toxoplasma gondii. *Science* **240**, 516-518

27. Noor, S., Habashy, A. S., Nance, J. P., Clark, R. T., Nemati, K., Carson, M. J., and Wilson, E. H. (2010) CCR7-dependent immunity during acute Toxoplasma gondii infection. *Infect Immun* **78**, 2257-2263

28. Wilson, E. H., Harris, T. H., Mrass, P., John, B., Tait, E. D., Wu, G. F., Pepper, M., Wherry, E. J., Dzierzinski, F., Roos, D., Haydon, P. G., Laufer, T. M., Weninger, W., and Hunter, C. A. (2009) Behavior of parasite-specific effector CD8+ T cells in the brain and visualization of a kinesis-associated system of reticular fibers. *Immunity* **30**, 300-311

29. Ploix, C. C., Noor, S., Crane, J., Masek, K., Carter, W., Lo, D. D., Wilson, E. H., and Carson, M. J. (2010) CNS-derived CCL21 is both sufficient to drive homeostatic CD4+ T cell proliferation and necessary for efficient CD4+ T cell migration into the CNS parenchyma following Toxoplasma gondii infection. *Brain Behav Immun* **25**, 883-896

30. Harris TH, B. E., Christian DA, Konradt C, Tait Wojno ED, Norose K, Wilson EH, John B, Weninger W, Luster AD, Liu AJ, Hunter CA. (2012)

Generalized Lévy walks and the role of chemokines in migration of effector CD8+ T cells. *Nature* **486**, 545-548

31. Wilson, E. H., Weninger, W., and Hunter, C. A. (2010) Trafficking of immune cells in the central nervous system. *J Clin Invest* **120**, 1368-1379

32. Banchereau, J., and Steinman, R. M. (1998) Dendritic cells and the control of immunity. *Nature* **392**, 245-252

33. Sallusto, F., Palermo, B., Lenig, D., Miettinen, M., Matikainen, S., Julkunen, I., Forster, R., Burgstahler, R., Lipp, M., and Lanzavecchia, A. (1999) Distinct patterns and kinetics of chemokine production regulate dendritic cell function. *Eur J Immunol* **29**, 1617-1625

34. Sakai, N., Wada, T., Yokoyama, H., Lipp, M., Ueha, S., Matsushima, K., and Kaneko, S. (2006) Secondary lymphoid tissue chemokine (SLC/CCL21)/CCR7 signaling regulates fibrocytes in renal fibrosis. *Proc Natl Acad Sci U S A* **103**, 14098-14103

35. Wald, O., Weiss, I. D., Galun, E., and Peled, A. (2007) Chemokines in hepatitis C virus infection: pathogenesis, prognosis and therapeutics. *Cytokine* **39**, 50-62

36. Kahnert, A., Hopken, U. E., Stein, M., Bandermann, S., Lipp, M., and Kaufmann, S. H. (2007) Mycobacterium tuberculosis triggers formation of lymphoid structure in murine lungs. *J Infect Dis* **195**, 46-54

37. Tateyama, M., Fujihara, K., Misu, T., and Itoyama, Y. (2009) CCR7+ myeloid dendritic cells together with CCR7+ T cells and CCR7+ macrophages invade CCL19+ nonnecrotic muscle fibers in inclusion body myositis. *J Neurol Sci* **279**, 47-52

38. Sallusto, F., Lenig, D., Forster, R., Lipp, M., and Lanzavecchia, A. (1999) Two subsets of memory T lymphocytes with distinct homing potentials and effector functions. *Nature* **401**, 708-712

39. Scandella, E., Fink, K., Junt, T., Senn, B. M., Lattmann, E., Forster, R., Hengartner, H., and Ludewig, B. (2007) Dendritic cell-independent B cell activation during acute virus infection: a role for early CCR7-driven B-T helper cell collaboration. *J Immunol* **178**, 1468-1476

40. Hardtke, S., Ohl, L., and Forster, R. (2005) Balanced expression of CXCR5 and CCR7 on follicular T helper cells determines their transient positioning to lymph node follicles and is essential for efficient B-cell help. *Blood* **106**, 1924-1931

41. Zidar, D. A., Violin, J. D., Whalen, E. J., and Lefkowitz, R. J. (2009) Selective engagement of G protein coupled receptor kinases (GRKs) encodes distinct functions of biased ligands. *Proc Natl Acad Sci U S A* **106**, 9649-9654

42. Gunn, M. D., Tangemann, K., Tam, C., Cyster, J. G., Rosen, S. D., and Williams, L. T. (1998) A chemokine expressed in lymphoid high endothelial venules promotes the adhesion and chemotaxis of naive T lymphocytes. *Proc Natl Acad Sci U S A* **95**, 258-263

43. Yoshida, R., Nagira, M., Kitaura, M., Imagawa, N., Imai, T., and Yoshie, O. (1998) Secondary lymphoid-tissue chemokine is a functional ligand for the CC chemokine receptor CCR7. *J Biol Chem* **273**, 7118-7122

44. Handel, T. M., Johnson, Z., Crown, S. E., Lau, E. K., and Proudfoot, A. E. (2005) Regulation of protein function by glycosaminoglycans--as exemplified by chemokines. *Annu Rev Biochem* **74**, 385-410

45. Schumann, K., Lammermann, T., Bruckner, M., Legler, D. F., Polleux, J., Spatz, J. P., Schuler, G., Forster, R., Lutz, M. B., Sorokin, L., and Sixt, M. (2010) Immobilized chemokine fields and soluble chemokine gradients cooperatively shape migration patterns of dendritic cells. *Immunity* **32**, 703-713

46. Weber, M., Hauschild, R., Schwarz, J., Moussion, C., de Vries, I., Legler, D. F., Luther, S. A., Bollenbach, T., and Sixt, M. (2013) Interstitial dendritic cell guidance by haptotactic chemokine gradients. *Science* **339**, 328-332

47. Forster, R., Davalos-Misslitz, A. C., and Rot, A. (2008) CCR7 and its ligands: balancing immunity and tolerance. *Nat Rev Immunol* **8**, 362-371

48. Yanagawa, Y., and Onoe, K. (2002) CCL19 induces rapid dendritic extension of murine dendritic cells. *Blood* **100**, 1948-1956

49. Yanagawa, Y., and Onoe, K. (2003) CCR7 ligands induce rapid endocytosis in mature dendritic cells with concomitant up-regulation of Cdc42 and Rac activities. *Blood* **101**, 4923-4929

50. Lefkowitz, R. J., and Whalen, E. J. (2004) beta-arrestins: traffic cops of cell signaling. *Curr Opin Cell Biol* **16**, 162-168

51. Shenoy, S. K., McDonald, P. H., Kohout, T. A., and Lefkowitz, R. J. (2001) Regulation of receptor fate by ubiquitination of activated beta 2-adrenergic receptor and beta-arrestin. *Science* **294**, 1307-1313

52. Zhang, J., Ferguson, S. S., Barak, L. S., Menard, L., and Caron, M. G. (1996) Dynamin and beta-arrestin reveal distinct mechanisms for G protein-coupled receptor internalization. *J Biol Chem* **271**, 18302-18305

53. Min, J., and Defea, K. (2011) beta-arrestin-dependent actin reorganization: bringing the right players together at the leading edge. *Mol Pharmacol* **80**, 760-768

54. Zoudilova, M., Min, J., Richards, H. L., Carter, D., Huang, T., and DeFea, K. A. (2010) beta-Arrestins scaffold cofilin with chronophin to direct localized actin filament severing and membrane protrusions downstream of protease-activated receptor-2. *J Biol Chem* **285**, 14318-14329

55. Xiao, K., Sun, J., Kim, J., Rajagopal, S., Zhai, B., Villen, J., Haas, W., Kovacs, J. J., Shukla, A. K., Hara, M. R., Hernandez, M., Lachmann, A., Zhao, S., Lin, Y., Cheng, Y., Mizuno, K., Ma'ayan, A., Gygi, S. P., and Lefkowitz, R. J. (2010) Global phosphorylation analysis of beta-arrestin-mediated signaling downstream of a seven transmembrane receptor (7TMR). *Proc Natl Acad Sci U S A* **107**, 15299-15304

56. DeFea, K. A. (2010) Beta-arrestins as regulators of signal termination and transduction: how do they determine what to scaffold? *Cell Signal* **23**, 621-629

57. McGovern, K. W., and DeFea, K. A. Molecular mechanisms underlying beta-arrestin-dependent chemotaxis and actin-cytoskeletal reorganization. *Handb Exp Pharmacol* **219**, 341-359

58. DeFea, K. A. (2007) Stop that cell! Beta-arrestin-dependent chemotaxis: a tale of localized actin assembly and receptor desensitization. *Annu Rev Physiol* **69**, 535-560

59. Sullivan, S. K., McGrath, D. A., Grigoriadis, D., and Bacon, K. B. (1999) Pharmacological and signaling analysis of human chemokine receptor CCR-7 stably expressed in HEK-293 cells: high-affinity binding of recombinant ligands MIP-3beta and SLC stimulates multiple signaling cascades. *Biochem Biophys Res Commun* **263**, 685-690

60. Ott, T. R., Pahuja, A., Nickolls, S. A., Alleva, D. G., and Struthers, R. S. (2004) Identification of CC chemokine receptor 7 residues important for receptor activation. *J Biol Chem* **279**, 42383-42392

61. Campbell, J. J., Bowman, E. P., Murphy, K., Youngman, K. R., Siani, M. A., Thompson, D. A., Wu, L., Zlotnik, A., and Butcher, E. C. (1998) 6-C-kine (SLC), a lymphocyte adhesion-triggering chemokine expressed by

high endothelium, is an agonist for the MIP-3beta receptor CCR7. *J Cell Biol* **141**, 1053-1059

62. Bardi, G., Lipp, M., Baggiolini, M., and Loetscher, P. (2001) The T cell chemokine receptor CCR7 is internalized on stimulation with ELC, but not with SLC. *Eur J Immunol* **31**, 3291-3297

63. Kohout, T. A., Nicholas, S. L., Perry, S. J., Reinhart, G., Junger, S., and Struthers, R. S. (2004) Differential desensitization, receptor phosphorylation, beta-arrestin recruitment, and ERK1/2 activation by the two endogenous ligands for the CC chemokine receptor 7. *J Biol Chem* **279**, 23214-23222

64. Byers, M. A., Calloway, P. A., Shannon, L., Cunningham, H. D., Smith, S., Li, F., Fassold, B. C., and Vines, C. M. (2008) Arrestin 3 mediates endocytosis of CCR7 following ligation of CCL19 but not CCL21. *J Immunol* **181**, 4723-4732

65. Tsang, K. Y., Cheung, M. C., Chan, D., and Cheah, K. S. (2009) The developmental roles of the extracellular matrix: beyond structure to regulation. *Cell Tissue Res* **339**, 93-110

66. Hohenester, E., Sasaki, T., Giudici, C., Farndale, R. W., and Bachinger, H. P. (2008) Structural basis of sequence-specific collagen recognition by SPARC. *Proc Natl Acad Sci U S A* **105**, 18273-18277

67. Hynes, R. O. (2009) The extracellular matrix: not just pretty fibrils. *Science* **326**, 1216-1219

68. Houghton, A. M., Quintero, P. A., Perkins, D. L., Kobayashi, D. K., Kelley, D. G., Marconcini, L. A., Mecham, R. P., Senior, R. M., and Shapiro, S. D. (2006) Elastin fragments drive disease progression in a murine model of emphysema. *J Clin Invest* **116**, 753-759

69. Hunninghake, G. W., Davidson, J. M., Rennard, S., Szapiel, S., Gadek, J. E., and Crystal, R. G. (1981) Elastin fragments attract macrophage precursors to diseased sites in pulmonary emphysema. *Science* **212**, 925-927

70. Senior, R. M., Griffin, G. L., and Mecham, R. P. (1980) Chemotactic activity of elastin-derived peptides. *J Clin Invest* **66**, 859-862

71. Weathington, N. M., van Houwelingen, A. H., Noerager, B. D., Jackson, P. L., Kraneveld, A. D., Galin, F. S., Folkerts, G., Nijkamp, F. P., and Blalock,

J. E. (2006) A novel peptide CXCR ligand derived from extracellular matrix degradation during airway inflammation. *Nat Med* **12**, 317-323

72. Jones, E. V., and Bouvier, D. S. (2014) Astrocyte-secreted matricellular proteins in CNS remodelling during development and disease. *Neural Plast* **2014**, 321209

73. Mackay, C. R. (2008) Moving targets: cell migration inhibitors as new anti-inflammatory therapies. *Nat Immunol* **9**, 988-998

74. Frangogiannis, N. G. (2012) Matricellular proteins in cardiac adaptation and disease. *Physiol Rev* **92**, 635-688

75. Brekken, R. A., and Sage, E. H. (2000) SPARC, a matricellular protein: at the crossroads of cell-matrix. *Matrix Biol* **19**, 569-580

76. Mason, I. J., Murphy, D., Munke, M., Francke, U., Elliott, R. W., and Hogan, B. L. (1986) Developmental and transformation-sensitive expression of the Sparc gene on mouse chromosome 11. *EMBO J* **5**, 1831-1837

77. Reed, M. J., Puolakkainen, P., Lane, T. F., Dickerson, D., Bornstein, P., and Sage, E. H. (1993) Differential expression of SPARC and thrombospondin 1 in wound repair: immunolocalization and in situ hybridization. *J Histochem Cytochem* **41**, 1467-1477

78. Bradshaw, A. D., Puolakkainen, P., Dasgupta, J., Davidson, J. M., Wight, T. N., and Helene Sage, E. (2003) SPARC-null mice display abnormalities in the dermis characterized by decreased collagen fibril diameter and reduced tensile strength. *J Invest Dermatol* **120**, 949-955

79. Sangaletti, S., Gioiosa, L., Guiducci, C., Rotta, G., Rescigno, M., Stoppacciaro, A., Chiodoni, C., and Colombo, M. P. (2005) Accelerated dendritic-cell migration and T-cell priming in SPARC-deficient mice. *J Cell Sci* **118**, 3685-3694

80. Kzhyshkowska, J., Workman, G., Cardo-Vila, M., Arap, W., Pasqualini, R., Gratchev, A., Krusell, L., Goerdt, S., and Sage, E. H. (2006) Novel function of alternatively activated macrophages: stabilin-1-mediated clearance of SPARC. *J Immunol* **176**, 5825-5832

81. Lane, T. F., and Sage, E. H. (1990) Functional mapping of SPARC: peptides from two distinct Ca+(+)-binding sites modulate cell shape. *J Cell Biol* **111**, 3065-3076

82. Bradshaw, A. D., Francki, A., Motamed, K., Howe, C., and Sage, E. H. (1999) Primary mesenchymal cells isolated from SPARC-null mice exhibit altered morphology and rates of proliferation. *Mol Biol Cell* **10**, 1569-1579

83. Wang, H., Fertala, A., Ratner, B. D., Sage, E. H., and Jiang, S. (2005) Identifying the SPARC binding sites on collagen I and procollagen I by atomic force microscopy. *Anal Chem* **77**, 6765-6771

84. Frank, S., Stallmeyer, B., Kampfer, H., Kolb, N., and Pfeilschifter, J. (2000) Leptin enhances wound re-epithelialization and constitutes a direct function of leptin in skin repair. *J Clin Invest* **106**, 501-509

85. Sangaletti, S., Stoppacciaro, A., Guiducci, C., Torrisi, M. R., and Colombo, M. P. (2003) Leukocyte, rather than tumor-produced SPARC, determines stroma and collagen type IV deposition in mammary carcinoma. *J Exp Med* **198**, 1475-1485

86. Rotta, G., Matteoli, G., Mazzini, E., Nuciforo, P., Colombo, M. P., and Rescigno, M. (2008) Contrasting roles of SPARC-related granuloma in bacterial containment and in the induction of anti-Salmonella typhimurium immunity. *J Exp Med* **205**, 657-667

87. Mrass, P., Takano, H., Ng, L. G., Daxini, S., Lasaro, M. O., Iparraguirre, A., Cavanagh, L. L., von Andrian, U. H., Ertl, H. C., Haydon, P. G., and Weninger, W. (2006) Random migration precedes stable target cell interactions of tumor-infiltrating T cells. *J Exp Med* **203**, 2749-2761

88. Sharma, S. D., Mullenax, J., Araujo, F. G., Erlich, H. A., and Remington, J. S. (1983) Western Blot analysis of the antigens of Toxoplasma gondii recognized by human IgM and IgG antibodies. *J Immunol* **131**, 977-983

89. Contini, C., Cultrera, R., Seraceni, S., Segala, D., Romani, R., Fainardi, E., Cinque, P., Lazzarin, A., and Delia, S. (2002) The role of stage-specific oligonucleotide primers in providing effective laboratory support for the molecular diagnosis of reactivated Toxoplasma gondii encephalitis in patients with AIDS. *J Med Microbiol* **51**, 879-890

CHAPTER TWO

β-arrestin 2 mediates T cell migratory speed in the inflamed brain

2.1 Abstract

As regulators of cell migration, β-arrestins influence actin remodeling and chemokine receptor endocytotis. These functions are critically important in the generation and maintenance of an immune response, particularly during chronic infection. *In vitro* migration data suggests that T cells isolated from tissue depend on β-arr2, one of two commonly expressed β-arrestin family members, to migrate toward CCL21 and that the absence of β-arr2 is detrimental to migratory speed. β-arr2 is not required for T cells to infiltrate the inflamed brain. However, once T cells have entered and are migrating within the parenchyma, intravital microscopy reveals that β-arr2 is required for optimal T cell velocity. Together these data demonstrate the role of β-arr2 in regulating cell migration behavior within inflamed tissue.

2.2 Introduction

Cell migration is a critical aspect of both homeostatic lymphocyte homing and the immune response. There is a continuous redistribution of cells from the primary and secondary lymphoid organs to infection sites, which must be tightly controlled to provide efficient protection from invading pathogens while minimizing immune related pathology. Chemokines and their receptors are major regulators of the cell trafficking required to mediate an immune response. For example, the role of CCR7 and its ligands have been intensely studied during both basal and inflammatory conditions. Like most other 7 transmembrane domain receptors, CCR7 has two signaling axes. The best known axis is the activation of G protein signaling (1). Ligand binding to CCR7 causes a conformational change leading to the exchange of GDP for GTP in the $G\alpha_i$ subunit of the heterotrimeric G protein complex that is coupled to the receptor. This exchange leads to the dissociation of the heterotrimeric complex to form $G\alpha_i$ and $G\beta\gamma$ subunits, which go on to control a myriad of second-messenger molecules, including Ca^{2+}, necessary for CCR7 mediated cell migration (2,3). Agonist bound CCR7 is then targeted by G-protein coupled receptor kinases (GRKs) and phosphorylated at the C-terminal tail. Phosphorylated receptors recruit β-arrestins, the molecules responsible for the second signaling axis. β-arrestins are a family of four intracellular proteins, two of which, β-arrestin 1 and 2 (β-arr2) are ubiquitously expressed in mammalian cells (4,5). The most well known actions of β-arrestins include receptor internalization and recycling, but β-

arrestins can also scaffold actin remodeling proteins at the leading edge of a migrating cell, promoting gradient sensing and chemotaxis even without the actions of G proteins (6-9). These actions may vary depending on cell type, or may be temporally and spatially regulated within the same cell (10,11).

The differential signaling axes influenced by CCR7's ligands are just one example of the complex signaling cascades that mediate the tight control necessary for regulating an immune response. Exactly how T cells are directed to sites of inflammatory loci within tissue and if the signaling requirements for circulating T cells are distinct from those that have entered tissue are unknown. In this work, we asked what signaling events are required for T cells to migrate within tissue. *Toxoplasma gondii* was used to model CNS inflammation, as following a robust systemic Th1 immune response, this parasite establishes a chronic infection in the brain and requires a constant influx of IFNγ secreting T cells to control replication. CCR7 plays a critical role in host immunity to *T. gondii*. CCR7-/- mice succumb early during infection due to a significant decrease in IFNγ production (12). Further, there are increases in CCL21 expression in the brain during *T. gondii* infection and this chemokine appears as long linear strands associated with migrating T cells (13-15). Indeed, CCR7/CCL21 signaling within the brain is crucial to control parasite replication after *T. gondii* infection (16). Though the inflammatory environment is complex *in vivo*, the reluctance of CCR7 to be internalized upon stimulation with CCL21 (17)

suggests a specific mechanism for promoting the chemotaxis of infiltrating immune cells either by promoting intrinsic searching behaviors (18) or in a directed, gradient-dependent manner (19). In *in vitro* assays T cells isolated from tissue require β-arr2 to migrate toward CCL21 because CCL21 mediates the cell's migratory speed toward a CCL21 gradient. Further, while β-arr2 is not required to recruit T cells into the brain parenchyma, β-arr2 is necessary to maintain optimal migratory speed within the brain. Together these data define a role for β-arr2 in mediating efficient effector T cell responses in the inflamed brain.

2.3 Results

2.3.1 β-arrestin 2 is required for T cells to migrate toward soluble CCL21.

It had been previously reported that CCR7 dependent migration toward CCL21 is independent of β-arrestin signaling in a T cell lymphoma line (20). However, primary cells may behave differently than a cell line, possibly due to differences in CCR7 expression at the cell surface or differences in signaling downstream of CCR7. To determine if β-arr2 is required for naïve, $CCR7^{hi}$ T cells to migrate toward CCL21, T cells were isolated from the lymph nodes and spleens of naïve WT and β-arr2-/- mice and their chemotaxis toward increasing concentrations of soluble CCL21 was measured using a transwell assay (Fig. 2.1A and B). Migration of WT CD4+ T cells increased with increasing concentrations of CCL21, peaking at 1000ng/mL (Fig 2.1A). However, while migration of CD4+ T cells that lack β-arr2 modestly increased as the concentration of CCL21 increased, the ratio of cells migrated/input remained significantly lower than the ratio exhibited by WT cells (Fig 2.1A). Similar results were obtained for CD8+ T cells (Fig 2.1B). Therefore, naïve, primary CD4+ and CD8+ T cells require β-arr2 to migrate toward soluble CCL21. To determine if the differences seen in the T cell migratory behavior was due to differences in surface expression of CCR7, the proportion of CCR7+ T cells isolated from the lymph node was determined using flow cytometry (Fig 2.1C). CCR7 expression on both CD4 and CD8+ cells was similar between genotypes, therefore there is a requirement for β-arr2

signaling downstream of CCR7 during the chemotaxis of naïve primary cells, in contrast to previous reports (20).

To address if β-arr2 is required for activated T cells to respond to CCL21, chemotaxis assays were performed on leukocytes harvested from the spleens and brains of WT and β-arr2 mice infected with *T. gondii* for 28 days. Migration of WT CD4+ T cells isolated from the spleen sharply increased at a CCL21 concentration of 500ng/mL before leveling off at higher chemokine concentrations (Fig. 2.1D). β-arr2 -/- CD4+ T cells followed similar migration kinetics (Fig. 2.1D). Migration of activated WT CD8+ T cells steadily increased as the concentration of CCL21 increased, peaking at a concentration of 1500ng/mL (Fig. 2.1E). In contrast, the migration of β-arr2-/- CD8 T cells peaked at a CCL21 concentration of 500ng/mL and any further increases in CCL21 did not result in increased migration (Fig. 2.1E). Equivalent CCR7 expression was confirmed on T cells isolated from the spleen between genotypes (Fig 2.1F), but as expected, when compared to levels found in naïve T cells, CCR7 expression is reduced. These results indicate that circulating, activated T cells either lose the requirement for β-arr2 signaling to migrate toward CCL21 or are able to overcome it through compensatory mechanisms such as signaling through another isoform of β-arrestin.

As activated, antigen specific T cells infiltrate the brain, CCR7 expression is reacquired to leave the blood and enter the brain parenchyma (16,21). Therefore, the requirement for β-arr2 signaling to mediate migration toward CCL21 may also be reacquired. To test if T cells in the brain need β-arr2 to migrate toward soluble CCL21, brain mononuclear cells were isolated from chronically infected WT and β-arr2-/- mice and were subjected to the transwell assay. The migration of WT CD4+ T cells peaked at 1000ng/mL CCL21 (Fig. 2.1G), affirming previous data acquired in our lab (Noor et al., 2016, submitted). The migration of β-arr2-/- CD4+ T cells did not deviate from baseline migration until exposed to 2000ng/mL CCL21, when the ratio of cells migrated/input increased sharply to match that of the WT cells (Fig. 2.1G). Similar migration kinetics were seen for CD8+ T cells (Fig. 2.1H). Again, CCR7 expression was tested and found to be equivalent between genotypes with a frequency of approximately 20% (Fig. 2.1I). However, the recovery of CCR7 expression in the brain is not equal to naïve expression levels (Fig. 2.1C), therefore the migration differences in naïve, activated circulating, and activated infiltrating T cell populations cannot be attributed to CCR7 expression alone. These results indicate that CCR7 dependent migration toward CCL21 is dependent on β-arr2 signaling in primary murine T cells isolated from the brain. Together, these data suggest that the behavior of T cells isolated from the brain is more similar to those isolated from another tissue such as the lymph node than to T cells that are circulating in the blood, despite their activation status.

2.3.2 β-arrestin2 is required for efficient T cell migration toward a gradient of CCL21.

Transwell assays illustrate the chemotactic response toward soluble CCL21. However, within tissue CCL21 is not all soluble, but rather is immobilized to the extracellular matrix (19,22). It is possible that chemokines bound to the matrix may elicit migration behavior that differs from behavior generated by chemokines in their soluble form. Additionally, as CCL21 has been shown to be upregulated in the brain upon infection with *T. gondii* (13), it may be that CCL21 is secreted only on areas of the brain where parasites are found and that a gradient of CCL21 is generated, providing local guidance signals for T cells toward areas of infection. Further, the absence of β-arr2 may impact specific aspects of cell migration behavior, such as the ability to sense the presence of a gradient. To mimic T cell migration within tissue, $CCR7^{hi}$ WT dsRed and β-arr2-/- GFP T cells isolated from the lymph node were seeded in artificial matrix and their migration in response to no chemokine, a constant concentration of CCL21, or a gradient of CCL21 was imaged and quantified. Normalizing cell tracks to begin at the origin reveals that in both the presence and absence of β-arr2, cells migrate very little in the absence of chemokine (Fig. 2.2A), cover somewhat more distance in response to a constant concentration of chemokine (Fig. 2.2B), and that both groups travel farthest in the direction of an increasing chemokine gradient (Fig 2.2C). WT T cells have a baseline speed of almost 3 μm/min migrating in

response to media alone. When bathed in a constant concentration of CCL21 their velocity increases to 4 μm/min and when following a gradient, their speed averages nearly 6 μm/min but some cells can reach a speed of 9 μm/min (Fig 2.2B). While β-arr2-/- cells have a significantly higher starting velocity at 4 μm/min, the presence of constant chemokine does not change this speed. The presence of a gradient results in a small but significant increase in the speed of β-arr2 deficient cells over media alone, but the absence of β-arr2 results in a significantly slower velocity compared to WT cells (Fig. 2.2D). Treatment of cells with media does not lead to any differences in the displacement of cells between groups, nor does treatment with a constant concentration of CCL21 (Fig. 2.2E). Under the influence of a gradient, a large variation of cell displacement can be observed in both WT and β-arr2-/- cells, and while the mean displacement is lower in β-arr2-/- cells compared to WT, this difference did not reach statistical significance (Fig. 2.2E). Quantifying the cells' meandering index, where a value of zero indicates no directed movement while a value of one indicates ideal directed movement, revealed a small but statistically significant difference between WT and β-arr2-/- cells that were treated with media alone. Exposure to either constant or increasing CCL21 concentrations indicate that β-arr2-/- cells can overcome this initial defect and can be guided by CCL21 just as well as WT cells. Together these data show the absence of β-arr2 in T cells is detrimental to their migratory speed.

2.3.3 Infection indicates CD8+ T cell recruitment to the brain requires β-arrestin 2

Under homeostatic conditions, T cells are not present in the brain. Indeed, T cells only migrate to the brain as a result of immune insult or injury (23). During *T. gondii* infection, any delay in T cell recruitment to the initial infection site leads to uncontrolled parasite replication. Previous reports indicate β-arr2-/- exhibit poor disease control such as uncontrolled tumor growth (24) and sepsis (25). To test if such a defect in T cell recruitment would be detrimental to the mice at the chronic stage of infection, WT and β-arr2-/- mice were infected and a chronic infection was allowed to establish. The numbers of circulating cells isolated from the spleen were equivalent between genotypes (Fig. 2.3A). Flow cytometry analysis revealed approximately 14% of cells found in the spleens of WT mice were CD4+ while 17% were CD8+. In contrast, in β-arr2-/- spleens CD4+ and CD8+ T cells were both significantly reduced to 8% (Fig. 2.3B). Despite the reduced proportion of cells, the number of CD4+ T cells was unchanged between groups (Fig. 2.3C), but the number of CD8+ T cells was significantly reduced in the absence of β-arr2 (Fig. 2.3D).

The numbers of mononuclear cells (BMNCs) that migrated to the brain in response to infection were equivalent between groups (Fig. 2.3E). Consistent with previous reports, (26) at four weeks post infection approximately 24% of the cells recruited to the brains of WT mice were CD4+ and approximately 21% were

CD8+ (Fig 2.3F). In mice lacking β-arr2, the proportion of CD4+ T cells in the brain remained comparable to that of the WT at 22%. However, the proportion of CD8+ T cells in the brain dropped significantly to approximately 9% (Fig. 2.3F). Analysis of total T cell numbers revealed that the number of CD4+ T cells remained unchanged between groups (Fig. 2.3G). However, the number of CD8+ T cells found in the brains of β-arr2 -/- mice was significantly reduced (Fig. 2.3H). As both CD4+ and CD8+ T cells are required to control infection, it would be expected that the defect seen in the recruitment of CD8+ T cells to the brain in the absence of β-arr2 would lead to a higher parasite burden and possible impair survival. To test if fewer CD8+ T cells in β-arr2 -/- mice lead to differences in the ability to control parasite replication, the number of parasites in the brain was quantified using RT-PCR. Surprisingly, and in contrast to other infection studies using these mice (25), β-arr2 deficient mice were found to have significantly fewer parasites in the brain (Fig. 2.3I). Consequently these mice also have a significantly lower cyst burden in the brain (Fig. 2.3J). While there was considerable variability in the ability of β-arr2-/- mice survive the infection (data not shown), ultimately the mice live due to a failure of *Toxoplasma* to disseminate to the brain (Fig. 2.3I and J). Together these data indicate either a failure of CD8+ T cells to enter the brain in equal numbers to WT cells due to the lack of antigen in the CNS.

2.3.4 Adoptive transfer reveals T cell recruitment is β-arrestin2 -/- independent

Infection of whole knockout mice indicate some T cells can arrive at the brain in the absence of β-arr2, however differences in antigen load make it difficult to draw clear conclusions about to the role β-arr2 is playing within infiltrating T cells. T cells might indeed be slower to enter the brain in the absence of β-arr2, or they may be failing to expand and infiltrate at levels comparable to WT mice because less antigen makes it unnecessary. Therefore, to test if β-arr2 is required for T cell migration to the brain, CD45.2 CD3+ T cells were transferred from WT and β-arr2-/- mice into congenic CD45.1 WT animals one day prior to infection. Cell populations recruited to the brain during chronic *T. gondii* infection were analyzed. Of the CD4+ T cells that were in the brains of mice that received cell transfers, approximately 16% were the WT transferred population and roughly 25% were the β-arr2-/- cells (Fig. 2.4A). Analysis of the total number of transferred CD4+ T cells in the brain determined that while the difference in the number of WT and β-arr2 -/- cells never reached statistical significance, the variation in the number of β -arr2 -/- cells was significantly higher than the variation in WT cells (Fig. 2.4B). Immunohistochemistry of brain sections from adoptively transferred mice revealed that like WT cells, β-arr2 -/- CD4+ T cells are able to cross the blood-brain barrier into the brain parenchyma (Fig. 2.4C). Similar results were observed with CD8+ T cells: approximately 19% of the cells that made it to the brain were the transferred, CD45.2 population regardless of

the presence of β-arr2 (Fig. 2.4D), the absence of β-arr2 lead to an increased variance in the number of transferred cells in the brain (Fig. 2.4E), and the absence of β-arr2 had no effect on the cell's ability to leave the perivascular spaces and enter the brain parenchyma (Fig. 2.4F). Thus, both CD4 and CD8+ T cells do not require β-arr2 to enter the brain.

As β-arr have been shown to mediate endocytosis of surface receptors, a possible explanation for variable cell recruitment in β-arr2 deficient cells may be variable expression of chemokine receptors known to be critical for mediating T cell migration to and within the brain. Therefore, we used flow cytometry to analyze the expression of CCR7 on the surface of adoptively transferred T cells isolated from the brains of chronically infected congenic mice. Like data previously collected in our lab, approximately 20% of WT T cells found in the brain express CCR7 (Noor et al., 2016, submitted) and while the proportions and number of CCR7 expressing cells did not significantly differ between WT and β-arr2 -/- CD4+ T cells (Fig. 2.4G, H), the variability of β-arr2 -/- CD4+CCR7+ T cells was significantly higher than their WT counterparts (Fig. 2.4H). Similarly, chemokine receptor expression on transferred CD8+ T cells did not significantly differ between groups (Fig. 2.4I and J), yet the variability of β-arr2 -/- CD8+CCR7+ cells was significantly higher than that of the WT cells (Fig. 2.4J). Taken together, these data suggest that β-arr2 is required for optimal CCR7 expression on the surface of T cells infiltrating the brain, but the changes in

observed CCR7 expression are not sufficient to detrimentally affect T cell recruitment to the brain.

2.3.5 T cell velocity in the inflamed brain depends on β-arrestin 2

Since is was clear that both WT and β-arr2-/- T cells can access the brain parenchyma and do not accumulate in perivascular spaces as observed in *plt/plt* mice (16), T cells are still responsive to CCL21 in the brain in the presence and absence of β-arr2. However, immunohistochemistry and flow cytometry cannot determine if the migration behavior of T cells is in any way impaired without β-arr2. Therefore, we expanded on a previously utilized experimental system to test if β-arr2 deficient effector T cells can migrate as easily as WT cell in the inflamed brain. β-arr2-/- mice were crossed with GFP+ mice and their progeny were crossed with OTI mice to generate mice with β-arr2-/- GFP CD8+ T cells that were specific for ovalbumin. OTI mice were also crossed with dsRed mice to generate ovalbumin specific dsRed WT controls. T cells were expanded *in vitro* before being adoptively transferred into uncolored WT mice that were chronically infected with a strain of *T. gondii* that was engineered to express ovalbumin (Pru-OVA) (27-29). One week post-transfer, brains of recipient mice were excised and cell migration was imaged over time using two-photon microscopy. Both WT OTI dsRed and β-arr2-/- OTI GFP cells infiltrated the brain and were observed migrating along the network of fibers generated in the brain upon infection (Fig. 2.5A). Plotting cell tracks so that each track begins at the origin of a flower plot

reveals that the distance traveled by the cells of either genotype are equivalent (Fig 2.5B). Analysis of the behavior of individual cells revealed the average velocity of WT T cells was almost 8 μm/min, though individual cells were recorded at up to 20 μm/min, in line with previous reports (29). In contrast, β-arr2-/- T cells migrating in the same brain (and therefore under identical conditions) had a significantly smaller average velocity of approximately 5 μm/min (Fig. 2.5C). The differences in T cell velocity had no effect on the displacement of T cells. Cells in both groups traveled an average of approximately 23 μm away from their starting points (Fig 2.5D). Similarly, there were no statistical differences in the meandering indices of tracked cells, indicating no differences in the cells' ability to be guided by a chemokine gradient (Fig. 2.5E).

2.4 Discussion

Chemokine mediated cell trafficking is essential for any immune response. Immune cell infiltration must be tightly governed in any organ, but especially so in the CNS where any slight imbalance of cell effector functions can cause irreparable damage or death. Until recently, little was known about the signaling events for efficient cell migration within tissue. For example, it is unknown if the signals used to migrate within infected tissue differ from those that regulate migration within lymphoid organs. It is also unknown if those signals are cell-specific or merely specific to individual receptors regardless of the cell upon which those receptors are expressed. Finally, it is unknown if there could be tissue-specific signals that could govern the intensity of immune responses, such as in peripheral verses immune-privileged organs like the brain. Presently, we know the generalized levy walk behavior of infiltrating CD8+ T cells is mediated by Gαi protein signaling coupled to CXCL10 stimulated CXCR3 and that when CXCL10 is depleted, average cell velocity is significantly reduced (18). Further, we know CCL21 signaling through CCR7 mediates T cell entry into the inflamed brain and efficient control of parasitic infection (13,16,29). Knowing the signaling requirements for cell migration within tissue downstream of chemokine receptors like CCR7 is critical if we intend to influence, direct, or correct the location and magnitude of inflammation within infected organs or during inappropriate immune responses.

These studies provide insight into the subtle role β-arr2 plays in orchestrating T cell migration within the inflamed brain. *In vitro* data presented here indicates that naïve, $CCR7^{hi}$ T cells require β-arr2 to migrate toward CCL21 (Fig. 2.1A-C). Once cells become activated and enter the circulation, CCR7 is downregulated and the requirement for β-arr 2 is lost. (Fig. 2.1D-F). Therefore it is tempting to conclude that activation status regulates the requirement for β-arr2 in regulating cell migration. However, when those activated cells re-enter tissue, specifically the chronically infected brain, CCR7 expression is partially re-acquired, as is the necessity of β-arr2. CD4+ and CD8+ subsets respond to CCL21 in the same manner, which may indicate that any type of T cell (T_{reg}, T_{rm}, T_{eff}, etc.) from either inflamed tissue or naïve secondary lymphoid organs would respond similarly to CCL21 stimulation as long at they express sufficient levels of CCR7.

To further characterize the role β-arr2 plays in mediating T cell migration within tissue, T cells were seeded in artificial matrix to mimic migration behavior in a three dimensional space. Quantifying cell behavior revealed that both WT and β-arr2 deficient T cells increased their speed, displacement and meandering indices, indicating that β-arr2-/- T cells are capable of sensing a gradient is present and are able to respond to it. Indeed the only difference observed in β-arr2-/- cells is a slower average velocity (Fig 2.2D), similar to *in vivo* data demonstrating the role of CXCL10 mediating migratory speed (18). Therefore β-arr2 deficient T cells are able to get where they need to go, but need more time

to get there. This is supported *in vivo* with adoptive transfer data (Fig 2.4). Both transferred CD4+ and CD8+ β-arr2-/- T cells are present in the brain parenchyma in proportions equal to transferred WT cells and any variability in cell number can be explained by variability in the surface expression of CCR7. Further, the results observed in our T cell migration assay can be recapitulated *in vivo* in the inflamed brain (Fig 2.5). Both WT and β-arr2-/- T cells migrate similar distances (Fig 2.5D) and are equally capable of being guided by chemotactic signals (Fig. 2.5E), but β-arr2-/- T cells are slower than WT. Taken together, these data indicate the role of β-arr2 in T cell movement in the brain is more refined than simply pro- or anti-inflammatory. Rather, its role in mediating optimal migratory speed is independent of recruitment, infiltration, and gradient sensing.

2.5 Figures and Legends

Figure 2.1. β-arrestin 2 mediated migration toward CCL21. Ratios of CD4+ (A) and CD8+ (B) T cells isolated from spleen and lymph nodes of naïve WT and β-arr2-/- mice that migrated through transwells toward increasing concentrations of CCL21 (0-2000ng/mL) over input. (C) CCR7 expression on each T cell subset from spleen and lymph nodes of naïve WT and β-arr2-/- mice. Ratios of CD4+ (D) and CD8+ (E) T cells isolated from spleen and lymph nodes of chronically infected WT and β-arr2-/- mice that migrated through transwells toward increasing concentrations of CCL21. (F) CCR7 expression on each T cell subset from spleen and lymph nodes of chronically infected WT and β-arr2-/- mice. Ratios of CD4+ (G) and CD8+ (H) T cells isolated BMNCs of chronically infected WT and β-arr2-/- mice that migrated through transwells toward increasing concentrations of CCL21. (F) CCR7 expression on each T cell subset BMNCs of chronically infected WT and β-arr2-/- mice. Migration data in this figure was analyzed using ANOVA. CCR7 expression was compared using the student's T test. *$p<0.05$, **$p<0.01$, ***$p<0.001$

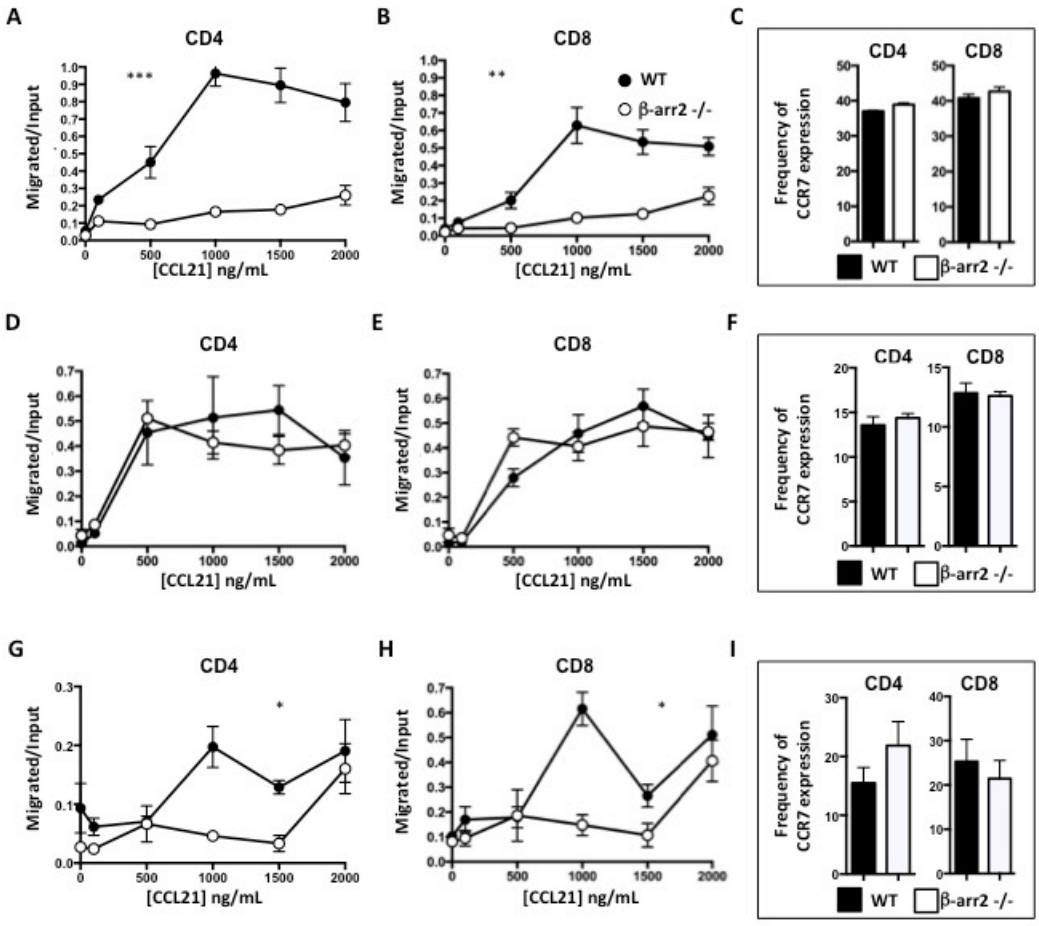
A
CD4
Migrated/Input
[CCL21] ng/mL
***
B
CD8
**
WT
β-arr2 -/-
C
CD4
CD8
Frequency of CCR7 expression
WT
β-arr2 -/-
D
CD4
E
CD8
F
CD4
CD8
G
CD4
*
H
CD8
*
I
CD4
CD8

Figure 2.2. β-arrestin 2 mediates efficient migratory speed in response to a gradient of CCL21. (A-C) Flower plots show migratory tracks of individual WT (green) or β-arr2-/- (pink) T cells with the start of each track placed at the graph origin. Cells were imaged migrating in response to media alone (A), a constant concentration of CCL21 (B), or a gradient of CCL21 (C). (D) Scatter plot of velocities of T cells migrating under each condition. (E) Scatter plot of displacement of T cells migrating under each condition. (F) Scatter plot of meandering indices of T cells migrating under each condition. Migration data was analyzed using the student's T test. *$p<0.05$, **$p<0.01$, ***$p<0.001$

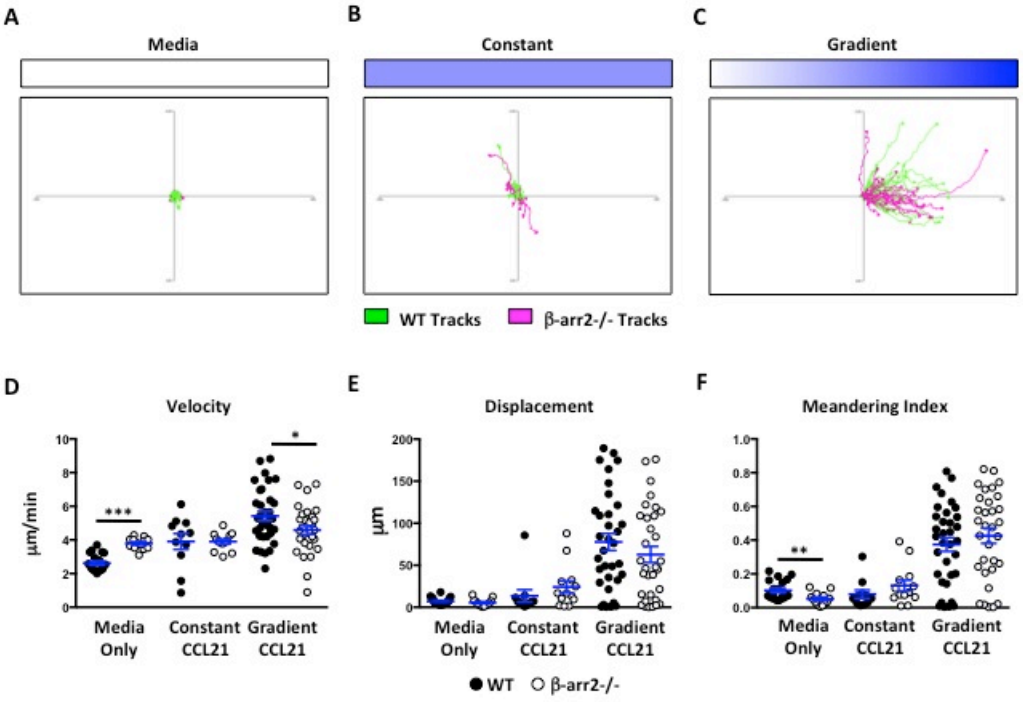
A
Media
B
Constant
C
Gradient
WT Tracks
β-arr2-/- Tracks
D
Velocity
µm/min
***
*
Media Only
Constant CCL21
Gradient CCL21
E
Displacement
µm
Media Only
Constant CCL21
Gradient CCL21
WT
β-arr2-/-
F
Meandering Index
**
Media Only
Constant CCL21
Gradient CCL21

Figure 2.3. T cell recruitment to the brain during chronic *T. gondii* infection. WT and β-arr2-/- mice were infected for 28 days and T cells recruited to the spleen and brain were quantified. (A) Absolute numbers of cells isolated from the spleen. (B) Flow cytomtery plots with the proportions of T cells found in the spleens of infected mice. Absolute number of CD4+ (C) and CD8+ (D) T cells found in the spleen were calculated. (E) Absolute numbers of BMNCs isolated from the brains of infected WT and β-arr2-/- mice. (F) Flow cytometry plots with the proportions of T cell subsets in BMNCs. Absolute number of CD4+ (G) and CD8+ (H) T cells isolated from the brain were calculated. (I) Parasite DNA was quantified from infected brain samples using qPCR relative to a standard curve. (J) Cyst burden in the brains of WT and β-arr2-/- was quantified. Flow cytometry data was analyzed using the student's T test. *$p<0.05$, **$p<0.01$, ***$p<0.001$

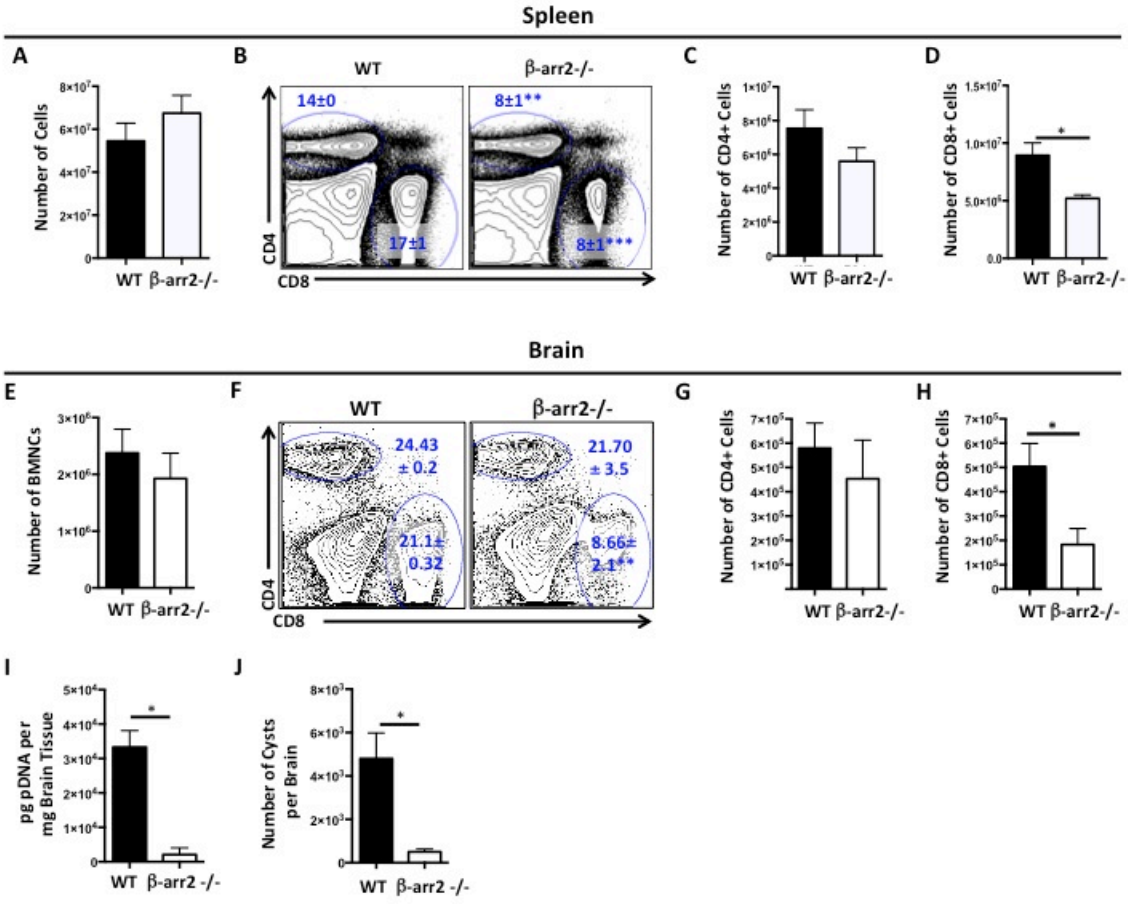
Spleen
A
Number of Cells
WT β-arr2-/-
B
WT
β-arr2-/-
14±0
8±1**
17±1
8±1***
CD4
CD8
C
Number of CD4+ Cells
WT β-arr2-/-
D
Number of CD8+ Cells
WT β-arr2-/-
Brain
E
Number of BMNCs
WT β-arr2-/-
F
WT
β-arr2-/-
24.43 ± 0.2
21.1± 0.32
21.70 ± 3.5
8.66± 2.1**
CD4
CD8
G
Number of CD4+ Cells
WT β-arr2-/-
H
Number of CD8+ Cells
WT β-arr2-/-
I
pg pDNA per mg Brain Tissue
WT β-arr2 -/-
J
Number of Cysts per Brain
WT β-arr2 -/-

Figure 2.4. Recruitment of adoptively transferred T cells to the brain is independent of β-arrestin 2. CD45.2+ CD3+ T cells from WT and β-arr2-/- were isolated and adoptively transferred into CD45.1 congenic mice one day before infection with *T. gondii*. At 28 days post-infection, cells that infiltrated the brain were phenotyped. Proportions (A) and absolute numbers (B) of transferred (CD45.2) CD4+ T cells. (C) IHC demonstrating transferred CD4+ T cells can enter the brain parenchyma. Proportions (D) and absolute numbers (E) of transferred CD8+ T cells in the brain. (F) IHC demonstrating transferred CD8+ T cells can enter the brain parenchyma. Proportions (G) and absolute numbers (H) of transferred CD4+ T cells that express CCR7. Proportions (I) and absolute numbers (J) of transferred CD8+ T cells that express CCR7. Flow cytometry data was analyzed using the student's T test. **p<0.01

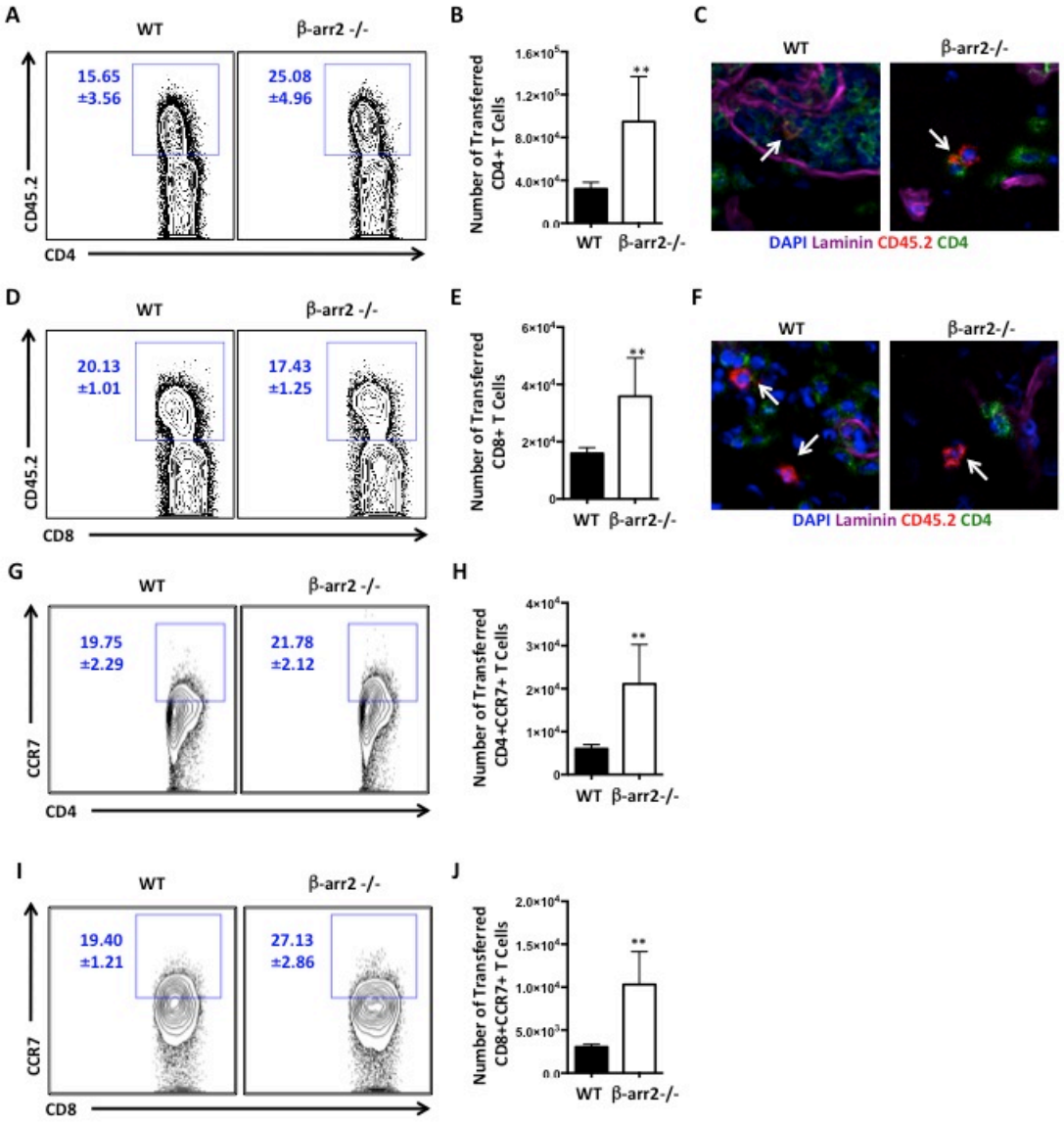
A
WT
β-arr2 -/-
15.65
±3.56
25.08
±4.96
CD45.2
CD4
B
Number of Transferred CD4+ T Cells
1.6×10^5
1.2×10^5
8.0×10^4
4.0×10^4
0.0
**
WT
β-arr2-/-
C
WT
β-arr2-/-
DAPI Laminin CD45.2 CD4
D
WT
β-arr2 -/-
20.13
±1.01
17.43
±1.25
CD45.2
CD8
E
Number of Transferred CD8+ T Cells
6×10^4
4×10^4
2×10^4
0
**
WT
β-arr2-/-
F
WT
β-arr2-/-
DAPI Laminin CD45.2 CD4
G
WT
β-arr2 -/-
19.75
±2.29
21.78
±2.12
CCR7
CD4
H
Number of Transferred CD4+CCR7+ T Cells
4×10^4
3×10^4
2×10^4
1×10^4
0
**
WT
β-arr2-/-
I
WT
β-arr2 -/-
19.40
±1.21
27.13
±2.86
CCR7
CD8
J
Number of Transferred CD8+CCR7+ T Cells
2.0×10^4
1.5×10^4
1.0×10^4
5.0×10^3
0.0
**
WT
β-arr2-/-

Figure 2.5. T cell velocity depends on β-arrestin 2 in the brain. WT mice were infected for 28 days with the OVA expressing Pru strain of *T. gondii* and then adoptively transferred with a 1:1 ratio of dsRed+ OVA specific WT CD8+ T cells and GFP+ OVA specific β-arr2-/- CD8+ T cells that had been expanded *in vitro*. (A) Still image of OVA specific WT and β-arr2-/- T cells in the inflamed brain. (B) Representative flower plot of WT and β-arr2-/- cell tracks. (C) Scatter plot of the velocity of individual T cells migrating in the inflamed brain. (D) Scatter plot of displacement of T cells in the infected brain. (E) Scatter plot of meandering indices of each cell migrating in the brain. Migration data was analyzed using the Mann-Whitney test. *$p<0.05$

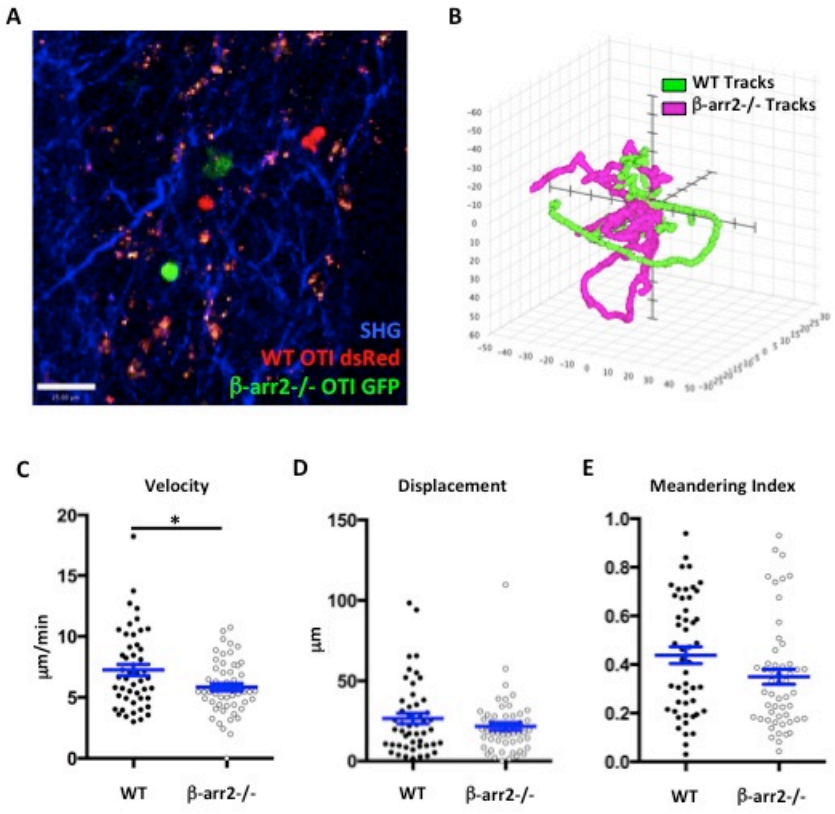
A
SHG
WT OTI dsRed
β-arr2-/- OTI GFP
B
WT Tracks
β-arr2-/- Tracks
C
Velocity
*
µm/min
20
15
10
5
0
WT
β-arr2-/-
D
Displacement
µm
150
100
50
0
WT
β-arr2-/-
E
Meandering Index
1.0
0.8
0.6
0.4
0.2
0.0
WT
β-arr2-/-

2.6 References

1. Lefkowitz, R. J., and Whalen, E. J. (2004) beta-arrestins: traffic cops of cell signaling. *Curr Opin Cell Biol* **16**, 162-168

2. Joseph, N., Reicher, B., and Barda-Saad, M. (2014) The calcium feedback loop and T cell activation: how cytoskeleton networks control intracellular calcium flux. *Biochim Biophys Acta* **1838**, 557-568

3. Thelen, M., and Stein, J. V. (2008) How chemokines invite leukocytes to dance. *Nat Immunol* **9**, 953-959

4. Shenoy, S. K., McDonald, P. H., Kohout, T. A., and Lefkowitz, R. J. (2001) Regulation of receptor fate by ubiquitination of activated beta 2-adrenergic receptor and beta-arrestin. *Science* **294**, 1307-1313

5. Zhang, J., Ferguson, S. S., Barak, L. S., Menard, L., and Caron, M. G. (1996) Dynamin and beta-arrestin reveal distinct mechanisms for G protein-coupled receptor internalization. *J Biol Chem* **271**, 18302-18305

6. Min, J., and Defea, K. (2011) beta-arrestin-dependent actin reorganization: bringing the right players together at the leading edge. *Mol Pharmacol* **80**, 760-768

7. Zoudilova, M., Min, J., Richards, H. L., Carter, D., Huang, T., and DeFea, K. A. (2010) beta-Arrestins scaffold cofilin with chronophin to direct localized actin filament severing and membrane protrusions downstream of protease-activated receptor-2. *J Biol Chem* **285**, 14318-14329

8. Xiao, K., Sun, J., Kim, J., Rajagopal, S., Zhai, B., Villen, J., Haas, W., Kovacs, J. J., Shukla, A. K., Hara, M. R., Hernandez, M., Lachmann, A., Zhao, S., Lin, Y., Cheng, Y., Mizuno, K., Ma'ayan, A., Gygi, S. P., and Lefkowitz, R. J. (2010) Global phosphorylation analysis of beta-arrestin-mediated signaling downstream of a seven transmembrane receptor (7TMR). *Proc Natl Acad Sci U S A* **107**, 15299-15304

9. DeFea, K. A. (2010) Beta-arrestins as regulators of signal termination and transduction: how do they determine what to scaffold? *Cell Signal* **23**, 621-629

10. McGovern, K. E., and DeFea, K. A. Molecular mechanisms underlying beta-arrestin-dependent chemotaxis and actin-cytoskeletal reorganization. *Handb Exp Pharmacol* **219**, 341-359

11. DeFea, K. A. (2007) Stop that cell! Beta-arrestin-dependent chemotaxis: a tale of localized actin assembly and receptor desensitization. *Annu Rev Physiol* **69**, 535-560

12. Noor, S., Habashy, A. S., Nance, J. P., Clark, R. T., Nemati, K., Carson, M. J., and Wilson, E. H. CCR7-dependent immunity during acute Toxoplasma gondii infection. *Infect Immun* **78**, 2257-2263

13. Noor, S., Habashy, A. S., Nance, J. P., Clark, R. T., Nemati, K., Carson, M. J., and Wilson, E. H. (2010) CCR7-dependent immunity during acute Toxoplasma gondii infection. *Infect Immun* **78**, 2257-2263

14. John, B., Harris, T. H., Tait, E. D., Wilson, E. H., Gregg, B., Ng, L. G., Mrass, P., Roos, D. S., Dzierszinski, F., Weninger, W., and Hunter, C. A. (2009) Dynamic Imaging of CD8(+) T cells and dendritic cells during infection with Toxoplasma gondii. *PLoS Pathog* **5**, e1000505

15. Wilson, E. H., Harris, T. H., Mrass, P., John, B., Tait, E. D., Wu, G. F., Pepper, M., Wherry, E. J., Dzierzinski, F., Roos, D., Haydon, P. G., Laufer, T. M., Weninger, W., and Hunter, C. A. (2009) Behavior of parasite-specific effector CD8+ T cells in the brain and visualization of a kinesis-associated system of reticular fibers. *Immunity* **30**, 300-311

16. Ploix, C. C., Noor, S., Crane, J., Masek, K., Carter, W., Lo, D. D., Wilson, E. H., and Carson, M. J. (2011) CNS-derived CCL21 is both sufficient to drive homeostatic CD4+ T cell proliferation and necessary for efficient CD4+ T cell migration into the CNS parenchyma following Toxoplasma gondii infection. *Brain Behav Immun* **25**, 883-896

17. Zidar, D. A., Violin, J. D., Whalen, E. J., and Lefkowitz, R. J. (2009) Selective engagement of G protein coupled receptor kinases (GRKs) encodes distinct functions of biased ligands. *Proc Natl Acad Sci U S A* **106**, 9649-9654

18. Harris TH, B. E., Christian DA, Konradt C, Tait Wojno ED, Norose K, Wilson EH, John B, Weninger W, Luster AD, Liu AJ, Hunter CA. (2012) Generalized Lévy walks and the role of chemokines in migration of effector CD8+ T cells. *Nature* **486**, 545-548

19. Weber, M., Hauschild, R., Schwarz, J., Moussion, C., de Vries, I., Legler, D. F., Luther, S. A., Bollenbach, T., and Sixt, M. (2013) Interstitial dendritic cell guidance by haptotactic chemokine gradients. *Science* **339**, 328-332

20. Byers, M. A., Calloway, P. A., Shannon, L., Cunningham, H. D., Smith, S., Li, F., Fassold, B. C., and Vines, C. M. (2008) Arrestin 3 mediates

endocytosis of CCR7 following ligation of CCL19 but not CCL21. *J Immunol* **181**, 4723-4732

21. Noor, S., and Wilson, E. H. (2012) Role of C-C chemokine receptor type 7 and its ligands during neuroinflammation. *J Neuroinflammation* **9**, 77

22. Yang, B. G., Tanaka, T., Jang, M. H., Bai, Z., Hayasaka, H., and Miyasaka, M. (2007) Binding of lymphoid chemokines to collagen IV that accumulates in the basal lamina of high endothelial venules: its implications in lymphocyte trafficking. *J Immunol* **179**, 4376-4382

23. Wilson, E. H., Weninger, W., and Hunter, C. A. (2010) Trafficking of immune cells in the central nervous system. *J Clin Invest* **120**, 1368-1379

24. Raghuwanshi, S. K., Nasser, M. W., Chen, X., Strieter, R. M., and Richardson, R. M. (2008) Depletion of beta-arrestin-2 promotes tumor growth and angiogenesis in a murine model of lung cancer. *J Immunol* **180**, 5699-5706

25. Fan, H., Bitto, A., Zingarelli, B., Luttrell, L. M., Borg, K., Halushka, P. V., and Cook, J. A. (2010) Beta-arrestin 2 negatively regulates sepsis-induced inflammation. *Immunology* **130**, 344-351

26. Neeley, S. P., and Conley, F. K. (1987) Extraction and immunocytochemical characterization of viable mononuclear inflammatory cells from brains of mice with chronic Toxoplasma gondii infection. *J Neuroimmunol* **15**, 159-172

27. Mrass, P., Takano, H., Ng, L. G., Daxini, S., Lasaro, M. O., Iparraguirre, A., Cavanagh, L. L., von Andrian, U. H., Ertl, H. C., Haydon, P. G., and Weninger, W. (2006) Random migration precedes stable target cell interactions of tumor-infiltrating T cells. *J Exp Med* **203**, 2749-2761

28. Pepper, M., Dzierszinski, F., Crawford, A., Hunter, C. A., and Roos, D. (2004) Development of a system to study CD4+-T-cell responses to transgenic ovalbumin-expressing Toxoplasma gondii during toxoplasmosis. *Infect Immun* **72**, 7240-7246

29. Wilson, E. H., Harris, T. H., Mrass, P., John, B., Tait, E. D., Wu, G. F., Pepper, M., Wherry, E. J., Dzierzinski, F., Roos, D., Haydon, P. G., Laufer, T. M., Weninger, W., and Hunter, C. A. (2009) Behavior of parasite-specific effector CD8+ T cells in the brain and visualization of a kinesis-associated system of reticular fibers. *Immunity* **30**, 300-311

CHAPTER THREE

Astrocytic SPARC facilitates T cell migration by binding CCL21

3.1 ABSTRACT

As discussed in chapters 1 and 2, CNS insult can result in profound changes in the brain including the release of the chemokine CCL21 to recruit lymphocytes to infected or injured tissue. Infection with the protozoan parasite *Toxoplasma gondii* results in a life-long infection in the brain. Control of parasite replication requires the continuous presence of IFNγ producing T cells to keep *T. gondii* in its slowly replicating, cyst form. Astrocytes contribute to resistance to the parasite via a variety of immune functions. These studies demonstrate infected astrocytes secrete the extracellular matrix remodeling protein SPARC (secreted protein acidic rich and cysteine) and that in this model, astrocytes are the predominant source of CCL21 in the brain. We also report SPARC can bind to CCL21 directly and enhances migration in vitro. In vivo, SPARC's presence plays a greater role in allowing effector T cells access to the inflamed CNS than contributing to optimal migration behavior within the brain parenchyma. Collectively, these data show how SPARC and CCL21 cooperate to contribute to T cell migration behavior within the inflamed brain.

3.2 INTRODUCTION

Cell migration is critical for all aspects of the immune response, especially the ability of effector cells to migrate to and within infected tissue. Cells need guidance to arrive at the correct organ and to infected areas within that organ. Cell migration is controlled by a multitude of individual processes, including but not limited to blood vessel permeability, remodeling of the extracellular matrix, and the production of both positive and negative chemotactic gradients. How these processes are controlled in a sensitive environment such as the brain is poorly understood. However, studies using *Toxoplasma gondii* as a model of CNS inflammation, as well as other brain infection models, have begun to discover how T cells are drawn into the parenchyma of the brain (1) and the behavior of T cells once they are inside (2,3).

As previously discussed in this dissertation*, T. gondii* is an intracellular parasite that results in a chronic infection in the brain. Parasitic cysts persist within neurons for the lifetime of the host. The continuous presence of IFNγ secreting T cells in the brain is required to keep parasite replication in check (4). An inflammatory response in the brain must require unique mechanisms of control. The skull limits the brain's capacity to swell and the blood-brain barrier limits access to the CNS. However, in otherwise healthy individuals, the immune response to *T. gondii* infection does not cause any apparent pathology. Therefore, *T. gondii* serves as a model of balanced CNS inflammation- potent to

control the parasite yet controlled to curb collateral damage in the brain.

During chronic *T. gondii* infection, chemokines like CCL21, CCL19, and CXCL10 are upregulated in the brain (1-3,5). These chemokines are thought to control distinct aspects of cell behavior in the brain, such as crossing into the parenchyma (1) and mediating Levy walk migration patterns to efficiently encounter infected cells (3). The movement of antigen specific T cells in the brain appears to be supported by the formation of a network of fibers of currently unknown composition. We now see a requirement for SPARC (secreted protein, acidic, rich in cysteine) in these remodeling events. SPARC is a matricellular protein whose function is important for ECM maintenance and remodeling. It can exert its functions through direct interaction with matrix proteins and on infiltrating immune cells via integrin signaling. Indeed the absence of SPARC can have a profound impact on the ability of immune cells to access inflamed tissue and to control infection (6-8), although its effects during the course of *T. gondii* infection appear to be more subtle, as any slight differences in cell populations and parasite burden resolve as infection progresses (Nance et al., manuscript in preparation). Building on previous studies from the Wilson lab, a nuanced role for SPARC is further defined in providing a protective immune response to *T. gondii* infection.

In this study, the hypothesis that increased expression of CCL21 and SPARC in the inflamed brain is a mechanism to guide immune cells within the brain

parenchyma to control parasite replication through the production of a chemokine-coated, fibrous reticulum in the brain was investigated. We determined that astrocytes are the source of both CCL21 and SPARC produced during *T. gondii* infection and that in the absence of SPARC, CCL21 transcripts are reduced. Further, SPARC and CCL21 production is intrinsic to astrocytes and does not require signaling from infiltrating T cells. Despite earlier work suggesting otherwise, CCL21 does not bind to the fibrous network but remains bound to its cellular source. In contrast, SPARC can bind directly to both CCL21 and CCL19, and that SPARC's presence enhances CCL21 driven chemotaxis of lymphocytes. In vivo, T cell access to the brain is patchy in the absence of SPARC and T cell migration is impaired. Together these data suggest that in addition to its influence on tissue malleability, SPARC works in combination with chemotactic cytokines to facilitate immune cell access to and migration within the parenchyma of the brain.

3.3 RESULTS

3.3.1 Reactive astrocytes are the source of CCL21 and SPARC during chronic *T. gondii* infection.

Previous studies demonstrated CCL21 is upregulated in the brain following infection with *T. gondii* (2,5) and T cells associate with CCL21 filaments (2). CNS stromal cells, neurons and astrocytes are capable of expressing CCL21 in various models of CNS disease (9-12), however astrocytes are thought to be the primary producers of chemokines in the CNS following infection with *T. gondii* (13-16). As chemokine production by astrocytes may be a result of direct infection or stimulation by the inflammatory milieu, we first tested the conditions in which astrocytes upregulate CCL21. At the peak of systemic infection with *Toxoplasma*, circulating cytokines activate astrocytes, even before the parasite is thought to enter the brain (13). Therefore, to test if exposure to systemic cytokines can trigger CCL21 induction, primary murine astrocytes were cultured with media alone and with IFNγ, a cytokine important for control of intracellular pathogens and required to combat *T. gondii* replication. RNA was isolated from astrocyte cultures and tested for the production of CCL21 transcripts relative to a standard curve. However, stimulation with IFNγ is not sufficient to trigger CCL21 induction by astrocytes (Fig 3.1A). In order for CCL21 to act as a directional signal for infiltrating T cells to combat the parasite, it must be produced following infection. Upregulation of CCL21 mRNA was observed after stimulation with live

avirulent type II (Pru) ($p<0.001$) and virulent type I (RH) ($p<0.001$) parasite strains, indicating that cultured astrocytes must be invaded by or interact with parasites to start producing the CCL21 (Fig 3.1A). However, it is possible that parasite antigens may be sufficient to upregulate CCL21. To test if *T. gondii* derived protein can prompt CCL21 production, astrocytes were stimulated with soluble *Toxoplasma* antigen (sTAg). While stimulation with sTAg resulted in an elevated CCL21/HPRT ratio, this change never reached statistical significance. Therefore, astrocytes that interact with live parasites begin producing CCL21 during *T. gondii* infection.

Past studies from our lab have demonstrated that like CCL21, SPARC is upregulated in the cortex following infection with *T. gondii* (Nance et al. manuscript in preparation). Therefore we probed the same stimulated astrocyte cultures for the induction of SPARC transcripts (Fig. 3.1B). When stimulated with IFNγ, we observe no induction of SPARC. Similarly to our results with CCL21, stimulation with sTAg causes an increase in the average number of SPARC transcripts but this change did not result in statistical significance. SPARC transcripts were significantly induced following infection with Pru parasites ($p<0.05$), but not following infection with the more virulent RH strain (Fig. 3.1B), indicating there is a role for parasite strain-specific rhoptry proteins in the induction of SPARC.

To confirm that direct invasion by *T. gondii* is required to induce CCL21 production, rather than exposure to *Toxoplasma* protein or interaction that result in uninfected, injected cells, primary astrocytes were cultured in the presence of RH parasites (MOI 1:3) for three hours before any remaining extracellular parasites were removed and cells were incubated for an additional 21 hours. Cultured naïve and infected astrocytes were then fixed and stained for both SPARC and CCL21 by immunohistochemistry. Mirroring our PCR results, little SPARC or CCL21 protein is expressed in naïve astrocytes, while in infected astrocytes both proteins stain brightly (Fig 3.1C). In situ, low levels of constitutive SPARC and CCL21 expression have been reported in the CNS (17). In our hands, very little SPARC and CCL21 expression is detected in the cortex of naïve brains and staining for GFAP, an astrocyte marker, is dim (Fig. 3.1D). In chronically infected brains, and consistent with previous reports (2,14), GFAP is upregulated in the cortex, indicative of the morphological changes astrocytes undergo in response to CNS pathology. SPARC and CCL21 staining co-localize with reactive astrocytes (Fig. 3.1D), confirming that while damaged neurons can produce CCL21, astrocytes are the primary source of this chemokine and SPARC during chronic *T. gondii* infection. In addition, while few astrocytes in the brain interact with *Toxoplasma* (18), astrocytes throughout the cortex are expressing SPARC and CCL21, indicating that while infection may trigger initial upregulation, once the infection reaches the chronic stage astrocytes throughout the cortex secrete both molecules (Fig. 3.1D).

3.3.2 Production of CCL21 and SPARC transcripts is independent of parasite reactivation.

Results from figure 3.1 suggest that continued parasite invasion would lead to increased CCL21 production by astrocytes. Uncontrolled parasite replication occurs in the absence of IFNγ-secreting T cells (4). Therefore, to determine if CCL21 is induced due to increased parasite burden during re-activation of a latent infection, mice were infected with *T. gondii* and a chronic infection was allowed to establish. Then, mice were treated with a regimen of depleting antibodies targeting either CD4+ or CD8+ T cells. After treatment, mononuclear cells from the brain, spleen, and cervical lymph nodes were isolated from each group and flow cytometry was used to confirm cell depletion (Fig. 3.2A and data not shown). Parasite burden was assessed with control and T cell depleted mice, confirming that the loss of either CD4+ or CD8+ T cells leads to a sharp increase in the number of parasites found in the brain ($p<0.05$ and $p<0.01$, respectively) (Fig. 3.2B). Absolute copy numbers of SPARC and CCL21 were quantified using RT-PCR after RNA was extracted from the brains of T cell depleted and control mice. No changes in transcripts levels of these molecules were detected (Fig. 3.2C). In addition, absolute copy numbers of CCL19 and CXCL10 were quantified to access the impact on increased parasite burden on the expression levels of these chemokines. No changes in transcript levels were detected with the exception of a reduction in CXCL10 transcripts ($p<0.001$) in the

absence of CD4+ T cells (Fig. 3.2C). Taken together, these data demonstrate that neither SPARC nor chemokine production is enhanced in the brain upon parasite reactivation once a chronic infection is established.

3.3.3 Infection induced CCL21 transcripts are reduced in the absence of SPARC.

As CCL21 and SPARC have the same cellular source in the *T. gondii* infected brain, it was possible that the expression of CCL21 may be influenced by the absence of SPARC either directly through SPARC's role in regulating astrocyte proliferation (19) or indirectly through differences in astrocyte activation in an altered matrix environment (20)(Nance et al. manuscript in preparation). Therefore, primary astrocytes from WT and SPARC-/- mice were cultured with the same stimulants as those featured in Fig 3.1, as well as with a few additional treatments. As expected, WT astrocytes cultured with media and IFNγ, exhibited a low production of CCL21 transcripts. When astrocytes were stimulated with TNFα, another pro-inflammatory cytokine released early in response to a variety of insults, CCL21 mRNA levels were comparable to media alone (Fig. 3.3A). Cultures were stimulated with TGFβ, an anti-inflammatory and neuroprotective cytokine released during CNS inflammation, but this cytokine does not change CCL21 expression compared to the media control (Fig 3.3A). Stimulation with sTAg again did not increase transcript levels, while infection with both Pru

($p<0.01$) and RH ($p<0.05$) parasites caused an increase in CCL21 in WT astrocytes (Fig 3.3A).

For CCL21 to accurately draw T cells only toward infection sites, its expression must also be controlled by the absence of parasites. IFNγ stimulated astrocytes inhibit parasite replication through the activation of IFNγ induced GTPases (13) and are thought to help control parasite dissemination in the brain (21). Therefore, cultured astrocytes were primed with IFNγ for three hours prior to infection with RH parasites to determine if CCL21 transcripts are reduced if infection can be controlled. Indeed, the induction of CCL21 is abolished when cells are primed with IFNγ (Fig. 3.3A). In addition to producing CCL21, astrocytes express the two receptors for CCL21 (CCR7 and CXCR3) (22,23). Moreover, CCR7 is upregulated in response to inflammatory stimuli (22) and CCL21 stimulation can elicit astrocyte proliferation and Ca^{2+} signaling (23). Consequently, cultured astrocytes were stimulated with recombinant CCL21 protein to test if CCL21 induction can be propagated in a paracrine like manner. Astrocytes stimulated with CCL21 increase production of CCL21 transcripts, suggesting that the presence of CCL21 in the parenchyma is sufficient to drive CCL21 induction in neighboring astrocytes (Fig 3.3A).

In contrast to WT astrocytes, no significant induction of CCL21 transcripts can be observed in SPARC deficient astrocytes. Indeed, stimulation of SPARC-/-

astrocytes with IFNγ leads to a reduction of transcripts compared to cultures stimulated with media alone (Fig 3.3A). To examine the kinetics of CCL21 production in the brain over the course of infection, WT and SPARC-/- mice were infected and RNA was extracted from tissue samples taken at days 7, 14, 21, 28, and 42 post infection. CCL21 transcripts in the brains of infected WT mice followed kinetics similar to those previously reported (2,5) (Fig. 3.3B). In contrast, CCL21 production in the brain in the absence of SPARC peaks at day 7- much earlier than we would expect to see parasites and infiltrating T cells in the brain. Following this peak, transcripts steadily decline, returning to baseline levels late into the chronic phase of infection (Fig 3.3B). Despite these differences at the RNA level, CCL21 protein is produced in the brains of SPARC deficient mice at the chronic stage of infection and all of the CCL21 staining colocalizes with GFAP, indicating astrocytes are still the source of this chemokine in the absence of SPARC (Fig. 3.3C).

3.3.4 CCL21 does not coat the fibrous reticulum that forms during brain inflammation.

Previously published data from our lab has implicated SPARC in the formation of the reticular fibers that form upon infection in the brain (Nance et al. manuscript in preparation). This network, detected through second harmonic generation via multiphoton microscopy is associated with cell migration through the inflamed parenchyma (2). It was postulated that the network facilitates cell migration

through the brain because it is coated with CCL21 (2), similar to the collagenous network observed in the lymph node (24-26). Visualizing the reticulum in preserved/stained tissue sections is technically challenging because fixation abolishes the SHG signal (data not shown). Yet when tissue is flash frozen, we can find a few areas where the signal is preserved (Fig. 3.4A). Like previously published results (2), CCL21 staining can be observed as strands which appear similar to reticular strands. However, imaging these sections with two-photon microscopy reveals the fibers of CCL21 are separate from the SHG signal (Fig. 3.4A). Staining frozen sections for CCL21 and GFAP confirmed astrocytes as the cellular source of the chemokine (Fig. 3.4B). The SHG signal has already been reported as distinct from reactive astrocytes (2). Using this method we are able to observe CCL21 staining is entirely confined to areas of astrocyte staining in both WT and SPARC-/- mice (Fig 3B). This data, together with previous studies, show that while the SHG network is not coated in CCL21 and immune cells migrating along it are still responsive to CCL21 (Noor et al., 2016, submitted) bound to the surface of reactive astrocytes.

3.3.5 SPARC binds CCR7 ligands.

SPARC is well known to facilitate extracellular matrix remodeling (ECM) by binding to matrix components (27). Many matrix components are thought to be structural in nature to provide a scaffold for tissue growth and cell migration. However, chemokines are also secreted into the extracellular space and may be

subject to the same remodeling mechanisms as matrix constituents. Further, although we determined CCL21 in the brain does not bind to the reticular fibers generated in the brain upon infection, CCL21 in particular is known to bind matrix molecules through its basic C-terminal domain and has been theorized to prompt haptotaxis, cellular movement driven by matrix-bound chemokines within tissue (28). Indeed, as SPARC's N-terminal domain is acidic, we theorized that SPARC and CCL21 might interact directly, either facilitate remodeling within the extracellular space or to present CCL21 in the correct confirmation to elicit movement of infiltrating T cells. To test if they interact, recombinant SPARC and CCL21 were mixed and applied to a 50mL size exclusion column packed with Sephadex G-50. The absorbance at 280nm of each 2mL fraction eluted from the column was plotted on an elution profile (Fig. 3.5A). Three peaks appear on the elution profile, indicating that some of the proteins applied to the column elute together as a complex. To confirm this finding, the fractions that contained protein were concentrated and subjected to western blot. Both SPARC and CCL21 are detected in the first peak. The remaining SPARC elutes in the second peak and the remaining CCL21 elutes in the third peak (Fig. 3.5A). Next, microscale thermophoresis was used to independently verify the interaction and to quantify the dissociation constant. CCL21 was diluted using a 3:1 serial dilution ratio and titrated against SPARC. Using this method, the dissociation constant was calculated to be 772.3±250.4nM (R^2=0.84) (Fig. 3.5A), which is a value similar to SPARC's known interaction with collagen (1-2mM), but a much

weaker interaction than CCL21's known interaction with collagen (4.6nM). If SPARC binds CCL21 through its basic C terminus, we would expect that a chemokine that lacks such a domain would not interact with SPARC. Therefore, CCL19 was chosen to test if a basic C-terminus was necessary to bind to SPARC. Like CCL21, CCL19 binds to CCR7 to elicit cell migration, but unlike CCL21, it lacks a C terminal tail and consequently remains a soluble chemokine even when expressed in tissue (29). When gel filtration is repeated with recombinant CCL19, three distinct peaks are seen in the elution profile (Fig. 3.5B). Surprisingly, more protein elutes in the first peak than in the other peaks in the profile. Western blotting confirmed the majority of SPARC and CCL19 applied to the column elutes as a complex. Thermophoretic analysis using a 1:1 serial dilution ratio determined SPARC has a much higher affinity for CCL19 than CCL21 (2.6±0.85nM, R^2=0.9) (Fig. 3.5B). To determine if SPARC has some specificity or if it sticks to any protein it encounters, SPARC's capacity to bind CXCL10 was also tested. CXCL10 is another chemokine known to have a major influence on the migratory behavior of infiltrating T cells in the brain during *T. gondii* infection (3). CXCL10 belongs to a different subfamily of chemokines than CCL19 and CCL21 and signals through the receptor CXCR3. Repeating the gel filtration with CXCL10 reveals no peak where a protein complex should elute and a distinct peak where SPARC elutes (Fig. 3.5C). CXCL10 does not elute in a single peak, as the chemokine forms dimers and tetramers in solution (30). Thermophoresis estimates a dissociation constant of 77.3nM. However, the

standard error of this measurement is 45nM and the fit is poor (R^2=0.61) (Fig. 3.5C). At the highest CXCL10 concentrations, there is some indication that bi-phasic binding may be taking place between CXCL10 and SPARC. However, further studies are necessary to determine how those proteins might interact.

3.3.6 SPARC facilitates T cell migration.

During chronic *Toxoplasma gondii* infection, continual surveillance of the brain by T cells is required to keep parasites sequestered within latent cysts. We know CCL21 facilitates T cell entry into the brain parenchyma (1).

However, SPARC's effect on the migration of primary T cells in the brain has not been reported. In cancer models, SPARC expression is associated with increased metastasis (31,32). Therefore we hypothesized that the presence of SPARC may contribute to T cell migration behavior. We can model migration through tissue by seeding lymphocytes in artificial matrix. CD8+ dsRed T cells were isolated and suspended in matrigel with or without recombinant SPARC. T cell migration was imaged in response to no chemokine, a constant concentration of CCL21, or a gradient of CCL21. Then cells were tracked and migratory behavior was quantified. Normalizing cell tracks reveals cells travel further from their starting position under the influence of chemokine regardless of whether the chemokine exists as a gradient (Fig. 3.6A). However, by analyzing each cell's migratory behavior, cell speed, the distance they traveled, their

meandering index all increased ($p<0.05$), indicating T cells migrate more directly when SPARC is present in the extracellular matrix (Fig. 3.6B).

3.3.7 Reticular fibers formed upon infection facilitate efficient T cell entry into the brain.

Reticular ECM structures that support cell migration have been observed in a variety of inflammatory models, including *Toxoplasma* infection (2,33,34)(Nance et al. manuscript in preparation). Indeed, studies from our laboratory reveal SPARC plays a role in ensuring the formation of a dense and linear network instead of a tangled one (Nance et al. manuscript in preparation) in the cortex of the brain, where the majority of parasites reside. While the majority of the in vivo data in this dissertation focuses on the cortex, brains were excised at the peak of network formation (two weeks post infection, Nance et al., manuscript in preparation) to determine the extent to which the network forms in other areas of the brain. Fresh brains were sliced coronally and imaged with two-photon microscopy to visualize the reticular fibers. In WT mice, the fibers can be seen throughout the cortex and beyond (Fig. 3.7A). Second harmonics can also be observed in SPARC deficient brains in the same areas as WT brains, but the signal is diminished, due to the reduced organization and volume of the network formed in these mice (Fig. 3.7A, Nance et al. manuscript in preparation).

In order to determine how the absence of SPARC and the network affects T cell infiltration into the brain, WT and SPARC -/- mice were infected with a *T. gondii* strain designed to secrete ovalbumin (Pru-OVA) (35) and a chronic infection was allowed to establish. Twenty-eight days after infection, the mice received OVA specific dsRed+CD8+ T cells that were expanded in vitro, as previously described (2,36). One week later, brains were excised and two-photon microscopy was used to image the dsRed+ T cells that have entered the brain (Fig. 3.7B). In WT mice, cells are evenly distributed and the majority are associated with the fibrous network (Fig. 3.7B, left). In SPARC deficient mice, while cells are also associated with the network, the distribution of T cells is discontinuous. The majority of cells appear in sparsely populated areas of the cortex (Fig. 3.7B, center) with the exception of a small number of densely populated cell clusters (Fig. 3.7B, right). Flow cytometry analysis reveals that at this timepoint, and despite patches that contain a large number of cells, there is a significantly smaller proportion (Fig. 3.7C) and number (Fig. 3.7D) of both endogenous and adoptively transferred CD8+ OVA specific T cells in the brains of SPARC-/- mice. Previous studies have revealed SPARC-/- mice exhibit delayed control of parasite burden in the brain (Nance et al. manuscript in preparation). However, by six weeks after infection, these differences resolve. Thus despite evidence that SPARC enhances cell migration in vitro (Fig. 3.6) and a deformed fibrous network is limiting the access of T cells to the infected CNS

(Fig. 3.7B), the survival of SPARC-/- animals is equivalent to that of WT mice (Fig. 3.7E).

3.3.8 SPARC facilitates optimal CD8+ T cell migration in the brain.

Control of chronic *T. gondii* infection requires a constant presence of IFNγ secreting T cells in the brain. Thus, if the presence of SPARC enhances chemokine guided T cell migration in vitro (Fig. 3.6) and a deformed fibrous network is limiting the access of T cells to the infected CNS (Fig. 3.7), it was surprising to discover that the survival of SPARC-/- mice is unchanged compared to WT mice. To test if the absence of SPARC has a detrimental effect on T cell migration in vivo, the movement of OVA specific CD8+dsRed+ T cells was imaged over time in the chronically infected brains of WT and SPARC-/- mice. Representative still images of cells and their tracks in WT and SPARC-/- brains are shown in Fig. 3.8A. Despite defects in network formation in SPARC-/- mice, infiltrating T cells can clearly be seen migrating in close association with second harmonics. The number of cells per movie recorded reveals cells within a cluster in SPARC-/- mice is much higher than in normal fields of view in the same animals or in WT mice (Fig. 3.8B) Therefore, clusters were defined as any area that contained more than 100 cells in the field of view. Flower plots of cell tracks show that the majority of CD8+ T cells in SPARC-/- are less displaced than in WT mice through cells within SPARC-/- clusters are capable of migrating distances similar to those migrating in the presence of SPARC (Fig. 3.8C).

Finally, data quantifying cell speed, displacement and meandering were plotted and compared (Fig. 3.8D-F). Cells migrating in SPARC deficient brains and a significantly lower velocity, displacement, and meandering index than cells migrating in WT brains ($p<0.0001$). When cell migrating within SPARC-/- clusters are compared to those migrating outside the clusters, cell velocity and meandering index is increased within the cluster (Fig 3.8G and I). This is in line with previous observations that cell speed is high when number of infiltrating T cells are also high (2). An increased meandering index among clustered cells may be in direct contrast with reports of more localized cell clustering with fewer cells (2,37). However, that behavior is consistently attributed to finding an infected target or a professional antigen-presenting cell. SPARC-/- clusters are large and densely populated with fast moving cells. Apart from a few outlying cells, the majority of cells migrating within a SPARC-/- cluster are significantly less displaced (Fig. 3.3H). Therefore it is more likely that SPARC-/- clusters identify an easy access point for T cells to gain access to the brain in mice with disordered matrix and lower CCL21 expression. Overall, while the differences between WT and SPARC-/- mice are significant, they are so slight that they are unlikely to be biologically significant, as there are plenty of cells in SPARC-/- brains that are migrating just as fast, far and in a directed manner as there are in WT brains.

3.4 DISCUSSION

Many studies have reported CCL21 and SPARC induction in the CNS in response to inflammation in the brain (17). We have also reported upregulation of both molecules following infection with *Toxoplasma gondii* (2,5)(Nance et al. manuscript in preparation). Indeed we have observed cables of both SPARC and CCL21 in association with parasites and infiltrating immune cells (2)(Nance et al. manuscript in preparation). This led us to theorize that infection in the brain leads to localized production of SPARC and CCL21 which bind to ECM molecules to optimize cell migration and provide directional cues resulting in an immobilized chemokine gradient. This could guide or facilitate migration of infiltrating T cells in infected areas of the brain.

This hypothesis is especially appealing as it would provide an underlying mechanism of control to explain why the majority of infected individuals show no symptoms of neurological disease despite a robust immune response in the brain. The immune response in the brain is very tightly controlled and a chemokine gradient would allow T cells to target infected cells while avoiding non-specific inflammation induced cell death. In support of this hypothesis, our lab has shown that CCL21 deficient animals have an increased parasite burden in the brain and that constitutive over-expression of CCL21 by astrocytes throughout the brain (i.e. in both infected and uninfected areas) causes a high degree of variability in parasite burden, indicating that T cells are less efficient at

homing to sites of infection if CCL21 is expressed at equivalent levels everywhere (1). Further, as critical components of the blood-brain barrier, it is likely that astrocytes are exposed to circulating cytokines like IFNγ, TNFα, and TGFβ even before the parasite can disseminate to the brain (38), yet these stimuli do not upregulate CCL21 (Fig. 3.3A). Therefore it was important to test if direct invasion by the parasite triggered CCL21 induction. Invasion by tachyzoites can lead to chemokine production in a variety of cells (13,39-42). Nonetheless, in order to exist as a gradient within tissue, CCL21 expression must be highest were active parasite replication is occurring (Fig 3.1). In vivo, it is extraordinarily unlikely that the parasite has infected or interacted with every astrocyte in the CNS (18,43). However, we observe astrocyte activation and CCL21 staining throughout the cortex (Fig 3.1D and 3.3C). Therefore our finding that CCL21 protein can promote CCL21 upregulation in naïve astrocytes offers a mechanism to explain the propagation of CCL21 signaling throughout the astrocyte network (Fig. 3.3).

Alternatively, it is possible that CCL21 expression by reactive astrocytes is simply a mechanism to attract T cells to the brain parenchyma from the extraparenchymal spaces (1). Further, while the parasite does not encyst within every neuron (18), neuronal damage appears to be more widespread than the rare individual infected neuron, as shown by patches of corrupted neurons observed in this model (44,45) indicating that the immune response in the brain

may target more than a few infected cells. Indeed, analysis of the migration of effector T cells in the brain reveals they exhibit a Levy walk behavior and show little to no directed movement (3), although CCL21 may be one of many signals the T cell uses to stop its Levy flight and investigate a particular area. Additionally, while we can't exclude some neurons might produce CCL21 in this model, the vast majority of the CCL21 we detect histologically is produced by astrocytes throughout the cortex of the brain and does not obviously exist as a gradient, either illustrating the limitation of the technique or supporting that the damage to the CNS is more prevalent in this model than originally appreciated.

SPARC expression by reactive astrocytes is also a common feature in the CNS during injury and disease (46). Therefore, it was not remarkable to discover the circumstances of SPARC expression in vitro are similar to those that lead to CCL21 induction (Fig. 3.1A and B). However, as CCL21 protein can be detected in the astrocytes of infected SPARC deficient mice (Fig. 3.3C and 3.4B), it was surprising to see SPARC is needed for optimal expression of CCL21 at the mRNA level (Fig. 3.3A), although a reduction in CCL21 expression may be a mechanism to explain increased accumulation of T cells in extraparenchymal spaces in chronically infected mice that lack SPARC (Nance et al. manuscript in preparation). Moreover, CCL21 does not bind to the reticular fibers that are formed in the brain during infection but rather remain bound to the surface of the astrocyte independently of the presence of SPARC.

The biological significance of SPARC's interaction with chemotactic cytokines in the inflamed brain is probably multifaceted. First, binding to SPARC may help keep chemokines in a confirmation that will most effectively interact with their respective receptors on the surface of a migrating cell, eliciting optimal movement so that the cell can find its target efficiently. SPARC's interaction with CCR7 ligands specifically, may contribute to the maintenance of an extracellular gradient of either CCL21 or CCL19. While CXCL10 needs to be present for ideal migratory speed (3), it does not necessarily need to exist in a gradient to exert its effects on T cells. In addition, SPARC may be needed to clear excess chemokine from the ECM to maintain a gradient, employing a stabilin-1 mediated mechanism similar to the way SPARC facilitates collagen remodeling (27,47). Additionally, SPARC's role in ECM remodeling likely helps to accommodate immune cell infiltration into the brain independently of its interaction with chemokines. Indeed, SPARC's presence in our in vitro assays of cell migration lead to increased cell velocity, which could support either scenario. Additional studies are necessary to determine the site(s) to which CCL21 and CCL19 bind to SPARC and whether those interactions would help or hinder SPARC's other known functions.

The astrocyte's capacity to produce both SPARC and CCL21 does not appear to depend on factors that are continually secreted from infiltrating T cells. These

results are in direct contrast to a recent report that SPARC expression in astrocytes is rapidly regulated by T cell derived cytokines in an animal model of multiple sclerosis (48). In vitro experiments indicate that CCL21 and SPARC are not upregulated in response to the effector cytokine IFNγ and only through interaction/infection with live parasites (Fig. 3.1A and 3.3A). As priming with IFNγ before infection lead to a decrease in CCL21 transcripts, control of parasite replication would diminish CCL21 production because T cell recruitment should no longer be necessary. Therefore continued parasite invasion in the absence of T cells should lead to an increase of CCL21 and SPARC expression. However, this is not the case (Fig. 3.2C). SPARC and CCL21 expression is independent of parasite burden as the depletion of CD4+ or CD8+ T cells from chronically infected mice did not change the expression of these molecules at the mRNA level, nor did it change the expression of CCL19 (Fig. 3.2C). The only change detected in the absence of T cells was a reduction in CXCL10 following the depletion of CD4+ T cells from the brain, perhaps as a compensatory mechanism to control the influx of cytotoxic T cells in the absence of CD4+ T regulatory cells (Fig. 3.2C). These results may point to a mechanism in which CCL21 expression in the parenchyma reaches a maximum limit after being prompted by infection or another, still unknown trigger. It is also possible that other mechanisms are in place to prevent overexpression of chemokines to avoid inflammation induced CNS damage even during reactivation of *T. gondii*, such as TGFβ signaling (44).

Independent of its interaction with chemokines, SPARC exerts influence on cell migration behavior by organizing the scaffold upon which cells migrate (Nance et al. manuscript in preparation) and facilitating cell movement, both in the presence and absence of chemokines in vitro (Fig. 3.6). Therefore it was important to determine the impact SPARC has on cell migration in vivo. The absence of SPARC leads to slight delays in the acute and adaptive immune response (Nance et al. manuscript in preparation), and a decrease in the number of antigen specific T cells recruited to the brain (Fig 3.7C and D). Further, T cell distribution is patchy in the absence of SPARC with large numbers of T cells accumulating in a few clusters in the cortex while the rest are sparsely distributed (Fig. 3.7B). These findings indicate that SPARC plays a role in regulating T cell entry and accumulation in the brain. Previous work has determined that the absence of SPARC leads to a transient increase in parasite burden in the brain (Nance et al. manuscript in preparation). This may be due to the ability of T cells to access the CNS or point to impaired cell migration within the brain. Thus it was important to quantify cell migration behavior with the CNS in the absence of SPARC. Measuring cell velocity, displacement and meandering indicated a small but significant decrease in all parameters in the absence of SPARC. Therefore it is tempting to conclude that SPARC is required to facilitate cell migration in vivo and that migratory defect is at least partially due to SPARC's role in maintaining chemokine gradients in the brain (due to the decrease in average meandering index in the absence of SPARC). However there are plenty

of cells that are migrating just as fast, far and in a directed manner in the absence of SPARC as they are in WT mice, especially those cells present in SPARC-/- clusters. Therefore the poor initial control of parasite burden is probably a better indicator of the importance of the reticular fibers early in infection to facilitate effector cell infiltration into the brain. Whereas later in infection, the fibers partially resolve along with differences in parasite burden between WT and SPARC-/- mice, indicating that once T cells have access to the CNS, they are able to control parasite replication regardless of the presence of SPARC.

In conclusion, these data show infection of astrocytes leads to increased CCL21 and SPARC production and the upregulation of those molecules propagates throughout the astrocyte network. Rather than binding to the network of fibers induced with SPARC's help by infection, CCL21 remains bound to the surface of the astrocyte. Therefore the ECM network provides structural support for the migration of infiltrating T cells while CCL21 exerts its influence on T cells while remaining bound to the astrocyte surface, much like the chemokine peppered fibroblast network found in the secondary lymphoid organs.

3.5 FIGURES AND LEGENDS

Figure 3.1. CCL21 and SPARC are expressed by murine astrocytes upon infection. (A and B) Primary astrocyte cultures were infected with the Pru or RH strain of *T. gondii*, or stimulated with sTAg or IFNγ or media alone. Real-time RT-PCR was conducted to determine the absolute copy numbers of CCL21 and SPARC transcripts compared to those of the reference gene HPRT using a standard curve. (C) Primary astrocyte cultures infected with *T. gondii* were stained for CCL21 (red) and SPARC (green). The red arrow indicates the small nuclei of replicating parasites. (D) Brains of naïve and chronically infected mice were stained for GFAP (white), CCL21 (red), and SPARC (green). Expression data was analyzed using the student's T test. *$p<0.05$, ***$p<0.001$

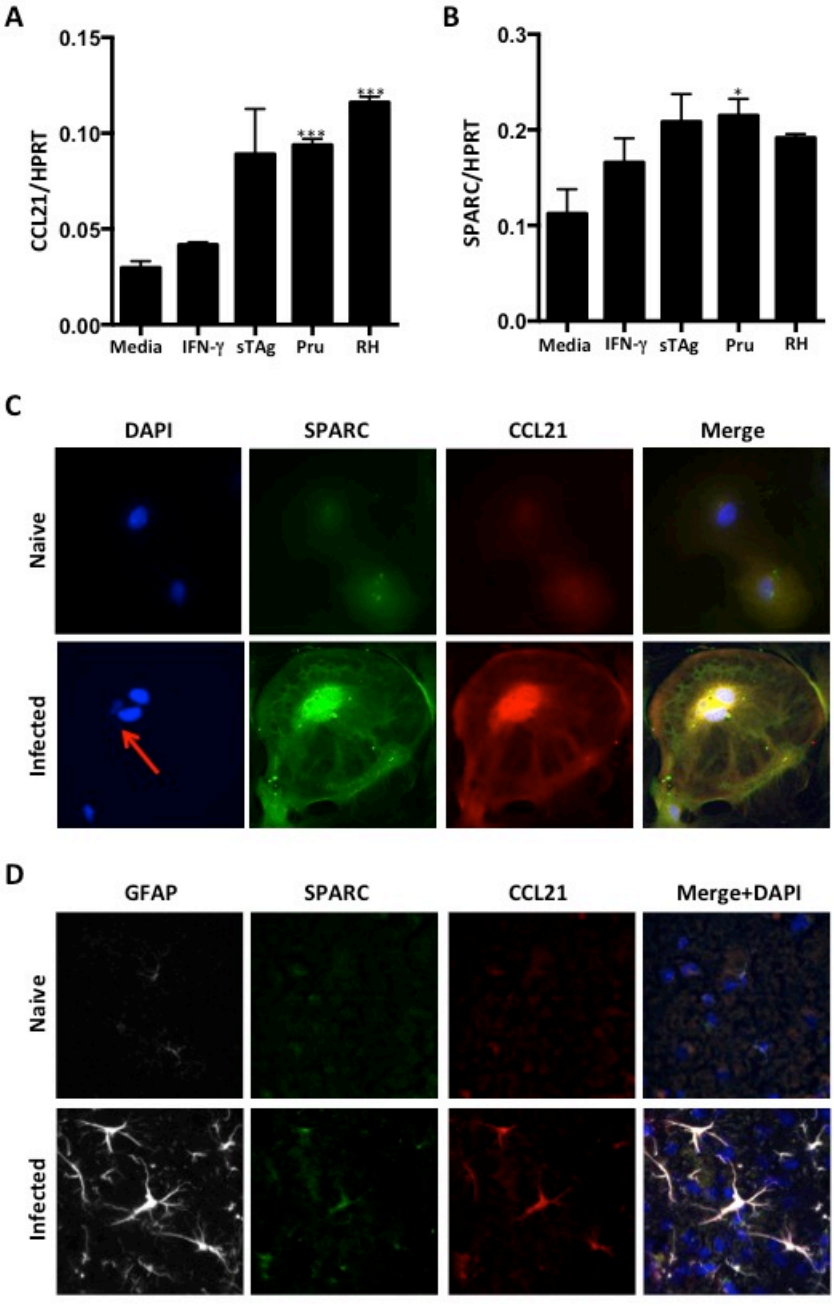
A
0.15
0.10
0.05
0.00
CCL21/HPRT
***
***
Media
IFN-γ
sTAg
Pru
RH
B
0.3
0.2
0.1
0.0
SPARC/HPRT
*
Media
IFN-γ
sTAg
Pru
RH
C
DAPI
SPARC
CCL21
Merge
Naive
Infected
D
GFAP
SPARC
CCL21
Merge+DAPI
Naive
Infected

Figure 3.2. SPARC and CCL21 expression does not increase during parasite reactivation. T cell subsets were depleted from chronically infected mice and RNA isolated from the brain was probed for SPARC and chemokine transcripts. (A) Flow cytometry analysis on brain mononuclear cells confirmed depletion of T cells in the brain. (B) Parasite burden increases in the absence of either subset of T cell. (C) RNA isolated from the brain was probed for SPARC, CCL21, CCL19, and CXCL10 transcripts. Flow cytometry and expression data was analyzed using the student's T test. *$p<0.05$, **$p<0.01$, ***$p<0.001$

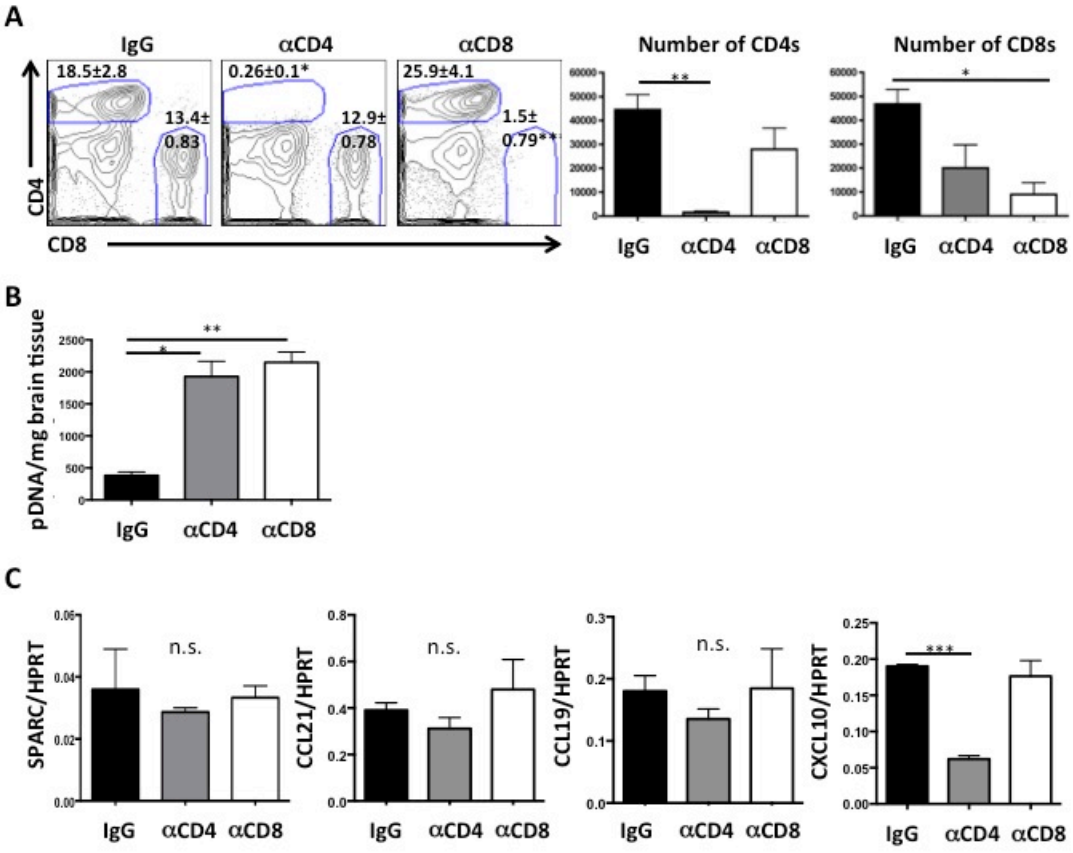
A
IgG
αCD4
αCD8
18.5±2.8
13.4±
0.83
0.26±0.1*
12.9±
0.78
25.9±4.1
1.5±
0.79**
CD4
CD8
Number of CD4s
Number of CD8s
**
*
IgG
αCD4
αCD8
B
pDNA/mg brain tissue
**
*
IgG
αCD4
αCD8
C
SPARC/HPRT
CCL21/HPRT
CCL19/HPRT
CXCL10/HPRT
n.s.
n.s.
n.s.
***
IgG
αCD4
αCD8

Figure 3.3. CCL21 expression in SPARC -/- mice is reduced. (A) Primary WT and SPARC -/- astrocytes were infected with the Pru or RH strain of *T. gondii*, or stimulated with sTAg, the cytokines IFNγ, TNFα, TGFβ, the chemokine CCL21, or media alone. Real-time RT-PCR was conducted to determine the absolute copy numbers of CCL21 and SPARC transcripts compared to those of the reference gene HPRT using a standard curve. B. Differences in CCL21 expression in the brains of naïve and infected WT and SPARC-/- mice were quantified by real-time RT-PCR using the standard curve method. Results are reported as a ratio of CCL21 transcripts over HPRT transcripts. C. Brains from chronically infected WT and SPARC-/- mice were stained for GFAP (white), SPARC (green), and CCL21 (red) by IHC. Expression data was analyzed using the student's T test. *$p<0.05$, **$p<0.01$

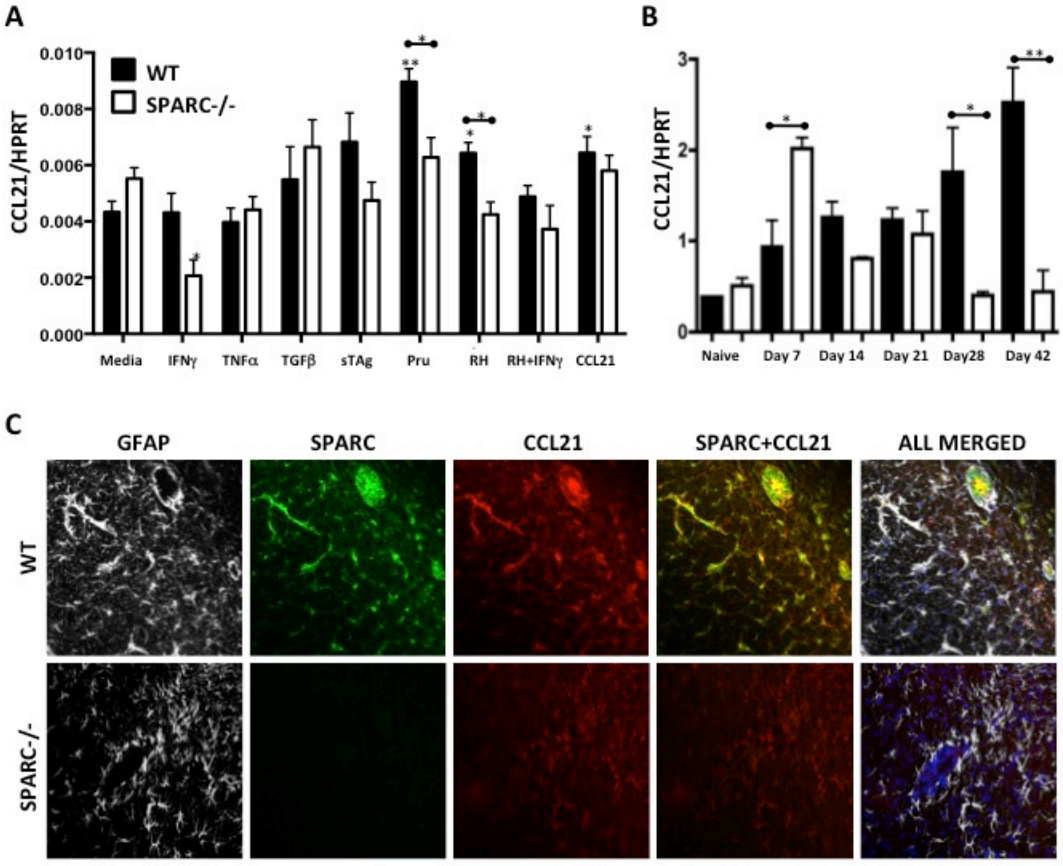
A
CCL21/HPRT
0.010
0.008
0.006
0.004
0.002
0.000
WT
SPARC-/-
Media
IFNγ
TNFα
TGFβ
sTAg
Pru
RH
RH+IFNγ
CCL21
B
CCL21/HPRT
3
2
1
0
Naive
Day 7
Day 14
Day 21
Day28
Day 42
C
GFAP
SPARC
CCL21
SPARC+CCL21
ALL MERGED
WT
SPARC-/-

Figure 3.4. CCL21 and SHG are distinct. Flash frozen WT and SPARC-/- tissue sections were stained for CCL21 and imaged using multiphoton microscopy to visualize second harmonic signals found in the brain. A. CCL21 appears as strands that are separate from strands of SHG. B. CCL21-stained sections were counterstained with GFAP.

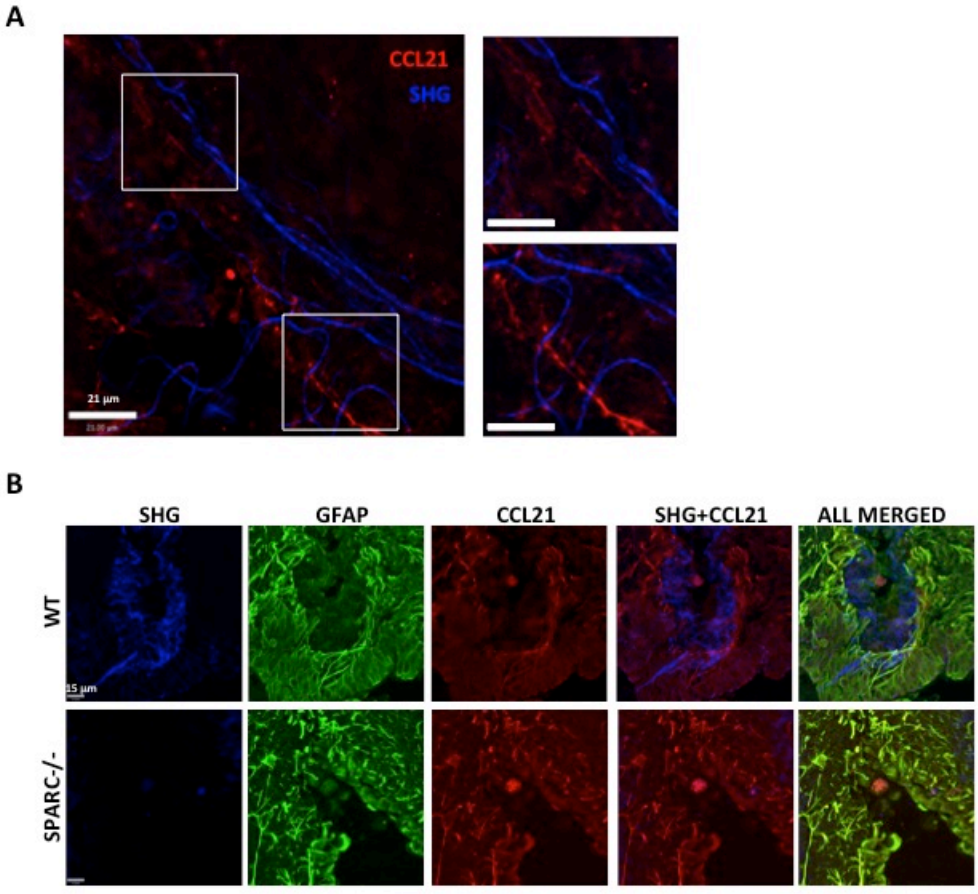
A
CCL21
SHG
21 µm
B
SHG
GFAP
CCL21
SHG+CCL21
ALL MERGED
WT
SPARC-/-
15 µm

Figure 3.5. SPARC interacts directly with CCR7 ligands. Recombinant SPARC was incubated with CCL21, CCL19, CXCL10, or BSA and the mixture was then applied to a Sephadex G-50 column. The elution profiles for SPARC+CCL21 (A), SPARC+ CCL19 (B), SPARC+CXCL10 (C) and the corresponding western blots and thermophoretic plots are shown. Values presented are the estimated dissociation constants ± SEM.

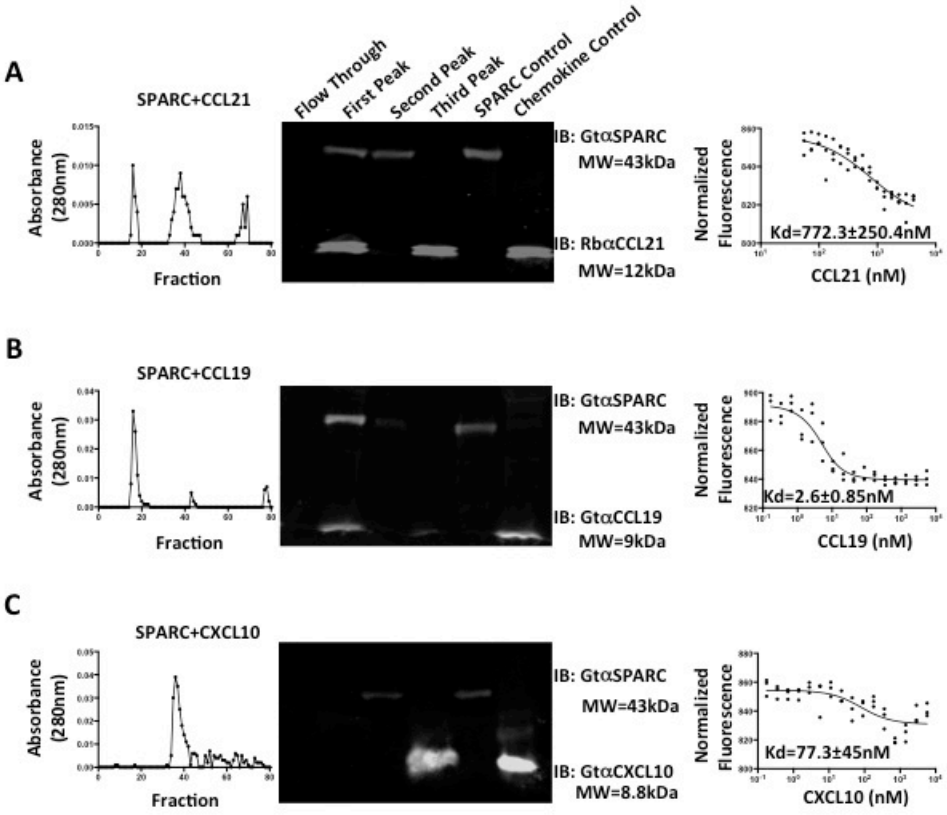
A
SPARC+CCL21
Flow Through
First Peak
Second Peak
Third Peak
SPARC Control
Chemokine Control
Absorbance (280nm)
Fraction
IB: GtαSPARC
MW=43kDa
IB: RbαCCL21
MW=12kDa
Normalized Fluorescence
Kd=772.3±250.4nM
CCL21 (nM)
B
SPARC+CCL19
Absorbance (280nm)
Fraction
IB: GtαSPARC
MW=43kDa
IB: GtαCCL19
MW=9kDa
Normalized Fluorescence
Kd=2.6±0.85nM
CCL19 (nM)
C
SPARC+CXCL10
Absorbance (280nm)
Fraction
IB: GtαSPARC
MW=43kDa
IB: GtαCXCL10
MW=8.8kDa
Normalized Fluorescence
Kd=77.3±45nM
CXCL10 (nM)

Figure 3.6. T cell migration is enhanced in the presence of SPARC. dsRed+ T cells were seeded in matrigel in the presence or absence of recombinant SPARC. Their migration was imaged in response to no chemokine, a constant concentration of chemokine, or a chemokine gradient over 20 min. Videos of cell migration were analyzed. (A) Tracks of T cells migrating in response to media alone, a constant chemokine stimulation, or in response to a gradient of CCL21 were normalized to begin at the origin to visualize migration trends. Cell velocity (B), displacement (C), and meandering index (D) were quantified. Migration data was analyzed using the student's T test. *$p<0.05$, ***$p<0.001$

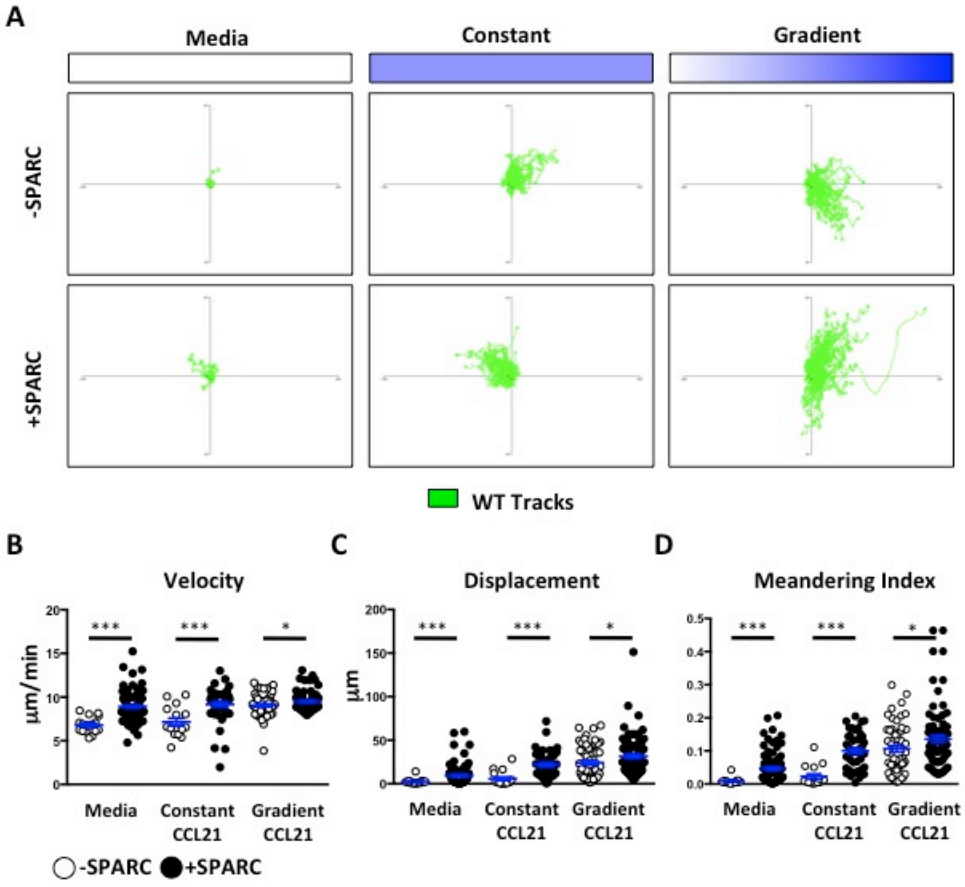
A
Media
Constant
Gradient
-SPARC
+SPARC
WT Tracks
B
Velocity
µm/min
***
***
*
Media
Constant CCL21
Gradient CCL21
-SPARC
+SPARC
C
Displacement
µm
***
***
*
Media
Constant CCL21
Gradient CCL21
D
Meandering Index
***
***
*
Media
Constant CCL21
Gradient CCL21

Figure 3.7. SHG network facilitates efficient T cell entry into the brain. (A) Brain were excised from mice two weeks post-infection, then whole coronal sections were imaged with two-photon microscopy. (B) WT and SPARC-/- mice were infected with Pru-OVA for 28 days then adoptively transferred with OVA specific CD8+ T cells. 2x2 tiled images were taken of the cortex using two-photon microscopy to visualize the distribution of T cells infiltrating the brain. (C) Flow cytometry plots of endogenous and transferred OVA specific T cells in chronically infected WT and SPARC-/- mice. (D) Absolute cell numbers of both endogenous and transferred OVA specific T cells isolated from chronically infected WT and SPARC-/- mice. (E) Survival curve of WT and SPARC-/- mice. Flow cytometry data was analyzed using the student's T test. Survival data was analyzed using the log-rank test. *$p<0.05$

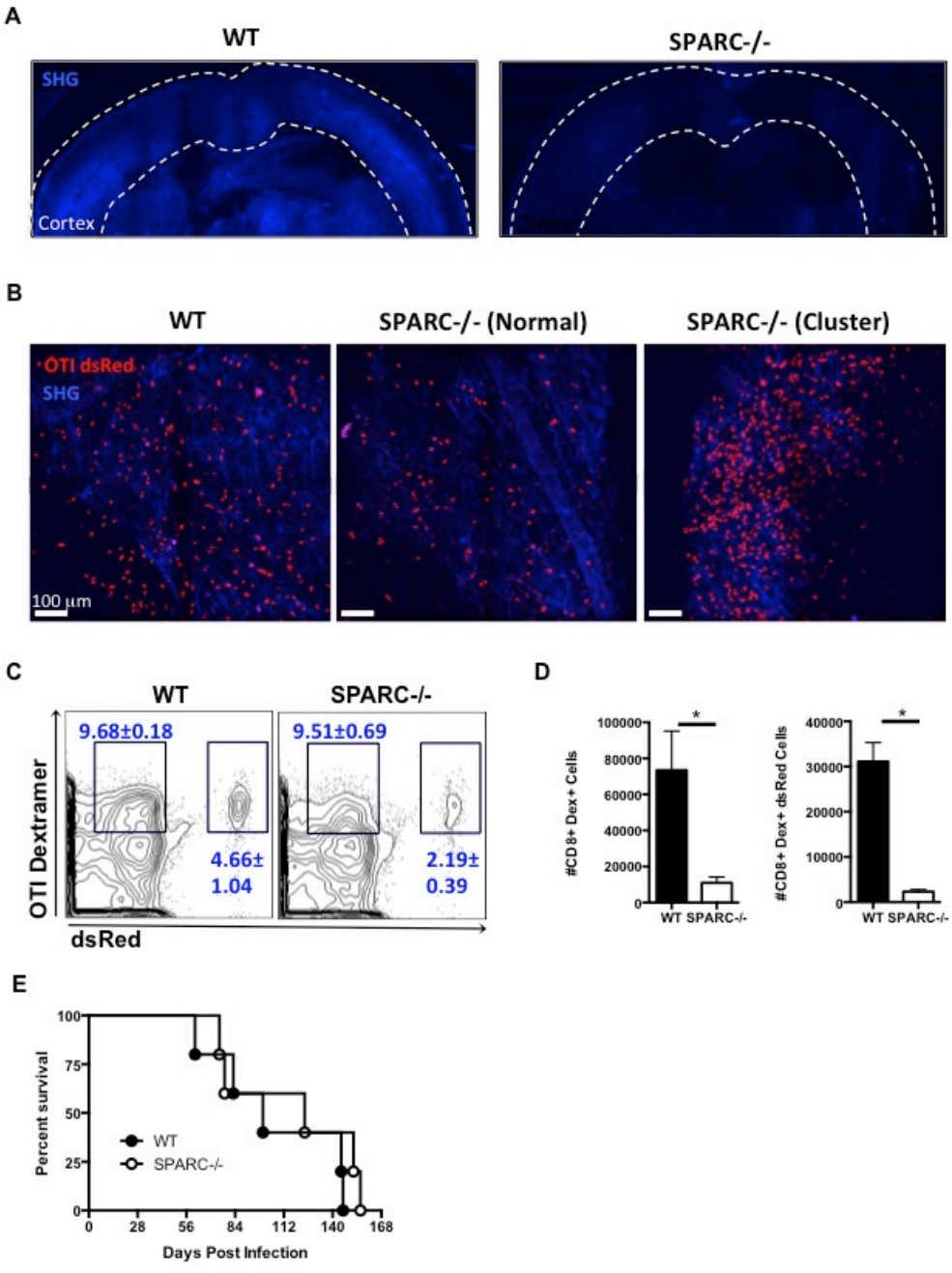
A
WT
SPARC-/-
SHG
Cortex
B
WT
SPARC-/- (Normal)
SPARC-/- (Cluster)
OTI dsRed
SHG
100 µm
C
WT
SPARC-/-
9.68±0.18
9.51±0.69
4.66±
1.04
2.19±
0.39
OTI Dextramer
dsRed
D
#CD8+ Dex+ Cells
#CD8+ Dex+ dsRed Cells
WT SPARC-/-
WT SPARC-/-
E
Percent survival
WT
SPARC-/-
Days Post Infection

Figure 3.8. SPARC facilitates optimal CD8+ T cell migration in the brain. Videos imaged of cell migration in the infected brain were analyzed. (A) Still images of OTI-dsRed T cell behavior in WT and SPARC-/- mice. (B) Number of cells in the field of view per movie imaged for each genotype. (C) Flower plots showing cell tracks normalized to the origin. Velocity (D), displacement (E), and meandering index (F) for cells migrating in WT and SPARC-/- brains were quantified. Velocity (G), displacement (H), and meandering index (I) for cells migrating in SPARC-/- clusters brains were compared to cells migrating in normal areas of infiltration. Clusters were defined as any area that contained more than 100 cells in the field of view. Migration data was analyzed using the Mann-Whitney test. **p<0.01, ****p<0.0001

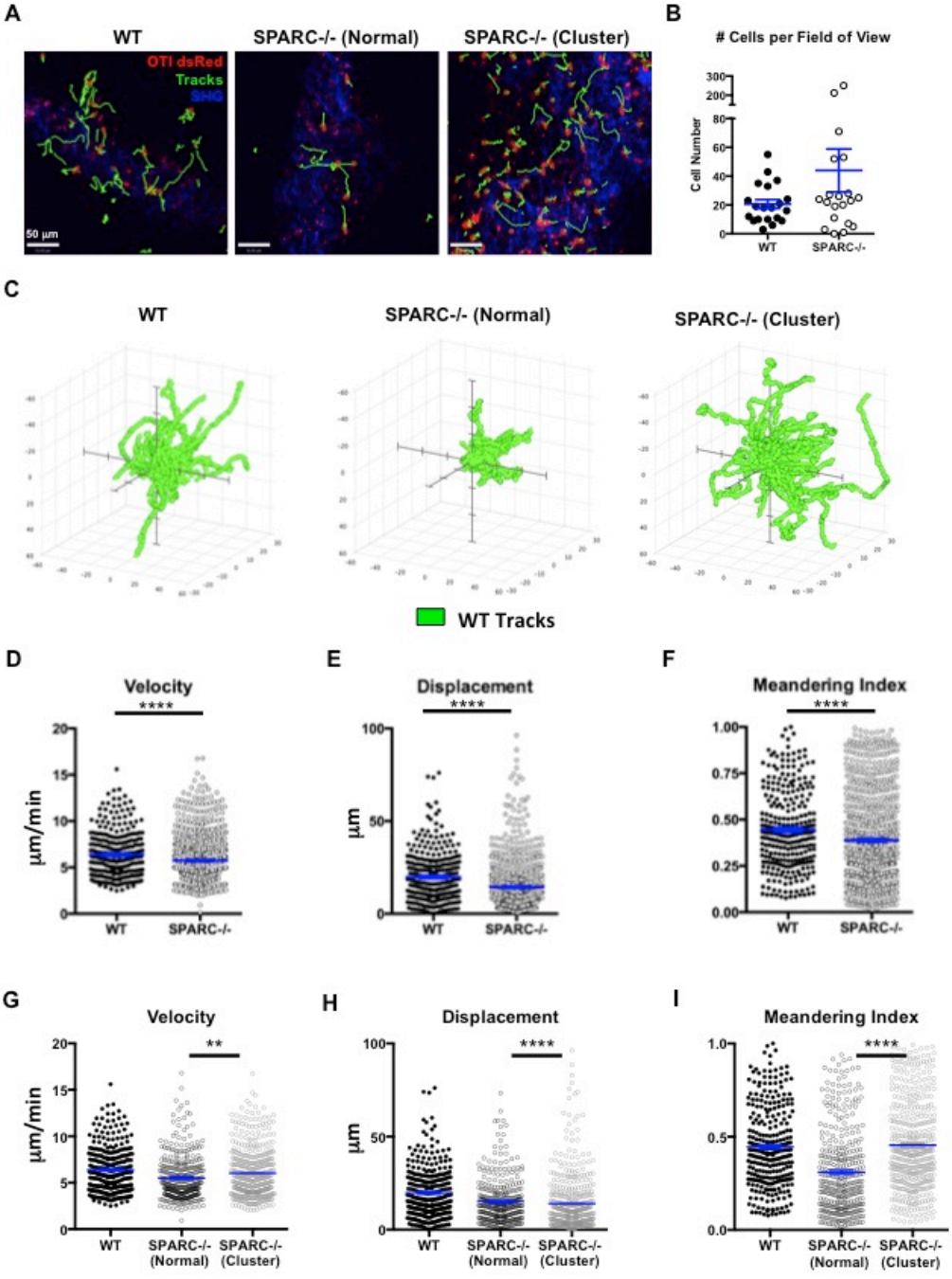
A
WT
SPARC-/- (Normal)
SPARC-/- (Cluster)
OTI dsRed
Tracks
SHG
50 µm
B
Cells per Field of View
Cell Number
WT
SPARC-/-
C
WT
SPARC-/- (Normal)
SPARC-/- (Cluster)
WT Tracks
D
Velocity
****
µm/min
WT
SPARC-/-
E
Displacement
****
µm
WT
SPARC-/-
F
Meandering Index
****
WT
SPARC-/-
G
Velocity
**
µm/min
WT
SPARC-/- (Normal)
SPARC-/- (Cluster)
H
Displacement
****
µm
WT
SPARC-/- (Normal)
SPARC-/- (Cluster)
I
Meandering Index
****
WT
SPARC-/- (Normal)
SPARC-/- (Cluster)

2.6 REFERENCES

1. Ploix, C. C., Noor, S., Crane, J., Masek, K., Carter, W., Lo, D. D., Wilson, E. H., and Carson, M. J. (2011) CNS-derived CCL21 is both sufficient to drive homeostatic CD4+ T cell proliferation and necessary for efficient CD4+ T cell migration into the CNS parenchyma following Toxoplasma gondii infection. *Brain Behav Immun* **25**, 883-896

2. Wilson, E. H., Harris, T. H., Mrass, P., John, B., Tait, E. D., Wu, G. F., Pepper, M., Wherry, E. J., Dzierzinski, F., Roos, D., Haydon, P. G., Laufer, T. M., Weninger, W., and Hunter, C. A. (2009) Behavior of parasite-specific effector CD8+ T cells in the brain and visualization of a kinesis-associated system of reticular fibers. *Immunity* **30**, 300-311

3. Harris TH, B. E., Christian DA, Konradt C, Tait Wojno ED, Norose K, Wilson EH, John B, Weninger W, Luster AD, Liu AJ, Hunter CA. (2012) Generalized Lévy walks and the role of chemokines in migration of effector CD8+ T cells. *Nature* **486**, 545-548

4. Gazzinelli, R., Xu, Y., Hieny, S., Cheever, A., and Sher, A. (1992) Simultaneous depletion of CD4+ and CD8+ T lymphocytes is required to reactivate chronic infection with Toxoplasma gondii. *J Immunol* **149**, 175-180

5. Noor, S., Habashy, A. S., Nance, J. P., Clark, R. T., Nemati, K., Carson, M. J., and Wilson, E. H. (2010) CCR7-dependent immunity during acute Toxoplasma gondii infection. *Infect Immun* **78**, 2257-2263

6. Sangaletti, S., Gioiosa, L., Guiducci, C., Rotta, G., Rescigno, M., Stoppacciaro, A., Chiodoni, C., and Colombo, M. P. (2005) Accelerated dendritic-cell migration and T-cell priming in SPARC-deficient mice. *J Cell Sci* **118**, 3685-3694

7. Sangaletti, S., Stoppacciaro, A., Guiducci, C., Torrisi, M. R., and Colombo, M. P. (2003) Leukocyte, rather than tumor-produced SPARC, determines stroma and collagen type IV deposition in mammary carcinoma. *J Exp Med* **198**, 1475-1485

8. Rotta, G., Matteoli, G., Mazzini, E., Nuciforo, P., Colombo, M. P., and Rescigno, M. (2008) Contrasting roles of SPARC-related granuloma in bacterial containment and in the induction of anti-Salmonella typhimurium immunity. *J Exp Med* **205**, 657-667

9. Biber, K., Sauter, A., Brouwer, N., Copray, S. C., and Boddeke, H. W. (2001) Ischemia-induced neuronal expression of the microglia attracting

chemokine Secondary Lymphoid-tissue Chemokine (SLC). *Glia* **34**, 121-133

10. Biber, K., Vinet, J., and Boddeke, H. W. (2008) Neuron-microglia signaling: chemokines as versatile messengers. *J Neuroimmunol* **198**, 69-74

11. de Haas, A. H., van Weering, H. R., de Jong, E. K., Boddeke, H. W., and Biber, K. P. (2007) Neuronal chemokines: versatile messengers in central nervous system cell interaction. *Mol Neurobiol* **36**, 137-151

12. Cupovic, J., Onder, L., Gil-Cruz, C., Weiler, E., Caviezel-Firner, S., Perez-Shibayama, C., Rulicke, T., Bechmann, I., and Ludewig, B. (2016) Central Nervous System Stromal Cells Control Local CD8(+) T Cell Responses during Virus-Induced Neuroinflammation. *Immunity* **44**, 622-633

13. Wilson, E. H., and Hunter, C. A. (2004) The role of astrocytes in the immunopathogenesis of toxoplasmic encephalitis. *Int J Parasitol* **34**, 543-548

14. Hunter, C. A., Roberts, C. W., and Alexander, J. (1992) Kinetics of cytokine mRNA production in the brains of mice with progressive toxoplasmic encephalitis. *Eur J Immunol* **22**, 2317-2322

15. Strack, A., Asensio, V. C., Campbell, I. L., Schluter, D., and Deckert, M. (2002) Chemokines are differentially expressed by astrocytes, microglia and inflammatory leukocytes in Toxoplasma encephalitis and critically regulated by interferon-gamma. *Acta Neuropathol* **103**, 458-468

16. Amichay, D., Gazzinelli, R. T., Karupiah, G., Moench, T. R., Sher, A., and Farber, J. M. (1996) Genes for chemokines MuMig and Crg-2 are induced in protozoan and viral infections in response to IFN-gamma with patterns of tissue expression that suggest nonredundant roles in vivo. *J Immunol* **157**, 4511-4520

17. Lalor, S. J., and Segal, B. M. (2010) Lymphoid chemokines in the CNS. *J Neuroimmunol* **224**, 56-61

18. Cabral, C. M., Tuladhar, S., Dietrich, H. K., Nguyen, E., MacDonald, W. R., Trivedi, T., Devineni, A., and Koshy, A. A. (2016) Neurons are the Primary Target Cell for the Brain-Tropic Intracellular Parasite Toxoplasma gondii. *PLoS Pathog* **12**, e1005447

19. Eroglu, C. (2009) The role of astrocyte-secreted matricellular proteins in central nervous system development and function. *J Cell Commun Signal* **3**, 167-176

20. Johnson, K. M., Milner, R., and Crocker, S. J. (2015) Extracellular matrix composition determines astrocyte responses to mechanical and inflammatory stimuli. *Neurosci Lett* **600**, 104-109

21. Stenzel, W., Rohn, G., Miletic, H., Radner, H., Deckert, M., and Ernestus, R. I. (2004) Diagnostic impact of ornithine decarboxylase in meningiomas. *J Neurooncol* **66**, 59-64

22. Gomez-Nicola, D., Pallas-Bazarra, N., Valle-Argos, B., and Nieto-Sampedro, M. (2010) CCR7 is expressed in astrocytes and upregulated after an inflammatory injury. *J Neuroimmunol* **227**, 87-92

23. van Weering, H. R., de Jong, A. P., de Haas, A. H., Biber, K. P., and Boddeke, H. W. (2009) CCL21-induced calcium transients and proliferation in primary mouse astrocytes: CXCR3-dependent and independent responses. *Brain Behav Immun* **24**, 768-775

24. Yang, B. G., Tanaka, T., Jang, M. H., Bai, Z., Hayasaka, H., and Miyasaka, M. (2007) Binding of lymphoid chemokines to collagen IV that accumulates in the basal lamina of high endothelial venules: its implications in lymphocyte trafficking. *J Immunol* **179**, 4376-4382

25. Worbs, T., Mempel, T. R., Bolter, J., von Andrian, U. H., and Forster, R. (2007) CCR7 ligands stimulate the intranodal motility of T lymphocytes in vivo. *J Exp Med* **204**, 489-495

26. Okada, T., and Cyster, J. G. (2007) CC chemokine receptor 7 contributes to Gi-dependent T cell motility in the lymph node. *J Immunol* **178**, 2973-2978

27. Bradshaw, A. D. (2009) The role of SPARC in extracellular matrix assembly. *J Cell Commun Signal* **3**, 239-246

28. Weber, M., Hauschild, R., Schwarz, J., Moussion, C., de Vries, I., Legler, D. F., Luther, S. A., Bollenbach, T., and Sixt, M. (2013) Interstitial dendritic cell guidance by haptotactic chemokine gradients. *Science* **339**, 328-332

29. Noor, S., and Wilson, E. H. (2012) Role of C-C chemokine receptor type 7 and its ligands during neuroinflammation. *J Neuroinflammation* **9**, 77

30. Swaminathan, G. J., Holloway, D. E., Colvin, R. A., Campanella, G. K., Papageorgiou, A. C., Luster, A. D., and Acharya, K. R. (2003) Crystal structures of oligomeric forms of the IP-10/CXCL10 chemokine. *Structure* **11**, 521-532

31. Yunker, C. K., Golembieski, W., Lemke, N., Schultz, C. R., Cazacu, S., Brodie, C., and Rempel, S. A. (2008) SPARC-induced increase in glioma matrix and decrease in vascularity are associated with reduced VEGF expression and secretion. *Int J Cancer* **122**, 2735-2743

32. Golembieski, W. A., Thomas, S. L., Schultz, C. R., Yunker, C. K., McClung, H. M., Lemke, N., Cazacu, S., Barker, T., Sage, E. H., Brodie, C., and Rempel, S. A. (2008) HSP27 mediates SPARC-induced changes in glioma morphology, migration, and invasion. *Glia* **56**, 1061-1075

33. Condeelis, J., and Segall, J. E. (2003) Intravital imaging of cell movement in tumours. *Nat Rev Cancer* **3**, 921-930

34. Herz, J., Paterka, M., Niesner, R. A., Brandt, A. U., Siffrin, V., Leuenberger, T., Birkenstock, J., Mossakowski, A., Glumm, R., Zipp, F., and Radbruch, H. (2011) In vivo imaging of lymphocytes in the CNS reveals different behaviour of naive T cells in health and autoimmunity. *J Neuroinflammation* **8**, 131

35. Pepper, M., Dzierszinski, F., Crawford, A., Hunter, C. A., and Roos, D. (2004) Development of a system to study CD4+-T-cell responses to transgenic ovalbumin-expressing Toxoplasma gondii during toxoplasmosis. *Infect Immun* **72**, 7240-7246

36. Mrass, P., Takano, H., Ng, L. G., Daxini, S., Lasaro, M. O., Iparraguirre, A., Cavanagh, L. L., von Andrian, U. H., Ertl, H. C., Haydon, P. G., and Weninger, W. (2006) Random migration precedes stable target cell interactions of tumor-infiltrating T cells. *J Exp Med* **203**, 2749-2761

37. Cockburn, I. A., Amino, R., Kelemen, R. K., Kuo, S. C., Tse, S. W., Radtke, A., Mac-Daniel, L., Ganusov, V. V., Zavala, F., and Menard, R. (2013) In vivo imaging of CD8+ T cell-mediated elimination of malaria liver stages. *Proc Natl Acad Sci U S A* **110**, 9090-9095

38. Wilson, E. H., Weninger, W., and Hunter, C. A. (2010) Trafficking of immune cells in the central nervous system. *J Clin Invest* **120**, 1368-1379

39. Fouts, A. E., and Boothroyd, J. C. (2007) Infection with Toxoplasma gondii bradyzoites has a diminished impact on host transcript levels relative to tachyzoite infection. *Infect Immun* **75**, 634-642

40. Sukhumavasi, W., Egan, C. E., and Denkers, E. Y. (2007) Mouse neutrophils require JNK2 MAPK for Toxoplasma gondii-induced IL-12p40 and CCL2/MCP-1 release. *J Immunol* **179**, 3570-3577

41. Mennechet, F. J., Kasper, L. H., Rachinel, N., Li, W., Vandewalle, A., and Buzoni-Gatel, D. (2002) Lamina propria CD4+ T lymphocytes synergize with murine intestinal epithelial cells to enhance proinflammatory response against an intracellular pathogen. *J Immunol* **168**, 2988-2996

42. Ju, C. H., Chockalingam, A., and Leifer, C. A. (2009) Early response of mucosal epithelial cells during Toxoplasma gondii infection. *J Immunol* **183**, 7420-7427

43. Koshy, A. A., Dietrich, H. K., Christian, D. A., Melehani, J. H., Shastri, A. J., Hunter, C. A., and Boothroyd, J. C. (2012) Toxoplasma co-opts host cells it does not invade. *PLoS Pathog* **8**, e1002825

44. Cekanaviciute, E., Dietrich, H. K., Axtell, R. C., Williams, A. M., Egusquiza, R., Wai, K. M., Koshy, A. A., and Buckwalter, M. S. (2014) Astrocytic TGF-beta signaling limits inflammation and reduces neuronal damage during central nervous system Toxoplasma infection. *J Immunol* **193**, 139-149

45. David, C. N., Frias, E. S., Szu, J. I., Vieira, P. A., Hubbard, J. A., Lovelace, J., Michael, M., Worth, D., McGovern, K. E., Ethell, I. M., Stanley, B. G., Korzus, E., Fiacco, T. A., Binder, D. K., and Wilson, E. H. (2016) GLT-1-Dependent Disruption of CNS Glutamate Homeostasis and Neuronal Function by the Protozoan Parasite Toxoplasma gondii. *PLoS Pathog* **12**, e1005643

46. Jones, E. V., and Bouvier, D. S. (2014) Astrocyte-secreted matricellular proteins in CNS remodelling during development and disease. *Neural Plast* **2014**, 321209

47. Kzhyshkowska, J., Workman, G., Cardo-Vila, M., Arap, W., Pasqualini, R., Gratchev, A., Krusell, L., Goerdt, S., and Sage, E. H. (2006) Novel function of alternatively activated macrophages: stabilin-1-mediated clearance of SPARC. *J Immunol* **176**, 5825-5832

48. Blakely, P. K., Hussain, S., Carlin, L. E., and Irani, D. N. (2015) Astrocyte matricellular proteins that control excitatory synaptogenesis are regulated by inflammatory cytokines and correlate with paralysis severity during experimental autoimmune encephalomyelitis. *Front Neurosci* **9**, 344

CHAPTER FOUR

Conclusions and Perspectives

4.1 INTRODUCTION

While our grasp of immune cell migration to and away from infected tissues is rapidly evolving, gaps in our knowledge still remain. Parasitic infections are particularly complex but because of this they can teach us much about cell trafficking. Coordinated cell recruitment and maintenance of cell populations is required to combat all infections, including *T. gondii*. Many infections occupy a chronic niche within the host and therefore necessitate sustained chemokine dependent recruitment to specialized organs. Using these infection models will allow researchers to tease out the signaling requirements for cell migration within tissue and answer lingering questions about whether signals can be tissue specific, cell specific, influenced by chemokines, or influenced by other molecules present within tissue.

4.2 MOVING FORWARD

4.2.1 The complexity of chemokine signaling.

Currently chemokines are studied by manipulating them or their receptors one by one. Techniques have to be developed where it is recognized that a cell may be able to detect and/or respond to multiple chemokines simultaneously, a much more realistic situation for cell migration within infected tissue. In addition, immunologists spend a considerable amount of time phenotyping cell populations and demonstrating their heterogeneity. Even the swarming behavior of neutrophils is not a clonal response during infection (1). Rapid detection of changes in receptor expression, internalization and downstream signaling currently available *in vitro* and being newly developed in the field of developmental biology (2) need to be utilized *in vivo* to truly understand chemokine dynamics during infection.

As science progresses, the complexity surrounding chemokine signaling is increasingly appreciated. Of the 40 or so chemokines that are expressed by humans and mice (3), one group is thought of as homeostatic (constitutively expressed to maintain cell populations) while the rest are considered inflammatory (expressed upon activation, infection, or injury to attract or repel cell populations). However, these categories are definitely not mutually exclusive- CCL21/CCR7 is a classic exception. Additionally, we know that several

chemokines can target the same receptor. CCL19 is also a ligand for CCR7, and in high concentrations, CCL21 has been shown to bind to CXCR3, a receptor that already has three other known ligands (CXCL9, CXCL10, CXCL11)! Thus, the concept of signaling bias is introduced (4). This hypothesis, for which there is considerable evidence, states that the binding of one ligand as opposed to another will preferentially activate one of many possible signaling pathways. These pathways can be as straightforward as favoring G protein signaling over β-arrestin recruitment, or even go so far as to favor one of several isoforms of G protein. For example, five different Gα proteins have been reported to associate with CCR7 ($G\alpha_{i1}$, $G\alpha_{i2}$, $G\alpha_{i3}$, $G\alpha_{01}$, $G\alpha_{02}$) (5).

We also now understand that chemokine receptors themselves are decorated with post-translational modifications such as glycosylation and siliation (6). Those modifications can alter the manner in which ligands are able to bind to their receptors. Further, those modifications can be altered by enzymes released by one cell type, such as dendritic cells, to enhance or diminish the migration of another cell type, such as T cells (6). Changes induced by enzymes can also have a direct impact of the chemokines themselves. For instance, dendritic cells can convert immobilized CCL21 into a soluble form that is functionally distinct from both intact CCL21 and CCL19 (6,7). Each level of regulation may be at play during chemokine mediated cell responses and tweaking any or all of them can have a profound impact on the immune response in the brain and elsewhere.

4.2.2 The continuing mystery surrounding infection induced reticular fibers.

In 2009, the induction of a densely organized network of fibers seemingly emanating from the vasculature and visualized using second harmonic generation was reported in the brain upon infection with *T. gondii* (8). While this dissertation, and other work from the Wilson lab has identified the importance of SPARC in the proper assembly of this network (Nance et al, manuscript in preparation), seven years later we still don't know the composition of these fibers.

Second harmonic generation in biological samples is caused by noncentrosymmetric structures, the most abundant of which is collagen. Collagen networks have been described in other tissues such as the lymph node and seem to support cell migration. The generation of a network of collagen fibers at a time when cells need to infiltrate the brain would be further evidence of a conserved mechanism to assist cell infiltration. Also a major source of collagen in the brain is the vasculature and the observation that the fibers seem to branch from blood vessels would support the hypothesis that collagen is rearranged in the brain upon infection to facilitate cell invasion.

However, There is no evidence that collagen is upregulated at the mRNA level in the brain upon infection, though this could be due to remodeling at the protein

level. Immunohistchemistry staining for collagen is restricted to blood vessels and there is no evidence of immunoreactivity within the parenchyma. Further, there is anecdotal evidence that fixation destroys the reticular network and collagen is known to be preserved well within tissue by fixation. Therefore the composition of the system of reticular fibers is yet to be determined.

There are, however, more candidates for the composition of this network. An intriguing possibility is an extracellular matrix protein called elastin. Elastin can be visualized using multiphoton microscopy and is capable of forming an extensive network of straight fibers in other tissues (9-11). Further, the vasculature is also a source for elastin in the brain, as it is with collagen, its appearance as a network resembles the long, straight, interwoven fibers seen during *T. gondii* infection, and neutrophils are known to secrete elastases as they infiltrate tissue and have recently been reported to do so in experimental autoimmune encephalomyelitis (12). This may explain the early formation of the network in the brain and its eventual resolution as innate immunity to *T. gondii* wanes and the adaptive T cell response increases over time. Another intriguing candidate is β-amyloid peptide, which has recently been shown to act as a defense mechanism employed by neurons to protect themselves from a variety of infections (13). However, no one has yet demonstrated that β-amyloid can be visualized without a probe or dye. In short, while the composition of this network still remains unknown, there are numerous avenues for further research.

4.3 CONCLUSION

All together, the data described in this dissertation begin to characterize the structural and signaling requirements for cells to migrate efficiently within the brain. I hope that further studies can build on these findings so that one day the T cell response can be enhanced, leading to new therapies for chronic *Toxoplasma gondii* infection- a condition for which there is still no cure.

4.4 REFERENCES

1. Ng, L. G., Qin, J. S., Roediger, B., Wang, Y., Jain, R., Cavanagh, L. L., Smith, A. L., Jones, C. A., de Veer, M., Grimbaldeston, M. A., Meeusen, E. N., and Weninger, W. (2011) Visualizing the neutrophil response to sterile tissue injury in mouse dermis reveals a three-phase cascade of events. *J Invest Dermatol* **131**, 2058-2068

2. Dona, E., Barry, J. D., Valentin, G., Quirin, C., Khmelinskii, A., Kunze, A., Durdu, S., Newton, L. R., Fernandez-Minan, A., Huber, W., Knop, M., and Gilmour, D. (2013) Directional tissue migration through a self-generated chemokine gradient. *Nature* **503**, 285-289

3. Zlotnik, A., and Yoshie, O. (2012) The chemokine superfamily revisited. *Immunity* **36**, 705-716

4. Steen, A., Larsen, O., Thiele, S., and Rosenkilde, M. M. (2014) Biased and g protein-independent signaling of chemokine receptors. *Front Immunol* **5**, 277

5. Hauser, M. A., and Legler, D. F. (2016) Common and biased signaling pathways of the chemokine receptor CCR7 elicited by its ligands CCL19 and CCL21 in leukocytes. *J Leukoc Biol*

6. Hauser, M. A., Kindinger, I., Laufer, J. M., Spate, A. K., Bucher, D., Vanes, S. L., Krueger, W. A., Wittmann, V., and Legler, D. F. (2016) Distinct CCR7 glycosylation pattern shapes receptor signaling and endocytosis to modulate chemotactic responses. *J Leukoc Biol*

7. Schumann, K., Lammermann, T., Bruckner, M., Legler, D. F., Polleux, J., Spatz, J. P., Schuler, G., Forster, R., Lutz, M. B., Sorokin, L., and Sixt, M. (2010) Immobilized chemokine fields and soluble chemokine gradients cooperatively shape migration patterns of dendritic cells. *Immunity* **32**, 703-713

8. Wilson, E. H., Harris, T. H., Mrass, P., John, B., Tait, E. D., Wu, G. F., Pepper, M., Wherry, E. J., Dzierzinski, F., Roos, D., Haydon, P. G., Laufer, T. M., Weninger, W., and Hunter, C. A. (2009) Behavior of parasite-specific effector CD8+ T cells in the brain and visualization of a kinesis-associated system of reticular fibers. *Immunity* **30**, 300-311

9. Zoumi, A., Lu, X., Kassab, G. S., and Tromberg, B. J. (2004) Imaging coronary artery microstructure using second-harmonic and two-photon fluorescence microscopy. *Biophys J* **87**, 2778-2786

10. Yu, J., and Urban, J. P. (2010) The elastic network of articular cartilage: an immunohistochemical study of elastin fibres and microfibrils. *J Anat* **216**, 533-541

11. Yu, J., Tirlapur, U., Fairbank, J., Handford, P., Roberts, S., Winlove, C. P., Cui, Z., and Urban, J. (2007) Microfibrils, elastin fibres and collagen fibres in the human intervertebral disc and bovine tail disc. *J Anat* **210**, 460-471

12. Aube, B., Levesque, S. A., Pare, A., Chamma, E., Kebir, H., Gorina, R., Lecuyer, M. A., Alvarez, J. I., De Koninck, Y., Engelhardt, B., Prat, A., Cote, D., and Lacroix, S. (2014) Neutrophils mediate blood-spinal cord barrier disruption in demyelinating neuroinflammatory diseases. *J Immunol* **193**, 2438-2454

13. Kumar, D. K., Choi, S. H., Washicosky, K. J., Eimer, W. A., Tucker, S., Ghofrani, J., Lefkowitz, A., McColl, G., Goldstein, L. E., Tanzi, R. E., and Moir, R. D. (2016) Amyloid-beta peptide protects against microbial infection in mouse and worm models of Alzheimer's disease. *Sci Transl Med* **8**, 340ra372